NON-DESTRUCTIVE EVALUATION AND MATHEMATICAL MODELING OF BEEF LOINS SUBJECTED TO HIGH HYDRODYNAMIC PRESSURE TREATMENT

By

Anand Lakshmikanth

Thesis submitted to the Faculty of Virginia Polytechnic Institute and State University in partial fulfillment of the requirements for the degree of

Doctor of Philosophy

In

Biological Systems Engineering

Parameswarakumar Mallikarjunan, Chair

Justin Barone

George J. Flick

Morse B. Solomon

Jitendra R. Patel

August 13, 2009

Blacksburg, VA

Keywords: high hydrodynamic pressure processing, beef, ultrasound, video image analysis, wavelet features, rheology, finite element modeling, small-strain and large-strain behavior

ABSTRACT

High hydrodynamic pressure (HDP) treatment is a novel non-thermal technology that improves tenderness in foods by subjecting foods to underwater shock waves. In this study non-destructive and destructive testing methods, along with two mathematical models were explored to predict biomechanical behavior of beef loins subjected to HDP-treament.

The first study involved utilizing ultrasound and imaging techniques to predict textural changes in beef loins subjected to HDP-treatment using Warner-Braztler shear force (WBS) scores and texture profile analysis (TPA) features for correlation. Ultrasound velocity correlated very poorly with the WBS scores and TPA features, whereas the imaging features correlated better with higher *r*-values. The effect of HDP-treatment variables on WBS and TPA features indicated that amount of charge had no significant effects when compared to location of sample and container size during treatment.

Two mathematical models were used to simulate deformational behavior in beef loins. The first study used a rheological based modeling of protein gel as a preliminary study. Results from the first modeling study indicated no viscous interactions in the model and complete deformation failure at pressures exceeding 50 kPa, which was contrary to the real-life process conditions which use pressures in the order of MPa. The second modeling study used a finite element method approach to model elastic behavior. Shock wave was modeled as a non-linear and linear propagating wave. The non-linear model indicated no deformation response, whereas the linear model indicated realistic deformation response assuming transverse isotropy of the model beef loin.

The last study correlated small- and large-strain measurements using stress relaxation and elastic coefficients of the stiffness matrix as small-strain measures and results of the study indicated very high correlation between elastic coefficients c_{11}, c_{22}, and c_{44} with TPA cohesiveness ($r > 0.9$), and springiness ($r > 0.85$). Overall results of this study indicated a need for further research in estimating mechanical properties of beef loins in order to understand the dynamics of HDP-treatment process better.

DEDICATION

To my parents for their love and affection, support, and patience,

To my brother, Ajit for being the great sibling that he is,

To my wife-to-be, Bhaveeni and her family for all their love and affection, support, and patience,

To my pet cat, Lali, for being the bundle of joy that she is.

ACKNOWLEDGEMENT

I wish to express sincere gratitude to my advisor, Dr. P. Mallikarjunan for giving me the opportunity to pursue my doctorate in the BSE department and for his strong support, guidance, wisdom, amicability, and patience in helping me conduct my research and helping me gain experience in writing grant proposals. I would also like to thank my committee members, Dr. Morse Solomon and Dr. Jitendra Patel, from USDA-ARS for their guidance, providing me samples for my research, and giving me the opportunity to intern at their facility during the summer of 2006. I would also like to thank Dr. Justin Barone for his guidance and support, and especially for stepping in as my committee member at an inopportune time and Dr. Flick for his help and his assistance in helping me use his facilities to conduct primary research.

I am also grateful to the head of BSE, Dr. Mostaghimi, for providing me financial opportunities through scholarships and assistantships for continuing my program. I would also extend the gratitude to the faculty at Engineering Education, Dr. Griffin, Dr. Lohani, and Dr. Lo, who also provided me financial opportunities through teaching assistantships and helped me hone my teaching skills.

Special thanks go towards all the staff members at BSE for coming to my assistance in times of dire need, especially Amy Egan, Denton Yoder, and Laura Teany. I would also like to thank Harriet Williams, Joell Eiffert, Dr. Susan Sumner, and Dr. Joe Marcy at Food Science and Technology for providing me the use of the facilities.

Lastly, I would like to thank my fellow graduate students- Christan Whysong and Ahmad Athamneh for helping me with my initial stages of research, and former colleagues- Anurag

Mishra, Rhonda Bengtson, Tameshia Ballard, Xiaopei Hu, Amanda Martin, and Meg Orders, who were very good friends and have moved on to great careers. I wish you all very well.

TABLE OF CONTENTS

Page

Title Page i

Abstract ii

Dedication iv

Acknowledgements v

Table of Contents vii

List of Figures xi

List of Tables xiv

CHAPTER 1
INTRODUCTION 1
Rationale and Significance 1

CHAPTER 2
REVIEW OF LITERATURE 3

Background 3
High Hydrostatic Pressure Processing 4
High Hydrostatic Pressure Treatment and Microbial Inactivation 6
High Hydrostatic Pressure Treatment and Quality Attributes in Foods 7
High Hydrodynamic Pressure Processing 9
High Hydrodynamic Pressure Treatment and Microbial Inactivation 11
High Hydrodynamic Pressure Treatment and Quality Attributes in Foods 15
Tenderness in the Beef Industry 19
Methods for improving tenderness 20
Methods for measuring tenderness 21
Warner-Bratzler Shear Force Testing 21
Tenderness Probes 22
Near-Infrared Spectroscopy 24
Video Image Analysis 25
Miscellaneous Methods for Measuring Tenderness 27
Conclusions 29
References 31

CHAPTER 3
NON-DESTRUCTIVE EVALUATION OF TEXTURE IN HIGH HYDRODYNAMIC PRESSURE-TREATED BEEF LOINS USING MACHINE VISION AND ULTRASOUND TECHNIQUES 48

Abstract 48
Introduction 50
Materials and Methods 52
HDP Testing Procedure 52
Image Acquisition 53
Ultrasound Acquisition 54
Warner-Bratzler Testing and Texture Profile Analysis 56
Statistical Analysis 56
Results and Discussion 57
Correlation between Non-Destructive Analysis and WBS scores and TPA features 57
Effect of HDP treatment variables on WBS scores and TPA features 58
Effects of Charge Amount 59
Effects of Container Size 60
Effects of Sample Location during Treatment 60
Conclusions 64
References 66

CHAPTER 4
RHEOLOGICAL METHOD FOR MODELING DEFORMATION BEHAVIOR OF A VISCOELASTIC PROTEIN GEL UNDERGOING HIGH HYDRODYNAMIC PRESSURE TREATMENT 84

Abstract 84
Introduction 86
Model Development 88
Results and Discussion 96
Sensitivity Analysis 100
Effects of Material Parameters 100
Effects of Process Conditions 101
Conclusions 102
References 104
MATLAB Code 119

CHAPTER 5
FINITE ELEMENT METHOD FOR MODELING MECHANICAL BEHAVIOR IN BEEF LOINS UNDERGOING HIGH HYDRODYNAMIC PRESSURE-TREATMENT 124

Abstract....124
Introduction....126
Model Development and Governing Equations....127
Constitutive Relationships for Mechanical Properties....127
Constitutive Relationships for Shock Wave Propagation....132
Modeling on FEMLAB 2.3....136
Materials and Methods....138
Ultrasound Velocity and Material Constants....138
Sample Testing and preparation....140
Results and Discussion....142
Estimation of Elastic Coefficients using Ultrasound Velocity....142
Effect of HDP-treatment on Elastic Coefficients....144
Results of Numerical Modeling....145
Stress Analysis....145
Modeling Linear Shock Wave Propagation....147
Isotropic Behavior....148
Transversely Isotropic Behavior....149
Conclusions....150
References....152

CHAPTER 6
CORRELATING SMALL-STRAIN AND LARGE-STRAIN BEHAVIOR IN BEEF LOINS USING AGING AND HIGH HYDRODYNAMIC PRESSURE-TREATMENT STUDIES....174

Abstract....174
Introduction....175
Materials and Methods....176
Correlating Relaxation Time and TPA Features....176
Aging of Samples....177
Stress Relaxation Estimation....177
Texture Profile Analysis....178
Statistical Analysis....178
Correlating Elastic Coefficients and WBS Scores and TPA Features....178
HDP Treatment of Sample....178
Estimation of Elastic Coefficients Using Ultrasound....179
Warner-Bratzler Shear and Texture Profile Analysis....182
Statistical Analysis....182
Results and Discussion....183
Aging Study: Correlation between Relaxation Time and TPA Features....183
HDP Study: Correlation between Elastic Coefficients and WBS Scores and TPA Features....185
Effects on Palatability....187
Conclusions....189
References....190

CHAPTER 7
SUMMARY AND CONCLUSIONS 208

Future Work.....211

LIST OF FIGURES

Page

Figure 3.1: Set-up of the performed HDP procedure....71

Figure 3.2: Image acquisition of beef loins....72

Figure 3.3: Close-up gray-scale image of beef loin....73

Figure 3.4: Acquisition of ultrasound data....74

Figure 3.5: Five-level wavelet decomposition using Haar wavelets....75

Figure 3.6: Ultrasound signal at 250 kHz....76

Figure 3.7: Distribution of samples in the canonical space based on charge amounts used in HDP-treatment using WBS and TPA scores as variables....77

Figure 3.8: Distribution of samples in the canonical space based on sample location during HDP-treatment using WBS and TPA scores as variables....78

Figure 3.9: Distribution of samples in the canonical space based on container size used in HDP-treatment using WBS and TPA scores as variables....79

Figure 4.1: Strain response to an applied sinusoidal shear stress....107

Figure 4.2: Four-element Burger model....108

Figure 4.3: Phasor diagram of the complex shear modulus, G*....109

Figure 4.4: Shear modulus vs protein content in a protein-stabilized emulsion gel....110

Figure 4.5: Pressure response of protein gel vs time....111

Figure 4.6: Deformation of a protein gel impacted by an oscillating pressure wave (P_{max} = 50 kPa, ω=120,000 rads/s)....112

Figure 4.7: Deformation of a protein gel impacted by an oscillating pressure wave (P_{max} = 50 kPa, ω=240,000 rads/s)....113

Figure 4.8: Time-pressure graph of incident shock wave during HDP-treatment....114

Figure 4.9: Sensitivity analysis of material parameter inputs for rheological model....115

Figure 4.10: Sensitivity analysis of process parameter inputs (pressure wave frequency) for rheological model 116

Figure 4.11: Sensitivity analysis of process parameter inputs (pressure wave intensity) for rheological model 117

Figure 5.1: 3-D elastic body with displacements and forces 158

Figure 5.2: Schematic representation of incident shock wave (P_0) on sample 159

Figure 5.3: Elliptical plate model of beef with meshing 160

Figure 5.4: Extraction schematic for samples for elastic coefficient estimation using ultrasound 161

Figure 5.5: Frozen cylindrical segments of beef loins 162

Figure 5.6: Frozen beef samples extracted for elastic coefficient estimation using ultrasound 163

Figure 5.7: Time-pressure graph of incident shock wave during HDP-treatment 164

Figure 5.8: von-Mises stresses on beef model at 800 MPa for non-linear shock wave propagation 165

Figure 5.9: von-Mises stresses on beef model at 600 MPa for non-linear shock wave propagation 166

Figure 5.10: Deformation of beef model at 800 MPa for non-linear shock wave propagation 167

Figure 5.11: Deformation of beef model at 600 MPa for non-linear shock wave propagation 168

Figure 5.12: von-Mises stresses on beef model at 800 MPa for linear shock wave propagation assuming isotropy 169

Figure 5.13: Deformation of beef model at 800 MPa for linear shock wave propagation assuming isotropy 170

Figure 5.14: von-Mises stresses on beef model at 800 MPa for linear shock wave propagation assuming transverse isotropy 171

Figure 5.15: Deformation of beef model at 800 MPa for linear shock wave propagation assuming transverse isotropy 172

Figure 6.1: Aging of beef loins in vacuum-packaged bags 195

Figure 6.2: Estimation of relaxation time using tensile strain……...196

Figure 6.3: Extraction schematic for samples for elastic coefficient estimation using ultrasound……..197

Figure 6.4: Texture profile analysis curve 198

Figure 6.5: Curve-fitted graph for estimation of relaxation time (τ) 199

Figure 6.6: Variation of relaxation time with days of aging.....200

Figure 6.7: Variation of TPA features with aging…….201

Figure 6.8: Correlation between relaxation time and TPA chewiness.....202

Figure 6.9: Correlation between relaxation time and TPA cohesiveness 203

Figure 6.10: Correlation between relaxation time and TPA springiness 204

LIST OF TABLES

Page

Table 3.1: Correlation coefficients and P- values for WBS and TPA features with ultrasound velocity (α =0.05) 80

Table 3.2: Correlation coefficients and P-values for WBS and TPA features with imaging features (α = 0.05) 81

Table 3.3: R^2 values for regression fit of WBS and TPA features with imaging features (α = 0.05) 80

Table 3.4: Percentage reduction or increase in values of WBS scores and TPA features in treated samples when compared to controls 82

Table 3.5: Average percentage change in WBS scores and TPA features with changing HDP-treatment variables 83

Table 3.6: P>F values for test of significance for separate and combinatorial effects of HDP-treatment on WBS scores and TPA features 83

Table 4.1: Material properties of β-lactogloublin protein gel with transglutaminase cross-linkages 118

Table 5.1: Average values of diagonal coefficients of stiffness matrix, C_{ij} estimated using ultrasound techniques 173

Table 5.2: Percentage change in elastic coefficients post HDP-treatment 173

Table 6.1: Pearson's correlation and Mean-squared error estimation between TPA features and stress relaxation (τ) 205

Table 6.2: Average values of diagonal coefficients of stiffness matrix, C_{ij} estimated using ultrasound techniques 205

Table 6.3: Percentage change in WBS shear-force post HDP-treatment 206

Table 6.4: Percentage change in TPA features post HDP-treatment 206

Table 6.5: Pearson's correlation coefficients (r) and P-values for WBS and TPA features with elastic coefficients 207

CHAPTER 1

INTRODUCTION

With current interest in minimally processed foods, high hydrostatic pressure (HPP) and hydrodynamic pressure (HDP) treatments have become more attractive techniques. High hydrostatic pressure and hydrodynamic pressure processing techniques have been regarded by food scientists and the food industry as a novel means for pathogen inactivation and simultaneously have minimal adverse effects on the characteristics of the final product. Pressures required to process the raw meat without modifying the textural attributes adversely but to provide the required lethality for pathogens is a challenging issue and has not been addressed in its full entirety to allow a commercial application. In the case of HDP, much study needs to be done to focus on the effect high pressure on product texture to provide consistent product quality and associated inactivation effect in raw meat products.

RATIONALE AND SIGNIFICANCE

Considering the increase in research in the field of high pressure treatments in food processing, it is essential that both raw and processed foods subjected to treatments are evaluated for changes in texture, flavor, constituents, and microbial activity. Limited work has been reported in the literature to study the effect of high pressure processing on the quality of various food products compared to the vast amount of literature on inhibition of various bacterial pathogens using high pressure system. While HPP technology has seen significant research

conducted resulting in an increase in the commercial application of the technology, HDP technology remains an area that has not been explored much. One means of generating shockwaves is through explosives, which leads to security issues in its utilization. In addition, since the technology is based on utilizing explosive detonation to generate shock waves, there is very little control in the hands of the user in optimizing the variables of application to generate consistent results. There is also a need to identify the pressures required to process the raw meat without modifying the textural attributes adversely but to provide the required lethality for pathogens. This is a challenging issue and has not been addressed in its full entirety. To summarize, there is a need for research to focus on the effect of HDP on product texture to provide consistent product quality and associated inactivation effect in raw meat products.

This research is focused primarily on helping facilitate better process and product control in the HDP process by analyzing changes occurring in the food sample, viz. raw beef loin, undergoing HDP treatment. The focus of the research work is on:

- Developing non-destructive methods, video image analysis and ultrasound methods, to analyze textural changes in raw beef loin undergoing HDP treatment,
- Experimentally estimate mechanical properties of raw beef loin using ultrasound methods to utilize in the numerical model,
- Developing mathematical models, based on rheology and mechanical constitutive relationships, to describe changes in raw beef loin subjected to shockwaves,
- Establish statistical relationship between experimentally derived large-strain and small-strain features.

CHAPTER 2

REVIEW OF LITERATURE

BACKGROUND

Non-thermal processing methods offer benefit of minimal effect on flavor, color, and texture of the food product, when compared to conventional thermal treatment methods. Processing methods such as ionizing radiation, high pressure, pulsed electric fields (PEF), pulsed white light, ultrasound, and UV radiation offer physical alternatives to thermal processing. Among these novel treatment methods, high pressure technology has become a popular non-thermal treatment method in the food industry. Around early 1990's, the food industry and consumers began to shift towards non-thermal processing and preservation of foods (Knoor, 1995). The shift was primarily due to a need for obtaining products of high nutritional quality and appealing sensory characteristics, since heat treatment tends to degrade both, along with providing microbiologically safe products with longer shelf life (Welti-Chanes et al., 2005). Effects of high pressure on foods involve modification of physico-chemical properties of water in terms of density, phase transition, etc., protein denaturation, protein modification, inactivation of enzymes, etc. (Knoor, 1995). The technology has also been applied in tempering of chocolate, blanching of vegetables, reducing cooking time in beans, gelatinization of starch and protein, and tenderization of meats (Ohlsson and Bengtsson, 2002).

Currently, two methods of high pressure treatment technologies are in use in the food industry. The first is high hydrostatic pressure processing (HPP) which is a technology that

utilizes very high static pressures up to 600 MPa to food systems (Ramaswamy et al., 2009) and the latter is high hydrodynamic pressure technology (HDP) that utilizes dynamic shock waves to food systems. Although this study is focused only on HDP treatment, a brief insight in HPP technology is essential to understand the impact of high pressure treatment technology in the modern day food industry since commercial production of pressurized foods via HPP treatment has become a reality in countries such as Japan, France, and USA. Fruit-based products like orange juice, avocado spread etc. are being processed by high pressure treatment (Cheftel and Culioli, 1997). In addition, Fujichiku Co. of Japan devised a novel manufacturing process involving "raw ham" using high pressure technology in 1992 to induce faster curing and tenderization, accompanied by improvement in water retention. Other muscle foods such as, raw squid, fish, scallops have been treated by HPP technology and marketed in Japan. (Cheftel and Culioli, 1997).

HIGH HYDROSTATIC PRESSURE PROCESSING

High hydrostatic pressure processing utilizes high static pressures in the range of 100-600 MPa through a pressure transmitting medium, which is usually water combined with mineral or vegetable oil for lubrication (Welti-Chanes et al., 2005). Since HPP technology utilizes extremely high pressures in enclosed vessels, the technology is predominantly a batch process, but Avure Technologies, Kent, WA has been producing semi-continuous HPP systems that are restricted to liquid food systems and operate at much lower pressures than batch systems (Ramaswamy et al., 2009).

A typical HPP system consists of the following components (Flick, 2003)

- Pressure vessel and enclosure
- Pressure generation system
- Pressure and temperature control device
- Materials handling system

Most vessels are made of high tensile steel alloys that can withstand very high pressures and the machinery involved in this technology relies heavily on extremely high precision in its construction, utilization, and maintenance (Flick, 2003). Methods of generating high pressure include

- Direct compression
- Indirect compression

Direct compression involves pressurizing the high-pressure chamber directly using the small diameter end of a piston, while the large diameter end is driven by a low-pressure pump (Palou et al., 1999). The indirect method uses a high pressure intensifier to pump the pressure medium from a reservoir to the pressure vessel till the required pressure is reached (Palou et al., 1999). The direct compression method has the advantage of faster compression, but also carries the disadvantage of wear and tear on closure seals between the piston and the internal surface of the pressure vessel and is thus limited to small-scale laboratory and pilot-plant units. Most industrial units utilize the indirect compression method (Palou et al., 1999).

The effects of HPP are instantaneous and result in a uniform transfer of pressure energy throughout the food regardless of their geometry or size by obeying the Pascal's principle

(Knoor, 1995). The process is non-thermal even though there is a slight increase in temperature with increase in pressure in the enclosed vessel, in accordance with the ideal gas law. However this increase in temperature is negligible and does not affect characteristics of the food (Welti-Chanes et al., 2005). Although high hydrostatic pressure disrupts living cells, it does not degrade small molecules like vitamins and flavors and as a result, has minimal effects on the sensory quality of meat products (Ananth et al., 1998, Murano et al., 1999).

High Hydrostatic Pressure Treatment and Microbial Inactivation

Pathogen inactivation in food products using HPP technology has been widely explored. Most work related to pathogen activation in HPP has been done using buffer solution or growth media (Rademacher et al., 2001 and Yuste et al., 2004) and skim milk, however notable work has been done on food products like tomato puree (Krebbers et al., 2003), juices (Aleman et al., 1996, Zook et al., 1999, Ardia et al., 2003), etc..

Significant work in pathogen and microbial inactivation in meat products have been reported using HPP treatment. Berlin et al. (1999) studied the response of pathogenic *Vibrio* species to high hydrostatic pressure. Suspensions of V. *parahaemolyticus, V. vulnificus, V. cholerae, V. hollisae,* and *V. mimicus* were treated with 200-300 MPa pressures for 5-15 min at 25°C. The conditions inactivated all strains of pathogenic *Vibrio* species without triggering a viable but non-culturable stage. In meat products, successful utilization of HPP treatments in inactivating pathogens was reported by Moerman et al. (2001) in meat batters, Garriga et al. (2004) in commercial cooked, cured and marinated meat products like ham and beef loins, and by Moerman (2005) in pork Marengo.

High Hydrostatic Pressure Treatment and Quality Attributes in Foods

High pressure treatment causes three kinds of changes in the meat: enzymatic, protein modifications and structural modifications (Cheftel and Culioli, 1997). High pressure processing treatments can induce changes on the texture and structure of a given food. The resulting change could be beneficial. Changing the texture of the product can be used for the development of new products or to increase the functionality of some ingredients. Therefore, the areas of experimentation with this technology for its industrial application in the meat sector comprise establishing best treatment conditions in every product and commercial situation

The pressure effects on water (main constituent of meat) comprise mainly a decrease in the freezing point under pressure and an increase in the ionization leading to a decrease in pH under pressure. These variations are reversible at low pressures but they can contribute by modifying the characteristics of the products subjected to high pressure. Above 150 MPa there are color changes similar to those in cooked meat (Cheftel and Culioli, 1997). When pressure is higher than 400-MPa, ferrous myoglobin becomes ferric and the globin protein is denatured. Calpastatin is inhibited from 200 MPa while calpains are degraded above 400 MPa (Carlez et al., 1995).

At pressures lower than 200 MPa lysosomes break down, the autolytic activity increases and the resulting meat tenderization is higher. Cathepsin H and aminopeptidases are inactivated from 200 MPa and cathepsin D is inactivated when pressure reaches 500 MPa (Montero et al., 2002). In general, gel formation is inhibited by high pressure processing since the pressure can

modify the transition temperature from sol to gel. Gelation can be induced by pressure and then the gels formed are softer and brighter. High pressure processing brings about a reversible passage of lipids from liquid to solid state leading to gelation. When there is a mixture of lipids, high pressures can lead to a separation of different phases resulting in the destruction of cell membranes (Cheftel and Culioli, 1997). The primary structures of proteins are slightly sensitive to high pressures; the modification of weak bonds can lead to protein denaturation or on the contrary to enzyme activation. The effects are variable depending on the protein types and the processing conditions (Cheftel and Culioli, 1997).

Several studies have described the enhancement of protease activity in pressurized meat (Homma et al., 1995; Jung et al., 1998; Otsuka et al., 1998), and the degradation of myofibrillar proteins (Cheftel and Culioli, 1997). Concerning the ultrastructural changes, pressurization was responsible for changes in the A-band (Suzuki et al., 1991), the weakening of gap filaments (Locker et al., 1984), the loss of integrity and aggregation of I-band (Macfarlane et al., 1980) and breaks in Z-lines (Elgasim and Kennik, 1982). Tuboly et al. (2003) studied the effects of high pressure treatments on lipid oxidation in mechanically deboned turkey using high pressure treatments of 200 MPa and 400 MPa for 20 minute durations. The results indicated an increase in thiobarbituric acid reactive substances (TBARs) and cholesterol oxidation products (COPs), as a result of lipid oxidation.

The extent of pressure induced modifications is strongly dependent on the rigor mortis stage, type of muscle and samples (intact or comminuted) and conditions of treatment (pressure level and duration, temperature). Transmission electron micrographs (TEM) in ovine *M. semimembranosus* subjected to 100 MPa for 1 min at 25°C showed stretching of sarcomeres (Macfarlane and Morton, 1978). With the added utilization of heat to high pressure, Boulton et

al. (1977) observed more extensive modifications to the meat structure when compared to high pressure alone. High pressure treatment thus interferes with normal tenderization, of which the exact mechanism still remains unclear.

HIGH HYDRODYNAMIC PRESSURE PROCESSING

The principle of utilizing high hydrodynamic pressure (HDP) involves shock waves in water. Underwater shock waves have been the subject of many theoretical and experimental studies in the past 25 years (Loske, 2001). The technology was popularized by its use in non-invasive treatment of nephrolithiasis in medicine; a technique known as extracorporeal shock wave lithotripsy (ESWL) (Loske, 2001). In general ESWL pulses are called shock waves to denote the high-amplitude pulse generated. Since the first treatment in 1980, the technique has become the standard treatment for patients suffering from renal and ureteral calculi or kidney stones. Shock waves for ESWL are produced by 4 major means:

- Electrohydraulic
- Electromagnetic
- Piezoelectric
- Microexplosive.

Electro-hydraulic lithotripters induce low intensity shock waves by electrical breakdown of water between two electrodes. The normal voltage used for this application ranges from 15-30 kV and peak current at discharge is in the range of 10-20 kA (Loske, 2001). Electromagnetic lithotripters use a system similar to a loudspeaker, viz. generating shock waves using a metal

diaphragm in the base of a water-filled shock tube. Eddy currents are generated in the diaphragm as a result of sending an electrical pulse (16-22 kV) through a coil. The magnetic fields generated by the eddy currents oppose those generated by the coil, causing the diaphragm to repel and transmitting energy into the water. Piezoelectric lithotripters use piezoceramic crystals arranged on a concave surface of a spherical metallic dish, which when stimulated by an electrical discharge create pulses of different intensities. Micro-explosive lithotripters utilize ellipsoidal reflectors to concentrate the energy generated by the explosion of small 10 mg lead or silver azide pellets. A major disadvantage of this technique is the amount of noise produced by the system (Loske, 2001). In addition to the medical utilization in removing renal calculi, other medical applications of shock waves include orthopedics, oncology, gene therapy and ophthalmology (Loske, 2001).

In food processing applications, the technology utilizes the principle of impedance or acoustic matching. Since foods such as meats contain 75% water, they form a close acoustical match to the water medium they are immersed in and the shock waves pass through the foods and reflect off of any surface that is not an acoustical match (Kolsky, 1963).

Application of hydrodynamic pressure treatments in foods have involved utilizing of electro-hydraulic generators and explosive charges to create shock waves. Applications in food have been studied in microbial inactivation and modification of textural properties which are discussed in detail in the next section.

High Hydrodynamic Pressure Treatment and Microbial Inactivation

Effects of shock waves on tubular cells of kidney in dogs (Delius et al., 1988) and on human red blood corpuscles (Delius et al., 1998) have been studied. The destructive effects of shock waves on eukaryotic cells extended its application to microbial inactivation and as a result, several studies have been reported in the field of HDP treatment and its effects on microbial inactivation.

Bactericidal effects were observed on suspensions of *Pseudomonas aeruginosa*, *Streptococcus faecalis*, *Staphylococcus aureus*, and *Escherichia coli* using 4000 shock waves at 20 kV at the rate of 100 shocks per minute (Kerfoot et al., 1992).

Loske et al. (1999) evaluated the possibility of using underwater shock waves to kill *Escherichia coli* in foods using an electrohydraulic shock generator. The organism was chosen because it is well known and easy to handle. Results of the study indicated that using a shockwave number between 500-2000 waves, at a voltage of 20 kV, a single log reduction was achieved at about 570 shock waves. Loske et al. (2002) studied the effect of HDP treatment on *E. coli* inactivation in 0.9% NaCl solution using electrohydraulic-generated shock waves. Influence from light generated from the spark-gap, number of shock waves applied, acoustic cavitation, and treatment temperature was studied. A reduction of 4.06 log CFU/ml at the rate of 350 shock waves for duration of 14.5 min was observed.

Alvarez et al. (2004) reported inactivation of *E.coli* O157:H7, *Salmonella Typhimurium*, and *Listeria monocytogenes* using underwater shock waves. The effect of acoustic cavitation, light produced by the discharge, shock wave dosage, and phase of growth was studied. *L.monocytogenes* was most susceptible with 3.17 log CFU/ml reduction with 350 shock waves.

With same dosage, *S.Typhimurium* reduction was by 1.68 log CFU/ml and *E.coli* O157:H7 was the least susceptible with 0.56 log CFU/ml reduction.

Aside from treatments on suspensions, work has been reported on HDP treatment on meat products and its effect on microbial inactivation. Williams-Campbell and Solomon (2001) investigated the effects of HDP treatment in reducing microorganisms on pork/beef stew pieces and ground beef. They reported a 2 log reduction using 100 g of explosive charge placed at 30.5 cm from the product. Williams-Campbell and Solomon (2002) also investigated HDP to reduce spoilage microorganisms in fresh beef products- ground beef and beef roasts. The packaged meat samples were placed in a 54-liter capacity shock wave container, 30.5 cm away from the explosive. HDP treatments reduced bacteria in both meat types. Based on days of storage after the treatments, the initial population was reduced by 2.0, 1.5, 4.5 logs for 0, 7 and, 14 days of storage, respectively, at 5°C. A reduction of 2-3 log was found in ground beef using 50, 75, or 100 g of charge at the given distance.

Patel and Solomon (2005) studied the effects of HDP-treatment on strongly-attached and loosely-attached bacteria- *E. coli* O157:H7, *L. monocytogenes*, and *S. typhimurium* on surfaces of beef cubes using a 100 g explosive charge at 30.5 cm from the meat surface. HDP treatment inactivated strongly-attached surface bacteria at a greater rate than loosely-attached bacteria and the reductions were very significant with for all three bacteria with 0.52, 0.37, and 0.43 $\log_{10}$ CFU/g respectively for *E. coli* O157:H7, *L. monocytogenes*, and *S. typhimurium*.

Podolak et al. (2006) studied the effects of HDP treatment using a 100 g explosive charge in inactivating a six strain cocktail of *E. coli* O157:H7- 3027-93, 3055-93, C7927, 43888, C9490, and green fluorescent protein-expressing *E. coli* O157:H7 B6-914 (GFP EC) at different

concentrations of 10^3, 10^4, and 10^6 CFU/g. Reductions observed in the population of the *E. coli* strains were found to be statistically significant post-treatment, but were not large enough for practical applications.

Patel et al. (2007) evaluated the effectiveness of a combinatorial treatment to control growth of *L. monocytogenes* in ready-to-eat meat products, like frankfurters by dipping them in antimicrobial solutions of sodium lactate, sodium diacetate, and nisin, followed by HDP treatment. Effectiveness in reducing the population of a five strain cocktail of *L. monocytogenes* was observed to be 2 $\log_{10}$ CFU/g when using nisin followed by HDP treatment indicating a synergistic effect of both treatments.

Sharma et al. (2008) compared both HPP and HDP treatments, in combination with chemical treatments, in inactivating food-borne viruses and non-pathogenic surrogates in pork sausage product. Sausages were inoculated with feline calicivirus (FCV), hepatitis A virus (HAV) or bacteriophage (MS2, phiX174, or T_4) after immersing them in distilled water, 100-ppm EDTA, or 2% lactoferrin. Combination of distilled water immersion and HDP-treatment significantly reduced titers of FCV by 2.70 $\log_{10}$ $TCID_{50}$/ml, and 1.10 $\log_{10}$ $TCID_{50}$/ml, and titers of bacteriophages T_4 and MS2 were reduced by 1.10 $\log_{10}$ PFU/g and 0.96 $\log_{10}$ PFU/g, respectively, when compared to non pressure-treated controls. It was reported that inoculation of viruses and bacteriophage on the meat may have protected viruses from complete inactivation using HDP-treatments.

Despite studies indicating success in microbial inactivation due to HDP treatments, unsuccessful treatments such as the one by Moeller et al. (1999) reported no significant differences in coliform bacterial counts between control and HDP-treated samples. This study

indicated that microbial inactivation due to HDP treatments wasn't very significant as that of HPP. Treatment by hydrodynamic pressure was also explored on eliminating the infectivity of *Trichinella spiralis*, a parasite in pork (Gamble, et al. 1998). Numbers of the parasite recovered from infected pork were significantly reduced by treatment with the HDP treatment, when compared to untreated and infected pork. However, treatment with the hydrodynamic force (55 to 60 MPa) did not eliminate the infectivity of this parasite when the larvae from treated meat were inoculated into mice.

Studies have also indicated penetration of pathogenic bacteria into the meat upon HDP treatment. Lorca et al. (2002) explored the effects of electrically-generated hydrodynamic shock waves on the microbial flora of ground beef. The study was on the penetration of surface inoculated *E. coli* into the ground beef samples, when subjected to HDP treatment. A penetration depth of 300 μm was observed using laser scanning confocal microscopy, which was deemed safe with respect to posing as a human hazard. Similar penetration depth studies were also done by Lorca et al. (2003) on boneless and skinless chicken breasts. Another study by Patel et al. (2005) evaluated destruction of E. coli O157:H7 in beef steaks treated with blade tenderization (BT), a non-thermal HDP, or combination of BT followed by HDP (BTH). Beef steaks, intentionally contaminated with five strain cocktail of E. coli O157:H7 were treated with BT, HDP, or BTH; and cooked to 54.4ºC (undercooked), 62.8ºC (medium rare), and 71.1ºC (medium). The potential translocation of E. coli O157:H7 from the surface to the interior of the muscle by blade tenderization treatment resulted in higher survival rate after cooking of BT treated steaks compared to those in control or HDP treated steaks. Patel et al. (2006) also studied the efficacy of HDP treatment using a 50 g explosive charge in reducing *Salmonella* in minced chicken. Population reduction of *Salmonella* in minced chicken post-treatment was 0.2-0.3 $\log_{10}$

CFU/g and found to be very marginal and practically insignificant. The authors noted the shock waves generated during the HDP process had low pressure intensities for fractions of milliseconds and may not have the required magnitude and duration to kill microorganisms such as *Salmonella spp.* when compared to HPP treatment.

These studies indicate that the effect of HDP treatments are not very consistent in microbial/pathogenic inactivation as HPP treatments are, and need more study to understand the dynamics behind the efficacy of shock waves in microbial inactivation.

High Hydrodynamic Pressure and Quality Attributes in Foods

The effect of HDP treatment has been found to have beneficial effects on meat texture, especially with respect to improving tenderness characteristics. Significant work in the field of HDP processes on muscle attributes has been reported from the USDA Beltsville facility in Maryland.

Solomon et al. (1997a) used three explosive charge amounts of 50, 75, and 100 g in improving tenderness in beef longissimus, semimembranosus, biceps femoris and semitendinous muscles using HDP-treatment. Shock pressures in the range of 6-7 MPa were reported on the contact surface of the meat. Samples indicated reduction of around 72% in Warner-Bratzler shear force (WBS) scores in longissimus muscles when using 100 g charge and as much as 30-59% of reduction was reported for other muscles. Solomon (1997b) reported the efficacy of HDP-treatment on “cold shortened” beef muscle using a 100 g explosive charge. The treatment was effective at tenderizing the “cold shortened” cuts of meat, irrespective of muscle origin by 53-66%. Solomon et al. (1997c) studied the effects of HDP-treatment, performed at 3 days post-

mortem, in comparison to 3, 17, 21, 28, and 35 days of aging. WBS reduction for the HDP-treatment was found to reduce by 33% whereas the samples subjected to aging reported WBS reduction by 24-33%, with no significant difference between the aging periods.

Zuckerman and Solomon (1998) reported reduction in WBS scores in beef longissimus samples by 37% when subjected to HDP-treatment using a 100 g charge. In addition they reported that transmission electron microscopy of treated samples indicated myofibrillar fragmentation in the Z-lines of bovine *longissimus dorsi* muscle upon HDP treatment at 150 MPa. A resultant of this fragmentation was increase in intramyofibrillar spaces, which resulted in a significant increase in tenderness.

Impact of HDP on tenderness and sensory characteristics were reported by Moeller et al. (1999) on pork *longissimus* muscle. The treatment resulted in a 17% reduction in WBS scores. No significant differences were reported on color score, firmness, drip loss and Minolta L* and Y scores between untreated and HDP-treated samples. Sensory evaluation, however, showed no improvement despite the reduction of WBS scores.

Claus et al. (2000) also reported reduction in WBS scores in chicken and turkey breasts subjected to electrically produced shock waves. The results indicated reduction in WBS scores by 22% for HDP-treated chicken breasts and a reduction in WBS scores by 12% for HDP-treated turkey breasts, when compared to the control.

Hydrodynamic shock waves were also used to evaluate quality and sensory characteristics of selected post-rigor and early deboned broiler breast meat (Meek et al., 2000). Different amounts of explosives and distance of the explosive to the meat surface were studied. It was found that HDP treatment at 20 cm distance, using 350 g of explosive produced 28.3%

reduction in WBS scores. Control aged samples were compared to HDP-treated and early deboned (non-HDP-treated) and it was found that control samples resulted in juicier, flavorful and more tender breasts.

Schilling et al. (2003) also compared the effect of HDP treatment, blade tenderization (BT), and a combination of both BT and HDP on bovine *longissimus lumborum* sample. These treatments were followed by aging for 7 and 14 days. WBS scores, total energy, thaw and cooking losses, and sensory evaluation indicated that aging time was more effective in reducing peak shear force values than the treatments. Sensory values, thaw and cooking losses were not affected significantly by the treatments.

Holzer et al. (2004) also utilized HDP treatments to negate the effects of koshering on meat. A significant problem resulting from salted/koshered meat is the loss of red lean color. Vacuum packaged koshered meat has been criticized for undergoing a rapid color change (red to brown) and developing an objectionable odor during refrigerated storage. The results of this study indicated that HDP treatment alone was more effective at reducing the surface micro-flora of the meat after 14 days of refrigerated storage than either salting or the combination of salting with HDP. Color stability was assessed by both a subjective panel and using a color meter. Both methods found a dramatic discoloration in the salted meat. This discoloration was significantly reduced when HDP was combined with the salting process. It appeared that HDP may diminish the undesirable discoloration resulting from salting/kosher processing of meat.

Solomon et al. (2008) studied tenderness improvement in fresh and frozen/thawed beef steaks, treated with HDP using a 100 g charge. A 29% reduction in shear force was observed for HDP-treated fresh samples. Freezing accounted for a further 14% reduction in shear force.

HDP-treatment followed by freezing resulted in a 30% reduction in shear force compared to the frozen control samples.

Bowker et al. (2007) evaluated the effects of HDP using a 100 g explosive charge and blade tenderization (BT) on collagen solubility and tenderness-related protein characteristics in top round steaks from Brahman cattle. It was found that HDP-treatment alone increased the amount of soluble collagen, when compared to controls, by 47.8% whereas a combination of blade tenderization and HDP (BTH) increased the amount of soluble collagen by 54.4%. Residual collagen was found to increase by 26.5% when using BTH, but no significant change was observed due to HDP-treatment alone. HDP and BTH treatments were also found to increase the content of a 100-110 kDa protein in myofibrillar protein fractions.

Bowker et al. (2008) further investigated the effects of aging at 0, 5, and 8 days of aging and HDP-treatment using a 100 g explosive charge, on myofibrillar proteins and tenderness of beef strip loins. Effects of HDP-treatment on MFI, protein solubility, and pH were studied, and MFI was found to be 25% higher in HDP-treated samples at day 0 when compared to controls, and protein solubility data also indicated significant effects due to HDP treatment. pH however did not indicate any significant effects due to HDP-treatment. Aging along with HDP-treatment was found to improve tenderness by 45% at day 8 of aging when compared to aging alone, which only improved tenderness by 29%. Overall, HDP-treatment was found to improve tenderness by 23% when compared to control samples. The authors inferred that even though protein solubility changes were not highly correlated to tenderness, increases in myofibrillar protein solubility after HDP-treatment indicated that the technology could have beneficial effects on protein functionality for further processed meat products.

Bowker et al. (2007) also established correlations between collagen and MFI and WBS tenderness at 0 and 7 days in their study on HDP-treatment on top round steaks. They reported that correlation between collagen and WBS tenderness at 0 and 7 days was not very high, and similarly low correlations were established between estimated parameters of myofibrillar protein- myofibrillar fragmentation index (MFI), protein solubility, and gel electrophoresis profile measurements, and WBS scores at 0 and 7 days. Correlation coefficient *r*-values between MFI and WBS scores were -0.57 and -0.62 at 0 and 7 days, respectively. The study by Bowker et al. (2008) on the effects of HDP-treatment on beef strip loins however established a better correlation between MFI and WBS scores with *r*-value of -0.75.

Since this study focuses on HDP treatment and its effect on texture in beef muscle, it is essential to understand the implication of textural attributes to the beef industry and various procedures utilized to detect and improve tenderness. This is discussed in detail.

TENDERNESS IN THE BEEF INDUSTRY

In the beef industry, tenderness is a quality attribute of beef that is widely accepted as important and a critical factor in a consumer's perception of beef quality (Koohmaraie et al., 1995). Tenderness also plays a major role in impacting the economic situation in the beef industry. It was estimated in 1995 that the beef industry had an annual loss of $217 million, due to lack of tenderness in beef cuts (Smith et al., 1995). These losses are mainly attributed to many tender and palatable carcasses being discounted in value because of insufficient marbling and yet sensory panel tests at the USDA Meat Animal Research Center at Clay Center, Nebraska indicate that marbling accounts for only 10% of the variation in beef rib eye tenderness (USDA,

1999). In 2004, researchers from Colorado State University determined that a 1% increase in beef tenderness would appreciate value of "select" cuts by 4.2% and a 10% improvement in tenderness would add $150-170 million to the industry (NCBA, 2009).

Considering the large amount of money involved in an important attribute, it is essential that sufficient research must be conducted in improving and measuring textural attributes, especially tenderness, in beef muscle.

Methods for improving tenderness

Financial implication of good textural attributes in beef have led commercial packers to utilize several methods to improve tenderness in beef, like aging, special packaging, avoiding animal stress prior to slaughter, and electrical stunning. Considerable amount of research has also been conducted on beef tenderness improvement. Packers generally employ nutritional methods, like incorporating vitamin D_3 in cattle feed (Karges et al., 2001) and genetic manipulation by biological engineering and selective breeding, are methods that have been researched to improve tenderness in beef. Plant derivatives, such as 'papain' from papaya, have been found to contain proteolytic enzymes that increase tenderness by 25-30% (Ashie et. al., 2002). Enzymes of the calpain system in the muscle, calpain I and calpain II, increase tenderness in beef by inducing proteolysis and have a natural inhibitor known as calpastatin. Injection of calcium chloride in the carcass (Whipple and Koohmaraie, 1992) and electrical stimulation (Ferguson et al., 2000) are also two methods that have been found to increase the activity of the calpain system enzymes.

Methods for measuring tenderness

Warner-Bratzler Shear Force Testing

The current industry accepted test for measuring tenderness is the Warner-Bratzler shear-force or WBS test. The shear-force test is a standardized procedure recommended by the American Meat Science Association (AMSA, 1995). The WBS test is assumed to simulate the chewing action of the teeth during the consumption of beef and eliminates the subjective grading assessment of a taste panel. Currently, a majority of the research institutions cook the meat to 71°C as required by the AMSA standard. The WBS test procedure outlined in the AMSA (1995) standard is as follows:

1. Determine sample size based on appropriate statistical analysis or consult statisticians.
2. Remove primals from the carcasses no sooner than 24 h post mortem.
3. Time post-mortem for processing into cuts and freezing should be 14 days, including time for aging.
4. Thickness of the beef steaks should be 2.54 cm.
5. Steaks should be vacuum packaged or packaged in material with low oxygen permeability, and frozen to a temperature no higher than -18°C.
6. Steaks should be evaluated within 6 months of frozen storage time.
7. Thaw steaks until the internal temperature is 2-5°C.
8. Insert iron/constantan or copper/constantan thermocouple wires with a diameter less than 0.05 cm and error limits less than 2°C.
9. Roast or broil the steaks, as per recommended procedure, until the internal temperature is 71°C.

10. Chill the cooked samples overnight at 2-5°C or cool the samples (if they are not chilled) until they attain a uniform temperature between 24-28°C, prior to coring.
11. Obtain at least 6 cores from the samples, either manually or by machine drill coring, parallel to the longitudinal orientation of the muscle fibers. Cores should be 1.27 cm in diameter.
12. Shear each core once in the center using a Universal Testing Machine, with a Warner-Bratzler shear head attachment. The crosshead speed of the machine should be 250 mm/min.

Tenderness Probes

The Armour Tenderometer (AT) was one of the first developed probe systems (Belk et al., 2000). The system utilized a group of probes that predicted tenderness as a measure of the force required to penetrate the ribeye muscle. Huffman (1974) reported an R^2 of 0.22 when the AT readings were correlated with WBS scores. No relationship was established between the AT readings and taste panel scores. Smith et al. (1984) reported a low correlation coefficient value of 0.10 ($P<0.05$) between the AT readings and taste panel scores. These studies concluded that the method was ineffective due to its inability to accurately predict tenderness.

The Meat Industry Research Institute of New Zealand (MIRINZ) developed a torsion-based tenderness probe. The instrument consists of two concentric sets of radially placed pins. The outer set of pins is static, while the inner set rotates. The meat is impaled on the pins, and the torque to the inner set of pins is generated by a synchronous motor. The torque and degree of rotation required to tear the meat are determined (Swatland, 1995). Jeremiah et al. (2000)

evaluated the performance of the MIRINZ probe and reported that the probe was a faster alternative to WBS testing. However, the correlation coefficients for the relationships between the probe values and WBS scores, a trained sensory panel, and consumer ratings ranged from *r*-values of -0.19 to -0.26.

The Tendertec Mark III Beef Grading Instrument is a probe system developed by the Australian Meat Research Corporation to measure the amount of connective tissue and other factors contributing to meat toughness (Belk et al., 2000). The probe was a hand-held, battery-powered tenderometer (Swatland, 1995). The meat surface resistance to penetration of the needle in the probe was plotted as a function of depth. Belk et al. (2001) evaluated the effectiveness of the Australian Tendertec probe and found significant correlation between the probe readings and other variables, i.e. WBS score, muscle fiber tenderness, overall tenderness, and amount of connective tissue. The variables; muscle fiber tenderness, overall tenderness, and amount of connective tissue were based on sensory panel scores. The probe, however, failed at sorting carcasses of young animals consistently, and the correlation coefficient declined for steaks as the degree of doneness increased. Higher correlation coefficient values were observed for steaks that were cooked to a rare or medium-rare degree of doneness. This study showed that the Tendertec probe had limited capacity to be used commercially.

The CT-probe or Connective Tissue probe is a prototype probe developed by the University of Guelph, Canada, supported by Ontario Cattlemen's Association and the Danish Meat Research Institute (Swatland et al., 1997). Functioning of the probe is based on ultra-violet fluorescence of the connective tissue. Most collagen types in meat have a peak excitation at 375 nm (Swatland, 1995). The CT-probe is hand-held, and has an optical window that penetrates the meat. This probe measures the whole band of the fluorescence emission spectrum against the

depth of penetration of the probe. Peaks in the spectrum are recorded whenever the probe penetrates a layer of connective tissue. Damage to the carcass due to penetration was found to be imperceptible. Swatland et al. (1998) evaluated the CT-probe for use in predicting taste and tenderness of broiled beef steaks. Samples were tested after aging periods of 3 days and 21 days. Probe readings were correlated with taste panel scores, with correlation coefficients ranging from 0.42 to 0.58.

Near-Infrared Spectroscopy

Near-infrared (NIR) spectroscopy has been demonstrated to be a promising method for assessing meat quality, because it offers a non-invasive, and usefully accurate approach to predicting tenderness. Hildrum et al. (1995) studied the use of NIR reflectance spectroscopy in the prediction of sensory hardness, tenderness, and juiciness of bovine *Longissimus dorsi* muscles. For these three sensory features, principal component regression analysis of NIR reflectance data and sensory panel scores yielded correlation coefficients of 0.74, 0.70, and 0.61, respectively.

Park et al. (1998) used NIR reflectance spectra from a sample set of 119 steaks to predict WBS tenderness scores. Absorption was higher for extremely tough steaks, than for tender steaks. A partial least-square (PLS) model was developed to predict meat tenderness and a multi-linear regression (MLR) model was developed for meat tenderness classification. The PLS model yielded an R^2 value of 0.67 for the training set, and 0.63 for the validation set. The MLR model correctly classified 89% of the samples as “tender” or “tough.”

Rodbotten et al. (2001) used NIR absorbance spectra to predict WBS scores. Two models were developed. The first model utilized the NIR spectra alone, and the second utilized NIR spectra in combination with information about post-slaughter treatments. Prediction models from NIR spectra alone gave correlation coefficients in the range of 0.52-0.83. When variables for post-slaughter treatments were included in the models, the correlation coefficients for predicting WBS scores were in the range of 0.71-0.85. Based on these prediction models, the beef samples were classified into two tenderness groups. When classified into two groups, 73-98% of the samples were correctly classified.

Video Image Analysis

Video image analysis also offers a non-invasive approach to meat grading. One of the earliest efforts to develop an objective method of grading beef carcasses was carried out by the National Aeronautics and Space Administration (NASA). In 1978, NASA conducted research to determine the application of its technology to beef grading. They concluded that ultrasound and image analysis were the best available methods for automated and objective beef grading (Biju, 1998). The 1994 National Beef Instrument Assessment Plan (NBIAP) Symposium identified VIA systems, among the systems evaluated, as most promising for improving consistency and quality of beef (Wyle et al., 1999).

A popular VIA system called, BeefCam®, developed by Colorado State University and Hunter Associates Laboratory (Reston, VA) is commercially utilized by graders for predicting tenderness in beef (Wyle et al., 1999). BeefCam® is a self-contained, portable, handheld video-imaging unit that utilizes an internal mirror to reflect the image onto a horizontally positioned

camera lens, while maintaining proper focal length. BeefCam® operates based on measurements of lean and fat color reflectance that are captured using VIA images containing up to 250,000 data points (pixels) per measurement (Belk, 1999). It can separate out different colors from irregularly shaped surfaces and be used to calculate relative areas that each color represents within the video image and utilizes the CIE L* a* b* color space, which is a perceptually uniform color space that simulates the functioning of the human eye (Hunterlab, 2009). Wyle et al. (1999) conducted two separate trials to predict tenderness and found that the BeefCam® was able to correctly classify as "tender" or "tough", 150 out of 156 carcasses in the first trial and 139 of 150 carcasses in the second trial. Further studies on BeefCam® by Vote et al. (2003) and Wyle et al. (2003) also indicated the effectiveness of the instrument in predicting tenderness of beef.

Early studies in VIA in predicting beef tenderness utilized color and marbling features. Belk (1999) reported that fat and lean color of beef muscle could indicate the ultra-structural status of the connective tissue. Fiems et al. (2000) used fat characteristics and lean color to predict tenderness in Belgian Blue bulls, using the Hunterlab Lab-Scan II. Lean color and fat characteristics both showed high correlation coefficient values, with respect to WBS scores, ranging from 0.70-0.85. In recent studies, image textural features have become more significant in the analysis of many types of images. Image textural features, such as pixel-value run length, pixel-value spatial dependence, gray-level cooccurrence matrix, wavelet textural features, etc. have been widely used in beef tenderness detection as is evident from studies by Li et al. (1999), Basset et al. (2000), Li et al. (2001), Jeyamkondan et al. (2001), Jackman et al. (2008), and Jackman et al. (2009). More recent studies are now focusing on using hyperspectral imaging.

Naganathan et al. (2008) utilized hyperspectral imaging in the visible/near-infrared to classify beef steaks into three categories of tenderness with 96.4% accuracy.

Miscellaneous Methods for Measuring Tenderness

Patel et al. (2006) utilized two sampling methods, high-performance liquid chromatography (HPLC) and capillary electrophoresis (CE), to examine changes in sarcoplasmic proteins during aging of beef and their relation to tenderness in *longissimus lumborum* muscle in beef. Water soluble proteins extracted from exudates from the meat via manual expression and using homogenization and centrifugation, were analyzed using HPLC and CE on days 2, 7, 10 and 14 postmortem. A pooled sample analysis for all aging periods indicated that manually expressed exudates from the meat samples explained 49% of variation in WBS scores compared to 25% of variation explained by the homogenized and centrifuged exudates using HPLC analysis. Eighty three percent of variation was explained using CE for the homogenized and centrifuged exudates and HPLC for the manually expressed exudates at day 2 post-mortem. Sixty percent of variability in WBS scores was explained using CE for homogenized and centrifuged exudates at day 7 post-mortem, and for days 10 and 14 post-mortem, the variability explained using either manually expressed or homogenized and centrifuged exudates was found to be <51%. Results from day 2 post-mortem indicated that both HPLC and CE analyses could be useful in sorting beef carcasses into tenderness groups.

A rapid artificial tactile sense technique, using a pressure sensor, was developed by Wang et al. (2009). Output voltage obtained from the pressure sensor for raw and cooked samples were compared to WBS scores and sensory evaluation. It was found that the *r*-values for correlation

between output voltage and WBS scores for raw and cooked samples were 0.95 and 0.90, respectively and those for the sensory panel scores for raw and cooked samples were 0.97 and 0.87, respectively. Further validation indicated 95% agreement with the established procedures, and a testing time period of 5 minutes indicated a good potential to replace WBS and sensory evaluation using the new technique.

Detecting tenderness in beef poses a major challenge since WBS testing is the only objective measure of tenderness in the beef industry. However, many issues exist with WBS testing. Wheeler et al. (1997) indicated differences in protocols between five different institutions with respect to preparation, cooking, type of instrument, and crosshead speed for WBS testing. One of the main reasons for the variation in procedures could be fact that consumers use different cooking methods based on consumer preference and as a result, tenderness of the cooked beef will vary based on the method and degree of doneness. In addition, WBS testing is destructive, labor and time intensive, and the procedure is not suited for on-line evaluation and correlation of WBS scores with sensory panel ratings have varied because the chewing process is a combination of compression, tension, and shear forces (Berry, 1983). Spadaro et al. (2002) reported that WBS correlations with measures of overall tenderness were very poor. Lu and Chen (1998) also reported that due to the structure of the WBS blade, the actual loading process during testing is difficult to interpret. These indicate that the approved standard of tenderness estimation using WBS testing may not be reliable after all.

Scientists have sought out methods of detecting tenderness that would be non-destructive, time and labor efficient, and compatible with online evaluation. Tenderness probes are rapid and less labor intensive than the WBS testing procedure, but many such probes like blunt-needle, blunt-blade, sharp-needle, sharp-blade, plumb bob, (Stephens et al., 2004) CT-probe, etc. exist

that utilize different principles, which creates issues with standardization. Detection of tenderness in the modern beef industry relies on rapidity and accuracy, and successful studies using VIA systems have indicated that this technology is best suited for utilization on a commercial scale. Although BeefCam® is a commercially utilized VIA system, it classifies beef based on tenderness using color and marbling features alone, whereas image textural features have been reported as better predictors of muscle texture since image texture features can represent muscle fiber characteristic such as size or arrangement, which can directly or indirectly correlate with tenderness (Li et al., 1999). However, since tenderness in beef is not a visual parameter, much study needs to be done in correlating image texture and sensory texture in beef muscle.

CONCLUSIONS

Textural tenderness of beef is an important attribute with significant financial ramifications on the beef industry, and is a complex characteristic to predict and quantify despite several studies being conducted to ascertain the chemistry behind tenderness and objectify detection methods.

With respect to improving textural tenderness in beef, non-thermal treatment methods like HDP offer a viable and microbiologically safe alternative to improving textural attributes in beef and other meat products. Studies on HDP treatment mentioned earlier in this chapter have indicated minimal to significant effects on tenderness due to treatment. It is essential to evaluate the efficacy of non-thermal treatment technology like HDP in improving tenderness, considering the financial implications of tenderness and good palatability attributes to the beef industry.

However, HDP-treatment conditions vary and include variables like method of wave generation, shape of charge, content of charge, distance of charge from the sample, orientation of sample, shape of vessel, intensity of electrical pulses, pulse frequency, etc.. This poses a significant amount of challenge for the experimenter as the large number of variables in the experiment can have any given outcome for a given set of conditions. In order to optimize the process, significant work needs to be done to better understand the effect of these variables on meat quality and texture. A thorough study on the efficacy of HDP-treatment on tenderness using modeling methods can address optimization issues and also eliminate the need for labor and time intensive procedures like WBS testing.

REFERENCES:

Alvarez, U.M., A.M. Loske, E. Castano-Tostado, and F.E. Prieto. 2004. Inactivation of *Escherichia coli* O157:H7, *Salmonella* Tymphimurium and *Listeria monocytogenes* by underwater shock waves. *Innov. Food Sci. & Emer. Tech.* 5, 459-463.

AMSA. 1995. Research guidelines for cookery, sensory evaluation, and instrumental tenderness of fresh meat. American Meat Science Association and National Livestock and Meat Board, Chicago, IL.

Aleman, G., E.Y. Ting, S. Mordre, A. Hawes, M. Walker, D. Farkas, and A. Torres. 1996. Pulsed ultra high pressure treatments for pasteurization of pineapple juice. *J. Food Sci.* 61(2), 388-390.

Ananth, V., J.S. Dickson, D.G. Olson, and E.A. Murano. 1998. Shelf life extension, safety, and quality of fresh pork loin treated with high hydrostatic pressure. *J. Food Prot.* 61(12):1649-1656.

Ardia, A., D. Knorr, G. Ferrari, and V. Heinz. 2003. Kinetic studies on combined high-pressure and temperature inactivation of *Alicyclobacillus acidoterrestris* spores in orange juice. *Appl. Biotech., Food Sci. & Policy* 1(3), 169-173.

Ashie, I.N.A., T.L. Sorensen, and P.M. Nielsen. 2001. Effects of papain and a microbial enzyme on meat proteins and beef tenderness. *J. Food Sci.* 67 (6). 2138-2142.

Basset, O., B. Buquet, S. Abouelkaram, P. Delachartre, and J. Culioli. 2000. Application of texture image analysis for the classification of bovine meat. *Food Chem.* 69, 437-445.

Belk, K.E.. 1999. Techniques to identify palatable beef carcasses: HunterLab BeefCam™. *Proceedings of the Range Beef Cow Symposium* XVI, Greely, CO.

Belk, K.E., J. A. Scanga, A. M. Wyle, and G. C. Smith. 2000. Prediction of beef palatability using instruments. Beef Improvement Federation Convention, Wichita, KS. Available at http://ansci.colostate.edu/files/meat_science/klb001.pdf. Accessed August 18, 2009.

Belk, K.E. M.H. George, J.D. Tatum, G.G. Hilton, R.K. Miller, M. Koohmaraie, J.O. Reagen, and G.C. Smith. 2001. Evaluation of the Tendertec beef grading instrument to predict the tenderness of steaks from beef carcasses. *J. Ani. Sci.* 79, 688-697.

Berlin, D.L., D.S. Herson, D.T. Hicks, and D.G. Hoover. 1999. Response of pathogenic *Vibrio* species to high hydrostatic pressure. *Appl. And Envtl. Micro*. 65(6). 2776-2780.

Berry, B.W.. 1983. Measurement of meat texture. *Reciprocal Meat Conference Proceedings* 36, 103-107.

Berry, B.W., A.M. Campbell, A.M. Spanier, and M.B. Solomon. 2004. Effect of koshering and hydrodynamic pressure on beef color, odor, and microbial loads. *J. Muscle Foods* 15: 69-82.

Biju, N. 1998. Beef quality grading with color video image analysis. MS Thesis, Oklahoma State University, Stillwater, OK.

Bouton, P.E., A.L. Ford, P.V. Harris, J.J. MacFarlane, and J.M. O'Shea. 1977. Pressure heat treatment of post-rigor muscle: effects on tenderness. *J. Food Sci.* 42. 132-135.

Bowker, B.C., M.N. Liu, M.B. Solomon, T.M. Fahrenholz, and J.S. Eastridge. 2007. Effects of hydrodynamic pressure processing and blade tenderization on intramuscular collagen and tenderness-related protein characteristics of top rounds from Brahman cattle. *J. Muscle Foods* 18, 35-55.

Bowker, B.C., T.M. Fahrenholz, E.W. Paroczay, J.S. Eastridge, and M.B. Solomon. 2008. Effect of hydrodynamic processing and aging on the tenderness and myofibrillar proteins of beef strip loins. *J. Muscle Foods* 19, 74-97.

Carlez, A., T. Veciana-Nogues and J.C. Cheftel. 1995. Changes in colour and myoglobin of minced beef meat due to high pressure processing, *Lebensm.-Wiss. u.-Technol* 28, 528–538.

Cheftel, J. C. and J. Culioli. 1997. Effects of high pressure on meat: a review. *Meat Sci*. 46, 211-236.

Claus, J.C., J.K. Schilling, N.G. Marriott, S.E. Duncan, M.B. Solomon, and H. Wang. 2000. Tenderization of chicken and turkey breasts with electrically produced hydrodynamic shockwaves. *J. Meat Sci.* (58). 283-286.

Delius, M., M. Jordan, H. Eizenhoefer, E. Marlinghaus, G. Heine, H.-G. Liebich, and W. Brendel. 1988. Biological effects of shock waves: Kidney haemorrhage by shcok waves in dogs-administration rate dependence. *Ultrasound in Med. & Biol.* 14(8), 689-694.

Delius, M., F. Ueberle, and W. Eisenmenger. 1998. Extracorporeal shock waves act by wave-gas bubble interaction. *Ultrasound in Med. & Biol.* 24(7), 1055-1059.

Elgasim, E.A. and W.H. Kennik. 1982. Effect of high pressure on meat microstructure. *Food Microstructure,* 1, 75-82.

Fiems L.O., S. De Campeneere, S. De Smet, G. Van de Voorde, J.M. Vanacker, and C. V. Boucqué. 2000. Relationship between the fat depots in carcasses of beef bulls and effect on meat colour and tenderness. *Meat Sci.* 56, 41-47.

Flick, G. 2003. High hydrostatic pressure processing has potential. Available at http://www.hpp.vt.edu/downloads/HPPPotential.pdf. Accessed August 1, 2009

Gamble, H.R., M.B. Solomon, and J.B. Long. 1998. Effects of hydrodynamic pressure on the viability of *Trichinella spiralis* in pork. *J. Food Prot.* 61. 637-639.

Garriga, M., N. Grebol, M.T. Ayemerich, J.M. Monfort, and M. Hugas. 2004. Microbial inactivation after high-pressure processing at 600 MPa in commercial meat products over its shelf life. *Innov. Food Sci. & Emer. Tech.* 5(4), 451-457.

Hildrum, K.I., T. Isaksson, T. Naes, B.N. Nilsen, M. Rodbotten, and P. Lea. 1995. Near infrared reflectance spectroscopy in the prediction of sensory properties of beef. *J. Near Infr. Spec.* 3, 81–87.

Holzer, Z., B.W. Berry, A.M. Williams Campbell, A. Spanier, and M.B. Solomon. 2004. Effect of koshering and hydrodynamic pressure on beef color, odor and microbial loads. *J. Muscle Foods*.(15). 69-82.

Homma, N., Y. Ikeuchi, and A. Suzuki. 1995. Levels of calpain and calpastatin in meat subjected to high pressure. *Meat Sci.,* 41, 251-260.

Huffman, D.L. 1974. An evaluation of the Tenderometer for measuring beef tenderness. *J. Ani. Sci.* 38, 287-294.

Hunterlab. 2009. Insight on color: CIE L*a*b* color scale. Available at http://www.hunterlab.com/appnotes/an07_96a.pdf. Accessed August 9, 2009.

Jackman, P., D.-W. Sun, C-J. Du, P. Allen, and G. Downey. 2008. Prediction of beef eating quality from colour, marbling, and wavelet texture features. *Meat Sci.* 80, 1273-1281.

Jackman, P. D.-W. Sun, and P. Allen. 2009. Comparison of various wavelet texture features to predict beef palatability. *Meat Sci.* 83, 82-87.

Jeremiah, L.E. and D.M. Phillips. 2000. Evaluation of a probe for predicting beef tenderness. *Meat Sci.* 55, 493-502.

Jeyamkondan, S., G.A. Kranzler, and A. Lakshmikanth. 2001. Predicting beef tenderness with computer vision. ASAE Paper # 013063 St. Joseph, MI.

Jung, S., M. De Lamballerie-Anton, and M. Ghoul. 1998. High pressure improvement of the meat ageing enzymes activity. In: ISAACS, N. S. (Ed.), High Pressure Food Science, Bioscience and Chemistry. Cambridge: The Royal Society of Chemistry, pp. 295-303.

Knoor, D. 1995. Advances in high-pressure food preservation methods. In R.K. Singh (Ed.), *Food process design and evaluation*, 159-174. Technomic Publishing Co., PA, USA.

Karges K., J. C. Brooks, D. R. Gill, J. E. Breazile, F. N. Owens and J. B. Morgan. 2001. Effects of supplemental vitamin D3 on feed intake, carcass characteristics, tenderness, and muscle properties of beef steers. *J. Ani. Sci.*79 (11), 2844-2850.

Kerfoot, W.W., A.Z. Beshai, and C.C. Carson. 1992. The effect of isolated high-energy shock wave treatments on subsequent bacterial growth. *Urol. Res.* 20. 183-186.

Kolsky, H. 1963. *Stress waves in solids*. Dover Publications, Inc., New York, NY.

Koohmaraie, M., T. L. Wheeler, and S. D. Shackelford. 1995. Beef tenderness: Regulation and prediction. Available at http://www.ars.usda.gov/SP2UserFiles/Place/54380530/19950004A1.pdf. Accessed April 10, 2009.

Krebbers, B., A.M. Matser, S.W. Hoogerwerf, R. Moezelaar, and M.M.M. Tomassen. 2003. Combined high-pressure and thermal treatments for processing of tomato puree: Evaluation of microbial inactivation and quality parameters. *Innov. Food Sci. & Emer. Tech.* 4**,** 377–385.

Lebail, A., L. Boillereaux, A. Davenel, M. Hayert, T. Lucas, , and J.Y. Monteau.2003. Phase transition in foods: effect of pressure and methods to assess or control phase transition. *Innov. Food Sci. & Emer.Tech*. 4. 15-24.

Li, J., J. Tan, F.A. Martz and H. Heymann.1999. Image texture features as indicators of beef tenderness. *Meat Sci.* 53, 17-22.

Li, J., J. Tan, and P. Shatadal. 2001. Classification of tough and tender beef by image texture analysis. *Meat Sci.* 57, 341-346.

Locker, R.H. and D.J.C. Wild. 1984. Tenderization of meat by pressure-heat involves weakening of the gap filament in the myofibril. *Meat Sci.* 10, 207-233.

Lorca, T.A., M.D. Pierson, J.R. Claus, J.D. Eifert, J.E. Marcy, and S.S. Sumner. 2002. Penetration of surface-inoculated bacteria as a result of hydrodynamic shock wave treatment of beef steaks. *J. Food Prot.* 65, 616-620.

Lorca, T.A., J.R. Claus, J.D. Eifert, J.E. Marcy, and S.S. Sumner. 2003. Penetration of surface-inoculated bacteria as a result of electrically generated hydrodynamic shock wave treatment of boneless skinless chicken breasts. *J. Poultry Sci.* 82, 1205-1210.

Loske, A.M., F.E. Prieto, M.L. Zavala, A.D. Santana, and E. Armenta. 1999. Repeated application of shock waves as a possible method for food preservation. *Shock Waves* 9, 49-55.

Loske, A.M.. 2001. Application of shockwaves in medicine. In G. Ben-Dor, G. Elperin, and O. Igra (Eds.) *Handbook of Shock Waves- 2nd Edition*. Academic Press, New York, NY, 415-440.

Loske, A.M., U.M. Alvarez, C. Hernandez-Galicia, E. Castano-Tostado, and F.E. Prieto. 2002. Bactericidal effect of underwater shock waves on *Escherichia coli* ATCC 10536 suspensions. *Innov. Food Sci. & Emer. Tech.* 3, 321-327.

Lu, R. and Y.R. Chen. 1998. Characterization of nonlinear elastic properties of beef products under large deformation. *Trans. ASAE* 41(1), 163-171.

MacFarlane, J.J. and D.J. Morton. 1978. Effects of pressure treatment on the ultrastructure of striated muscle. *Meat Sci.* 2. 281-288.

Macfarlane, J. J., I.J. Mckenzie, and R.H. Turner. 1980. Pressure treatment of meat: effects on thermal transitions and shear values. *Meat Sci.* 5, 307-317.

Meek, K.I., J.R. Claus, S.E. Duncan, N.G. Marriott, M.B. Solomon, S.J. Kathman, and M.E. Marini. 2000. Quality and sensory characteristics of selected post-rigor, early deboned broiler breast meat tenderized using hydrodynamic shock waves. *Poultry Sci.* 79, 126-136.

Moeller, S., D. Wulf, D. Meeker, M. Ndife, N. Sundararajan, and M.B. Solomon.1999. Impact of the hydrodyne process on tenderness, microbial load, and sensory characteristics of pork longissimus muscle. *J. Anim. Sci.* 77, 2119-2123.

Moerman, F., B. Mertens, L. Demey, and A. Huyghebaert. 2001. Reduction of *Bacillus subtilis*, *Bacillus stearothermophilus* and *Streptococcus faecalis* in meat batters by temperature-high hydrostatic pressure pasteurization. *Meat Sci.* 59(2), 115-125.

Moerman, F.. 2005. High hydrostatic pressure inactivation of vegetative microorganisms, aerobic and anaerobic spores in pork Marengo, a low acidic particulate food product. *Meat Sci.* 69(2), 225-232.

Montero, P., M.D. Fernandez-Diaz, and M.C. Gomez-Guillen. 2002. Characterization of gelatin gels induced by high pressure. *Food Hydrocoll.* 16, 197-2005.

Murano, E.A., P.S. Murano, R.E. Brennan, K. Shenoy, and R.G. Moreira. 1999. Application of high hydrostatic pressure to eliminate *Listeria monocytogenes* from fresh pork sausage. *J. Food Prot.* 62(5):480-483.

Naganathan, G.K., L.M. Grimes, J. Subbiah, C.R. Calkins, A. Samal, and G.E. Meyer. 2008. Visible/Near-infrared hyperspectral imaging for beef tenderness prediction. *Comp. & Elec. In Agr*. 64.225-233.

NCBA. 2009. Research shows one of the keys to tender beef. Available at http://www.beefusa.org/NEWSResearchShowsOneoftheKeystoTenderBeef3451.aspx. Accessed April 10, 2009.

Ohlsson, T. and N. Bengtsson. 2002. *Minimal processing technologies in the food industry*. Woodhead Publishing Inc., Cambridge, UK.

Otsuka, Y., N. Homma, K. Shiga, J. Ushiki, Y. Ikeuchi, and A. Suzuki. 1998. Purification and properties of rabbit muscle proteasome, and its effect on myofibrillar structure. *Meat Sci.* 49, 365-378.

Palou, E., A. Lopez-Malo, G.V. Barbosa-Canovas, and B.G. Swanson. 1999. High pressure treatment in food preservation. In S. Rahman (Ed.), *Handbook of food preservation- 1st Edition*, CRC Press, Boca Raton, FL, 533-576.

Park, B., Y.R. Chen, W.R. Hruschka, S.D. Shackelford , and M. Koohmaraie. 1998. Near-Infrared reflectance analysis for predicting beef longissimus tenderness. *J. Ani. Sci.* 76, 2115-2120.

Patel, J.R., A. Williams-Campbell, M.N. Liu, and M.B. Solomon. 2005. Effect of hydrodynamic pressure processing on inactivation of *Escherichia coli* O157:h7 in blade tenderized beef steaks. *J. Muscle Foods* 16, 342-353.

Patel, J.R., A.A. Bhagwat, G.C. Sanglay, and M.B. Solomon. 2006. Rapid detection of *Salmonella* from hydrodynamic pressure-treated poultry using molecular beacon real-time PCR. *Food Microbiol.* 23, 39-46.

Patel, J.R., M.B. Solomon, T. Fahrenholz, and E. Paroczay. 2006. Sorting for beef tenderness using high performance liquid chromatography and capillary electrophoresis: A research note. *Meat Sci.* 72, 574-580.

Patel, J.R., G.C. Sanglay, M. Sharma, and M.B. Solomon. 2007. Combining antimicrobials and hydrodynamic pressure processing for control of *Listeria monocytogenes* in frankfurters. *J. Muscle Foods* 18, 1-18.

Podolak, R., M.B. Solomon, J.R. Patel, and M.N. Liu. 2006. Effect of hydrodynamic pressure processing on the survival of *Escherichia coli* O157:H7 in ground beef. *Innov. Food Sci. & Emer.Tech.* 7, 28-31.

Rademacher, B., F. Werner, and M. Pehl. 2001. Effect of thepressurizing ramp on the inactivation of *Listeria innocua* considering thermofluidynamical processes. *Innov. Food Sci. & Emer.Tech.* 3. 19-24.

Ramaswamy, R., V.M. Balasubramaniam, and G. Kaletun. 2009. High pressure processing: Fact sheet for food processors. Available at http://ohioline.osu.edu/fse-fact/0001.html. Accessed August 1, 2009.

Rodbotten, R., B.-H. Mevik, and K.I. Hildrum. 2001. Prediction and classification of tenderness in beef from non-invasive diode-array detected NIR spectra. *J. Near Infr. Spec.* 9, 199–210.

Savell, J., R. Miller, T. Wheeler, M. Koohmaraie, S. Shackelford, B. Morgan, C. Calkins, M. Miller, M. Dikeman, F. McKeith, G. Dolezal, B. Henning, J. Busboom, R. West, F. Parrish, and S.Williams. 1994. Standardized Warner-Bratzler shear force procedures for genetic evaluation. Available at http://savell-j.tamu.edu/shearstand.html. Accessed on August 15, 2009.

Schilling, M.W., N.G. Marriott, H. Wang, and M.B. Solomon. 2003. Characteristics of USDA utility cow beef subjected to blade tenderization and hydrodynamic shock waves. *J. Muscle Foods* 14, 131-142.

Sharma, M., A.E.H. Shearer, D.G. Hoover, M.N. Liu, M.B. Solomon, and K.E. Kniel. 2008. Comparison of hydrostatic and hydrodynamic pressure to inactivate foodborne viruses. *Innov. Food Sci. & Emer.Tech.* 9, 418-422.

Smith, J.C., J.W. Savell, H.G. Dolezal, T.G. Field, D.R. Gill, D.B. Griffin, D.S. Hale, J.B. Morgan, S.N. Northcutt and J.D. Tatum. 1995. National Beef Quality Audit-1995. Conducted by Colorado State University, Texas A&M University, and Oklahoma State University for National Beef Cattlemen's Association: 270.

Smith, G.C. Z. L. Carpenter, H.R. Cross, G.E. Murphey, H.C. Abraham, J.W. Savell, G.W. Davis, B.W. Berry and F.C. Parrish, Jr. 1984. Relationship of USDA marbling groups to palatability of cooked beef. *J. .Food Qual.*7, 289-308.

Solomon, M.B. J.B. Long, and J.S. Eastridge. 1997a. The hydrodyne: A new process to improve beef tenderness. *J. Ani. Sci.* 75, 1534-1537.

Solomon, M.B., J.B. Long, and J.S. Eastridge. 1997b. The hydrodyne process for tenderizing cold-shortened beef . *Inst. Food Tecnol.* 21-9.

Solomon, M.B., J.S. Eastridge, H. Zuckerman, J.B. Long, and W.L. Johnson. 1997c. Hydrodyne treated beef: tenderness and meat ultrastructure. *Proc. 43rd Intl. Cong. Meat Sci. Technol*., 121-124.

Solomon, M.B.. 1998. The hydrodyne process for tenderizing meat. *Reciprocal Meat Conference Proceedings* 51, 171-176, Kansas City, MO.

Solomon, M.B., M.N. Liu, J.R. Patel, E. Paroczay, J.S. Eastridge, and S.W. Coleman. 2008. Tenderness improvement in fresh or frozen/thawed beef steaks treated with hydrodynamic pressure processing. *J. Muscle Foods* 19, 98-109.

Spadaro, V., Allen, D.H., Keeton, J.T., Moreira, R., and Boleman, R.M.. 2002. Biomechanical properties of meat and their correlation to tenderness. *J. Texture Studies* 33, 59-87.

Stephens, J.W., J.A. Unruh, M.E. Dikeman, M.C. Hunt, T.E. Lawrence, and T.M. Loughlin. 2004. Mechanical probes can predict tenderness of cooked beef longissimus using uncooked measurements. *J. Ani. Sci.* 82, 2077-2086.

Suzuki, A., N. Suzuki, Y. Ikeuchi, and M. Saito. 1991. Effects of high pressure treatment on the ultrastructure and solubilization of isolated myofibrils. *Agrl. & Biol. Chem.*, 55, 2467-2473.

Swatland, H.J. 1995. *On-line evaluation of meat*. Technomic Publishing Company Incorporated, Lancaster, PA.

Swatland, H.J., J.C. Brooks, and M.F. Miller. 1998. Possibilities for predicting taste and tenderness of broiled beef steaks using an optical-electromechanical probe. *Meat Sci.* 50 (1), 1-12.

Swatland, H.J. and C.J. Findlay. 1997. On-line probe prediction of beef toughness, correlating sensory evaluation with fluorescence detection of connective tissue and dynamic analysis of overall toughness. *Food Qual. & Pref.* 8(3), 233-239.

Tuboly, E., V.K. Lebovics, O. Gaal, L. Meszaros, and J. Farkas. 2003. Microbiological and lipid oxidation studies on mechanically deboned turkey meat treated by high hydrostatic pressure. *J. Food. Eng.* 56. 241-244.

USDA. 1999. Predicting Tenderness in Beefsteaks. Agricultural Research Magazine. Available at http://www.ars.usda.gov/is/AR/archive/nov99/beef1199.htm. Accessed April 10, 2009.

Vote, D.J., K.E. Belk, J.D. Tatum, J.A. Scanga, and G.C. Smith. 2003. Online prediction of beef tenderness using a computer vision system equipped with a BeefCam module. *J. Ani. Sci.* 81, 457-465.

Wang, X.-D., Y.-H. Sun, Y. Wang, T.-J. Hu, M.-H. Chen, and B. He. 2009. Artificial tactile sense technique for predicting beef tenderness based on FS pressure sensor. *J. Bionic Engg.* 6, 196-201.

Welti-Chanes, J., A. Lopez-Malo, E. Palou, D. Bermudez, J.A. Guerrero-Beltran, and G.V. Barbosa-Canovas. 2005. Fundamentals and applications of high pressure processing of foods. In G.V. Barbosa-Canovas, M.S. Tapia, and M.S. Cano (Eds.). *Novel food processing technologies*, 157-182. Marcel Dekker/CRC Press, Boca Raton, FL.

Whipple, G., and M. Koohmaraie. 1992. Freezing and calcium chloride marination effects on beef tenderness and calpastatin activity. *J. Ani. Sci.*. 70: 3081-3085.

Wheeler, T.L., S.D. Shackelford, L.P. Johnson, M.F. Miller, R.K. Miller and M. Koohmaraie. 1997. A comparison of Warner-Bratzler shear force assessment within and among institutions. *J. Ani. Sci.* 75, 2423-2432.

Williams-Campbell, A.M., and M.B. Solomon. 2001. New non-thermal postharvest technology to improve food safety: hydrodynamic pressure processing. *Proc. Of SPIE* 4206, 167-173.

Williams-Campbell, A.M., and M.B. Solomon. 2002. Reduction of spoilage microorganisms in fresh beef using hydrodynamic pressure processing. *J. Food Prot.* 65(3), 571-574.

Wyle, A.M., R.C. Cannell, K.E. Belk, M. Goldberg, R. Riffle, and G.C. Smith. 1999. An evaluation of the prototype portable HunterLab video imaging system (BeefCam) as a tool to predict tenderness of beef carcasses using objective measures of lean and fat color. *1999 Beef Program Report*. Department of Animal Sciences, Colorado State University.

Wyle, A.M., D.J. Vote, D.L. Roeber, R.C. Cannell, K.E. Belk, J.A. Scanga, M. Goldberg, J.D. Tatum, and G.C. Smith. 2003. Effectiveness of the SmartMV prototype BeefCam System to sort beef carcasses into expected palatability groups. *J. Ani. Sci.* 81, 441-448.

Yuste, J., M. Capellas, D.Y.C. Yung, and M. Mor-Mur. 2004. Inactivation and sublethal injury of foodborne pathogens by high pressure processing: Evaluation with conventional media and thin agar layer method. *Food Res. Intl.* 37. 861-866.

Zook, C. D., M.E. Parish, R.J. Braddock, and M.O. Balaban. 1999. High pressure inactivation kinetics of *Saccharomyces cerevisiae* ascospores in orange and apple juice. *J Food Sci.* 64(3).533-535

Zuckerman, H., and M.B. Solomon. 1998. Ultrastructural changes in bovine longissimus muscle caused by the hydrodyne process. *J. Muscle Foods* 9, 419-426.

CHAPTER 3

NON-DESTRUCTIVE EVALUATION OF TEXTURE IN HIGH HYDRODYNAMIC PRESSURE-TREATED BEEF LOINS USING MACHINE VISION AND ULTRASOUND TECHNIQUES

ABSTRACT: High hydrodynamic pressure treatment (HDP) is a novel non-thermal treatment method employing underwater shockwaves that combines microbial inactivation along with tenderization of muscle foods. Twenty four beef loins were chosen for this study, out of which six were control samples and the remaining eighteen were subjected to HDP treatment. Treatment variables used were amount of charge (50, 75, and 100g), container size (121 L and 98 L), and locations of samples (North, South, and middle) during treatment. Treated and control samples were subjected to non-destructive evaluation using ultrasound velocity and Fourier-Transform and Haar Wavelet features. The effects of treatment variables and the efficacy of the non-destructive methods were analyzed using Warner-Bratzler shear (WBS) scores and texture profile analysis (TPA) features. Ultrasound velocity correlated very poorly with the WBS scores and TPA features, whereas the imaging features correlated better with Pearson's correlation *r*-values of -0.38 with WBS scores, -0.36 with hardness, -0.52 with cohesiveness, -0.57 with springiness, -0.46 with chewiness, and -0.37 with resilience. A 75 g amount of explosive charge showed the highest average reduction of WBS scores (15.29%) and TPA hardness (28.26%) and chewiness (23.41%) respectively, and increase in springiness (2.82%) from the control samples. Container size of 98 L showed higher average reduction of WBS scores (12.01%) and increase in springiness (2.97%) whereas the 121 L container showed higher reductions of TPA hardness (28%) and chewiness by (25.45%). Samples placed in the North location indicated highest

reduction of WBS scores (21.91%) whereas those placed in the South location indicated highest reduction of TPA hardness (31.02%) and chewiness (25%), and increase in springiness (4.43%). Canonical discriminant analysis and Multivariate ANOVA results indicated that the effects of container size and location of samples were more significant between the treatment effects and control samples.

INTRODUCTION

Texture in beef, especially tenderness, is a critical factor in consumer perception of beef quality (Koohmaraie et al., 1995). Consumers have ranked beef tenderness as the most important characteristic for palatability, along with juiciness and flavor. This is corroborated by surveys conducted by the National Cattleman's Beef Association (NCBA), in order to assess tenderness in retail cuts and to provide a benchmark for beef tenderness in the United States (Beef Research, 2009). Currently, the only objective measure of beef tenderness is the Warner-Bratzler shear-force (WBS) test, which is a destructive method, hence requiring the need for a non-destructive and objective system to predict tenderness.

Video image analysis (VIA) and ultrasound methods offer a non-invasive approach to analyzing texture in muscle foods. One of the earliest efforts to develop an objective method of grading beef carcasses was carried out by the National Aeronautics and Space Administration (NASA). In 1978, NASA conducted research to determine the application of its technology to beef grading. They concluded that ultrasound and image analysis were the best available methods for automated and objective beef grading (Biju, 1998). In VIA, image texture is an important feature in the analysis of many types of images (Livens et al., 1997). Image texture refers to intrinsic properties of an image having irregular surface features. These intrinsic properties include irregularity, non-directionality, and structural complexity and also contain important information about the structural arrangement of the surfaces and their relationship to the surrounding environment (Haralick et. al., 1973). VIA has been widely used in beef tenderness detection as is evident from studies by Wyle et al. (1999), Basset et al. (2000), Jeyamkondan et al. (2001), Li et al. (2001), Jackman et al. (2008), and using hyperspectral analysis in the infrared and near-infrared regions by Naganathan et al. (2008).

Ultrasound and ultrasound imaging has been widely used in textural analysis of foods. Ultrasound imaging has been used using VIA methods to predict beef tenderness Low frequency ultrasonic measurements, like velocity and attenuation have been utilized successfully for textural measurements in cooked carrots (Nielsen and Martens, 1997), meat-based products (Llull et al., 2002), chilling injury in tomatoes (Verlinden, 2004), using attributes such as transmission loss, peak frequencies, peak force and total energy in evaluating sensory crispness in fried chicken nuggets (Antonova et al., 2003), and using energy absorbance determining mealiness in apples (Bechar et al., 2005). These studies indicate the viability of ultrasound and imaging techniques as non-destructive evaluation of texture in foods.

The objective of this study is to:

- Establish a correlation between image texture and ultrasound features with objective methods of texture analysis of beef, namely Warner-Bratzler shear force (WBS) scores and texture profile analysis (TPA) features.
- Evaluate the effect of the following HDP treatment variables on WBS and TPA features
    - Amount of charge
    - Size of container
    - Location of sample during treatment

MATERIALS AND METHODS

HDP Testing Procedure

Beef loins were acquired from the USDA-ARS Environmental Microbial and Food Safety Laboratory in Beltsville, MD. Six sets (identified by labels- AC1, AC3, AC4, AC6, BBE, FM3) of four beef loin samples each, totaling twenty four beef loins of 5.08 cm thickness each, were used for the experiment. Each set of four had one control sample (total 6), which was not subjected to HDP-treatment. The remaining three samples from each set (total 18) were subjected to HDP-treatment. First, the samples undergoing treatment were split into two sets each to be treated in disposable 98 L (AC3, AC6, and FM3) and 121 L (AC1, AC4, and BBE) Rubbermaid® containers. Since the height of the charge below the water line was constant, the distance of the charge from the product was varied in the two containers. In every batch of nine samples, three samples each were treated with rectangular-shaped explosive charges of 50g, 75g, and 100g quantities.

A metal plate was placed at the bottom of the container and then filled with water at a temperature of 5-10°C. The low temperature of water was maintained to prevent microbial contamination. Samples were packaged in puncture and abrasion resistant, Boneguard bags to prevent rupture during explosion, and placed on the metal plate. The function of the metal plate is to reflect the incident shock wave from the explosion, onto the sample, thereby maximizing the effect of the treatment.

During packaging in the Boneguard bags, each sample was kept at a specified location (North, South, and Middle) to add another variable. Samples AC1 and AC3 were placed facing North, AC4 and AC6 facing South, and BBE and FM3 placed in the middle, during all 3 charge

treatments. These procedures were carried out at the USDA-ARS facility in Beltsville, MD. The set-up of the procedure is described by figure 3.1. All samples were removed from their Boneguard bags after treatment, and loin was cut into two 2.54 cm thick slices to obtain two replicates, one each for WBS and TPA testing and non-destructive analysis using ultrasound and image analysis.

Image Acquisition

Image analysis of each loin was done using a Sony® XC-75 monochrome CCD camera under fluorescent lighting conditions. Prior to imaging, the loins were removed from their vacuum packages and allowed to bloom for 30 minutes to ensure uniformity in reflection. The bloomed samples were then placed on a black matted surface to reduce glare during acquisition and a height of the camera lens over the surface of the loin was 23.1 cm and a F-stop between 5.6 to 8 was chosen to allow proper contrast (fig. 3.2). Close-up images, detailing more textural features of the lean tissue and minimizing imaging of intramuscular fat or marbling, were taken instead of the whole loin (fig. 3.3). Images were acquired using ImagePro 4.1 software (Media Cybernetics, Inc., Bethesda, MD) at 640 x 480 pixel resolution for analysis using Matlab 7.0 (The Mathworks Inc., Natick, MA).

Fourier-Transform features and wavelet-texture (WT) features were extracted from the images of the beef loins. Maximum magnitude, average magnitude, energy, and variance were the Fourier features extracted for analysis. A two-dimensional wavelet decomposition using Haar wavelets was performed on each image. The 2-D decomposition occurs as a result of filtering by the product of two one- dimensional (1-D) wavelet transforms. Wavelet decomposition of a 2-D

image can be obtained by performing the filtering operations consecutively in the horizontal and vertical directions (Livens et al., 1997). Rows of the input image are passed through the low- and high- pass filter bank, followed by sub-sampling by a factor of 2. Columns of the resulting images from the filter bank are filtered further by low- and high-pass filters. This sequence of filtering is followed by sub-sampling by a factor of 2. The entire process represents a single level of decomposition. Each level of decomposition yields four sub-images, namely; approximation, horizontal, vertical, and diagonal. For the analysis, 5 levels of decomposition was performed (fig. 3.5) and the following features from each level of decomposition were extracted from the subimages- Energy, variance, kurtosis, skewness, and edge density. Due to the large amount of data acquired from the image features, a stepwise regression procedure was performed to reduce the set of features for ease of further analysis. Skewness features at every level of decomposition, except those extracted from the approximation image at the 5^{th} level of decomposition, were taken out of the analysis due to very small values generated during texture feature extraction.

Ultrasound Acquisition

Ultrasound analysis was performed on loins using Ultran W-series standard miniature contact transducers (The Ultran Group, State College, PA). Transducers were set to analyze in through-transmission mode, to prevent attenuation of waves in the samples due to the high water content in the sample. Three different transducers of 250 kHz, 500 kHz, and 1 MHz were utilized. On each sample, three points were chosen for measurement- at the extremities and at the middle of the loin. Thickness of the sample at these chosen points was measured using calipers.

Sonotech® Clear Image (Sonotech Inc., Bellingham, WA) ultrasound scanning gel was used as couplant.

Transducer pairs were mounted on a spring loaded unit specifically built for ultrasound acquisition. An Ultran BP-9400A signal transducer was used to generate acoustic pulses, which were received by an Ultran BR-640A broadband receiver (The Ultran Group, State College, PA) (fig. 3.4). Received pulses were sent to a 100 MHz Tektronix® oscilloscope, model 2232 with a GPIB interface (Tektronix Inc., Richardson, TX), connected to a computer which was used to acquire the signals.

Ultrasound time of flight through the sample was calculated using a fast Fourier transform method using a reference signal (without any medium in between transducers) and the signal acquired for the samples (fig. 3.6). The calculated time of flight was converted to velocity by dividing it by the sample thickness (l) using the following equation (Antonova et al., 2003)

$$v_{sample} = \frac{l}{(TOF - TOF_0)} \quad (1)$$

where, v_{sample} = Ultrasound velocity through the beef sample (m/s)

l = Path length of transmission (m)

TOF = Time of flight with the sample (m/s)

TOF_0 = Time of flight without the sample (m/s)

Warner-Bratzler Testing and Texture Profile Analysis

After imaging and ultrasound acquisition, the steaks were cooked according to American Meat Science Association (AMSA) guidelines to 71°C or medium doneness (AMSA, 1995). Cooked samples were chilled in a refrigerator to enable ease of coring. Samples were refrigerated during the course of testing. WBS testing and TPA (50% compression) were carried out on a Texture Analyzer TA-XT2 (Texture Technologies Corp., Scarsdale, NY) at Virginia Tech. A 50% compression level was chosen because an initial test on some samples resulted in the inability of them to recover from the initial compression when 75% compression was used. Claus (1995) mentioned that any level between 25%-75% was considered appropriate for meats and hence 50% was chosen.

WBS testing involved 6-8 cores per samples whereas 3 cores per sample (20 mm diameter and 15 mm height) were chosen for TPA testing. Crosshead speed for the WBS procedure was 200 mm/min as per AMSA guidelines and for the TPA a test speed of 1 mm/s was used. Hardness, chewiness, resilience, springiness, and cohesiveness were the TPA features evaluated in this study.

Statistical Analysis

Statistical analysis of correlation between WBS scores and TPA features and image texture features and ultrasound velocity was conducted. A canonical discriminant model was used for evaluating the effects of charge amount, container size, and location of samples during treatment on ultrasound velocity, image texture features and on WBS scores and TPA features were carried out using canonical discriminant analysis. This method utilizes a dimension

reduction and classification technique using canonical variables which are a linear combination of the variables in the experiment (Naganathan et al., 2008). This was followed by multivariate analysis of variance (MANOVA) which determined the significance of separation of the samples based on the treatment variables. Efficacy of the treatment variables were also analyzed using percent change in values between control and treated samples. All statistical analyses were conducted at a significance level of $\alpha = 0.05$ on SAS 9.1 (SAS Institute Inc., Cary, NC).

RESULTS AND DISCUSSION

Correlation between Non-Destructive Analysis and WBS scores and TPA features

Velocity of ultrasound acquired using all three transducers were used in the correlation model along with the image features. Stepwise regression procedure yielded thirteen image texture features which were used in the correlation model. The features that were used were

- Variance feature from Fourier transform (VarFT)
- WT Kurtosis features from the horizontal decomposition images at the 1st, 2nd, 3rd, and 5th levels and from the vertical decomposition image at the 1st level (KH1, KH2, KH3,KH5, and KV1)
- WT Energy features from horizontal decomposition images at the 1st and 3rd levels and from the vertical decomposition image at the 3rd level (EH1, EH3, and EV3)
- Wavelet edge density feature from the diagonal decomposition image at the 5th level (WED5)
- WT Variance features from the horizontal decomposition image at the 4th level and vertical decomposition image at the 1st level (VarH4 and VarV1)

- WT Skewness feature from the approximation decomposition image at the 5^{th} level (SkA5)

Ultrasound velocity correlated very poorly with the WBS scores and TPA features (Table 3.1). For ultrasound velocity, highest correlation (*r* at $\alpha = 0.05$) of -0.26 was observed between resilience and ultrasound velocity (250 kHz). Imaging features showed relatively better values (Table 3.2) of correlation coefficient with the WBS scores and TPA features. WBS scores showed the highest correlation value with WED5 (-0.40), hardness with EH1 (-0.36), cohesiveness with EH3 (-0.52), EH1 (-0.51), and VarH4 (-0.43), springiness with EH1 (-0.57), EH3 (-0.52), VarV1 (-0.50), and VarH4 (-0.44), chewiness with EH1 (-0.46), and resilience with KH3 (-0.40). Due to the low R-values for the ultrasound velocity, only the imaging features were considered for fitting in a regression model. The imaging features chosen in the regression model were those that showed the highest correlation values.

Table 3.3 indicates the R^2 values ($\alpha = 0.05$) of the regression fit between the imaging features and WBS and TPA features. Imaging features best explained the variations in cohesiveness and springiness R^2 values of 44% and 45% respectively, with the imaging features EH3 and VarH4 contributing most to the model. Imaging features could only explain 9% of variation in hardness, which was the poorest predicted feature.

Effect of HDP treatment variables on WBS scores and TPA features

Effects of charge amount (50, 75, and 100 g), container size (98 L and 121 L), and location of sample (North, South, and middle) during the treatment, on WBS scores and TPA features were analyzed based on percentage change in values during treatment when compared to

the values extracted during control (table 3.4). Eight out of the eighteen treated samples showed an improvement (reduction) of 10% or greater for the WBS scores after treatment, with five samples showing an increase in WBS scores post treatment, with 32.89% being the highest reduction in value. Hardness and chewiness were the features that showed the most samples with reduction post-treatment with fourteen and thirteen samples, respectively exhibiting improvement of 10% or greater. The highest values of reduction for hardness and chewiness were 46.95% and 44.96%, respectively. Springiness was found to increase in twelve samples, with a maximum increase of 12.42%. Cohesiveness and resilience both predominantly showed an increase in value post-treatment.

Effects of Charge Amount

Average percentage reduction (table 3.5) in WBS scores, hardness and chewiness and percentage increase in springiness was observed to be higher when using the 75 g charge. Using the 50 g charge indicated the least average percentage change in the WBS scores and TPA values. This indicated that the 75 g charge was very effective than the other two charge amounts in improving the palatability characteristics of the treated loins. The MANOVA analysis however indicated no significant difference between the charge amounts, using the four statistical tests in the analysis.

Effects of Container Size

Using different containers for the treatments indicated a significant difference in the WBS scores and TPA features as was indicated by the MANOVA analysis (table 3.6). The 121 L container indicated higher values of average percent reduction in chewiness and hardness, whereas the 98 L one performed better in reducing WBS scores and increasing springiness of the samples (table 3.5).

Effects of Sample Location During Treatment

Placement of the samples during treatment also showed significant differences in the WBS and TPA features by MANOVA analysis (table 3.6). Samples placed towards North had the most effect in reducing WBS scores, whereas the ones placed towards South had the most effect in reducing hardness and chewiness and improving the springiness of the samples. The only marked effect of the samples placed in the middle was in reducing the cohesiveness.

The canonical discriminant procedure utilized in this study was used for ultrasound velocity, image texture features, and WBS and TPA scores to classify the loins based on the treatment variables, viz. charge amount, locations of samples during treatment, and container size. Canonical discriminant analysis using ultrasound velocity and image texture features did not significantly classify the loins based on the treatment variables, with all four MANOVA tests indicating P>F values much greater than 0.05 because a strong correlation could not be established between the non-destructive analysis and the destructive analysis using WBS scores and TPA features. The issue with the ultrasound velocity characteristics could be attributed to factors such as attenuation, which resulted in different velocities from the same sample.

Ultrasound readings were taken from a 2.54 cm or 1” thick sample, which could have resulted in interference due to intramuscular fat or connective tissue that could have attributed to this discrepancy. Though a better correlation was established using the image texture features, when compared to the ultrasound velocity, the highest value was only -0.57 between springiness and EH1.

In this study, Haar wavelets were chosen for decomposition when conducting image analysis. Haar wavelets are the simplest of all wavelets, but also have the advantage of being easy to compute. Previous studies correlating image texture features derived from wavelet decomposition and meat texture and tenderness have reported varying degrees of success. Li et al. (2001) achieved an 83.3% success rate classifying the beef samples into categories of “tender” and “tough” using image features, like pixel-value run length and primitive fraction on wavelet-decomposed images. Studies by Du and Sun (2006) on cooked pork ham and Zheng et al. (2006) on cooked beef joints indicated that wavelet features combined with Gabor features were better predictors of tenderness when compared to spatial-based image texture features. Jackman et al. (2008 and 2009) also reported good predictions of beef eating quality using wavelet texture features. This study did not indicate good predictions of WBS scores and TPA features with wavelet and Fourier texture features primarily due to the values of WBS scores and TPA features in certain samples that did not follow a pattern of either increasing or decreasing post HDP-treatment. From table 3.4 it can be inferred that there were a minimum of two samples for each textural feature that can be considered as outliers. The lack of good correlation can also be attributed to conditions during image acquisition. The use of direct lighting during image acquisition due to the unavailability of a proper diffused lighting chamber, the presence of intramuscular fat in the acquired images, and the utilization of monochrome images that limited

extraction of textural features in red, green and blue (RGB) or the CIE L*a*b* color spaces, could have contributed to the lack of a good correlation. Therefore good image acquisition conditions and studies using other wavelets for extracting image texture features could possibly result in better correlation between the non-destructive features and WBS scores and TPA features.

The HDP-treatment process indicated reduction in values of WBS scores and TPA hardness, chewiness, and increase in springiness. The effect of treatment was very significant due to the size of the containers and locations of the samples during treatment. The amount of explosive charge, however, did not have a significant effect on the treatment. From figure 3.7 of the canonical plot for effects due to charge amount, it can be inferred that neither canonical variable was able to clearly discriminate the effects due to charge, whereas from figures 3.8 and 3.9 for the sample location and container size effects, it can be inferred that the first canonical variable was able to separate the effects of treatment variables between each other, despite the presence of a few outliers and that the controls were not clearly discriminated from the treated samples.

Reduction in WBS scores was much lower than the maximum of 72% reduction by a 100g explosive charge reported by Solomon et al. (1997). The results could have differed because the study by Solomon et al. (1997) was done in a larger container capacity of 208 L, which according to the current study has a significant effect on the WBS scores and TPA features. In addition, the shape of charge used by Solomon et al. (1997) is unknown, which also could have had an influence on the results. Solomon (1998) reported a summary on HDP-treatment studies conducted with different meats- beef, lamb, and pork, using different amounts of charge and container sizes. Solomon (1998) reported from studies on HDP-treatment on beef

longissimus muscle in 208 L containers using 50, 75, and 100 g charges that the 100 g charge had better values of reduction of WBS scores than 50 or 75 g charges and was utilized more often in HDP studies (Bowker et al., 2007, Bowker et al., 2008, Solomon et al., 2008). In this study it was found that the 75 g charge treatment performed better than the other two charge amounts (table 3.5), whereas according to Solomon (1998) the 50 g charge performed better than the 75 g charge in reducing WBS scores. This indicates that charge amounts did not seem to have a linear relationship with reduction in WBS scores, if all other treatment conditions were assumed to be constant and could indicate that the effects due to container size and location of shot are more significant on the outcome of the process than the amount of charge. In addition Solomon (1998) also reported no significant differences between the charge amounts in reducing WBS scores after treatment which was corroborated in this study using canonical discriminant analysis and MANOVA tests.

Among the TPA features, besides reduction in hardness and chewiness, and increase in springiness, cohesiveness and resilience also indicated an increase in value after HDP-treatment. In contrast, Schilling et al. (2002) reported no change in TPA springiness, chewiness, and cohesiveness at 50% compression and hardness at 75% compression in frankfurters made from *Biceps femoris* muscle in beef. Similarly, Callahan et al. (2005) reported no significant differences in hardness, cohesiveness, chewiness, and gumminess between HDP-treated and control hams and springiness was found to reduce post-treatment. This discrepancy could be attributed to the difference in behavior of frankfurters and hams undergoing HDP-treatment versus beef loins, which could have a different mechanical response to the treatment.

In a study done by Caine et al. (2003), negative correlation between palatability characteristics (juiciness, flavor desirability, flavor intensity, overall tenderness, and overall

palatability) and TPA hardness, chewiness, and cohesiveness and a positive correlation to springiness indicates that in this study, post treated samples had better palatability characteristics than the controls. Very little literature has been reported with respect to the effects of HDP-treatment on TPA features in beef loins and considering the study by Caine et al. (2003), more studies need to be done on the effects of HDP-treatment on TPA features in order to have better predictors of good beef palatability than WBS scores alone.

CONCLUSIONS

In this study a small-strain change in beef loins by the HDP treatment process was evaluated using large-strain evaluation methods like, WBS shear and TPA, which did not correlate very well with non-destructive analysis using ultrasound velocity and image texture features. In engineering applications, small-strain measurements are invalid once strains exceed certain limits that can result in unrealistic stress values and nonlinear elasticity must be considered using hyperelastic strain energy potential that can simulate these large-strain changes better (Bonet and Burton, 1998). However previous studies done in textural evaluation of HDP-treated muscle foods have involved evaluation using large strain measurements in cooked muscle, with WBS scores being the predominant means of testing. In addition, large strain measurements like, WBS and TPA measurements are performed on cooked samples and studies on the effects of heat treatment on muscle texture have reported increase in firmness (Martens et al., 1982) and reduction in hardness (Bertola et al., 1994) which could be attributed to denaturation of myofibrillar proteins, shrinkage in sarcomere length, and decrease in fiber diameter with increasing temperature (Palka and Daun, 1999, Wattanachant et al., 2005). These

destructive large-strain procedures are also labor intensive and time consuming which requires a need for estimating the small-strain changes occurring in the samples during HDP-treatment. Future studies must focus on mathematical models simulating the effects of HDP-treatment variables on behavior of meats and establish good correlation between numerically estimated parameters of small-strain behavior and large-strain WBS scores and TPA features in order to eliminate the need for destructive testing.

REFERENCES:

AMSA. 1995. Research guidelines for cookery, sensory evaluation, and instrumental tenderness of fresh meat. American Meat Science Association and National Livestock and Meat Board, Chicago, IL.

Antonova, I., P. Mallikarjunan, and S.E. Duncan. 2003. Correlating objective measurements of crispness in breaded fried chicken nuggets with sensory crispness. *J. Food Sci.* 68(4), 1308-1315.

Basset, O., F. Dupont, A. Hernandez, C. Odet, S. Abouelkaram, and J. Culioli. 1999. Texture image analysis: Application to the classification of bovine muscles from meat slice images. *Optical Engineering* 38(11). 1950-1959.

Bechar, A., A. Mizrach, P. Barreiro, and S. Landahl. 2005. Determination of mealiness in apples using ultrasonic measurements. *Biosys. Engg.* 95(3), 329-334.

Bertola, N.C., A.E. Bevilacqua, and N.E. Zaritzky. 1994. Heat treatment effect on textural changes and thermal denaturation of proteins in beef muscle. *J. Food Process. & Preserv.* 18, 31-46.

Biju, N. 1998. Beef quality grading with color video image analysis. MS Thesis, Oklahoma State University, Stillwater, OK.

Bonet, J. and A.J. Burton. 1998. A simple orthotropic, transversely isotropic hyperelastic constitutive equation for large-strain computations. *Comp. Methods Appl. Mech. Engg.* 162, 151-164.

Bowker, B., M. Liu, M.B. Solomon, J. Eastridge, T. Fahrenholz, and B. Vineyard. 2007. Effects of hydrodynamic pressure processing and blade tenderization on intramuscular collagen and tenderness-related protein characteristics of top rounds from Brahman cattle. *J. Muscle Foods* 18, 35-55.

Bowker, B., T. Fahrenholz, E. Paroczay, J. Eastridge, and M. B. Solomon. 2008. Effect of hydrodynamic pressure processing and aging on the tenderness and myofibrillar proteins of beef strip loins. *J. Muscle Foods* 19, 74-97.

Caine, W.R., J.L. Aalhus, D.R. Best, M.E.R. Dugan, and L.E. Jeremiah. 2003. Relationship of texture profile analysis and Warner-Bratzler shear force with sensory characteristics of beef rib steaks. *Meat Sci.* 64, 333-339.

Callahan, J., M. Liu, and M.B. Solomon. 2005. Effect of hydrodynamic pressure treatment before processing on pork ham quality. *Proceedings of the 51st International Congress of Meat Science and Technology*, August 7-12, 2005, Baltimore, Maryland. Paper No. T61.

Claus, J.R. 1995. Methods for the objective measurement of meat product texture. *Reciprocal Meat Conference Proceedings*, 48. 96-101.

Du, C.-J. and D.-W. Sun. 2006. Correlating image texture features by five different methods with the tenderness of cooked pork ham: A feasibility study. *Trans. ASABE* 49(2), 441-448.

Haralick, R.M., K. Shanmugam, and I. Dinstein. 1973. Textural features for image classification. *IEEE Trans. Sys. Man, & Cybernetics* SMC-3(6), 610-621.

Jackman, P., D.-W. Sun, C-J. Du, P. Allen, and G. Downey. 2008. Prediction of beef eating quality from colour, marbling, and wavelet texture features. *Meat Sci.* 80, 1273-1281.

Jackman, P., D.-W. Sun, and P. Allen. 2009. Comparison of various wavelet texture features to predict beef palatability. *Meat Sci.* 83, 82-87.

Koohmaraie, M., T. L. Wheeler, and S. D. Shackelford. 1995.Beef tenderness: Regulation and prediction. Available at http://www.ars.usda.gov/SP2UserFiles/Place/54380530/19950004A1 .pdf. Accessed April 10, 2009.

Li, J., J. Tan, and P. Shatadal. 2001. Classification of tough and tender beef by image texture analysis. *Meat Sci.* 57, 341-346.

Livens, S., P. Scheunders, G. Van de Wouver, and D. Van Dyck. 1997. Wavelets for texture analysis: An overview. 6th Int. Conf. on image processing and its applications, 581-585. Dublin, Ireland.

Llull, P., S. Simal, J. Benedito, and C. Rossello. 2002. Evaluation of textural properties of a meat-based product (sobrassada) using ultrasonic techniques. *J. Food Engg*. 53 (3), 279-285.

Martens, H., E. Stabursvik, and M. Martens. 1982. Texture and colour changes in meat during cooking related to thermal denaturation of muscle proteins. *J. Text. Studies* 13, 291-309.

Naganathan, G.K., L.M. Grimes, J. Subbiah, C.R. Calkins, A. Samal, and G.E. Meyer. 2008. Visible/Near-infrared hyperspectral imaging for beef tenderness prediction. *Comp. & Elec. In Agr*. 64.225-233.

Nielsen, M. and H.J. Martens. 1997. Low frequency ultrasonics for texture measurements in cooked carrots (*Daucus carota L.*). J. Food Sci. 62(6), 1167-1175.

Palka, K. and H. Daun. 1999. Changes in texture, cooking losses, and myofibrillar structure of bovine *M. semitendinosus* during heating. *Meat Sci.* 51, 237-243.

Schilling, M.W., J.R. Claus, N.G. Mariott, M.B. Solomon, W.N. Eigel, and H. Wang. 2002. No effect of hydrodynamic shock wave on protein functionality of beef muscle. *J. Food Sci.* 67(1), 335-340.

Solomon, M.B., J.B. Long, and J.S. Eastridge. 1997. The Hydrodyne: A new process to improve beef tenderness. *J. Ani. Sci.* 74, 1534-1537.

Solomon, M.B.. 1998. The hydrodyne process for tenderizing meat. *Reciprocal Meat Conference Proceedings* 51, 171-176.

Solomon, M.B., M. Liu, J. Patel, E. Paroczay, J. Eastridge, and S. Coleman. 2008. Tenderness improvement in fresh or frozen-thawed beef steaks treated with hydrodynamic pressure processing. *J. Muscle Foods* 19, 98-109.

Verlinden, B.E., V.D. Smedt, and B.M. Nicolai. 2003. Evaluation of ultrasonic wave propagation to measure chilling injury in tomatoes. *Postharv. Biol. & Tech.* 32, 109–113.

Wattanachant, S., S. Benjakul, and D.A. Ledward. 2005. Effect of heat treatment on changes in texture, structure, and properties of Thai indigenous chicken muscle. *Food Chem.* 93, 337-348.

Wyle, A.M., R.C. Cannell, K.E. Belk, M. Goldberg, R. Riffle, and G.C. Smith. 1999. An evaluation of the prototype portable HunterLab video imaging system (BeefCam) as a tool to predict tenderness of beef carcasses using objective measures of lean and fat color. *1999 Beef Program Report*. Department of Animal Sciences, Colorado State University.

Zheng, C. D.-W. Sun, and L. Zheng. 2006. Classification of tenderness of large cooked beef joints using wavelet and Gabor textural features. *Trans. ASABE* 49(5), 1447-1454.

LIST OF FIGURES

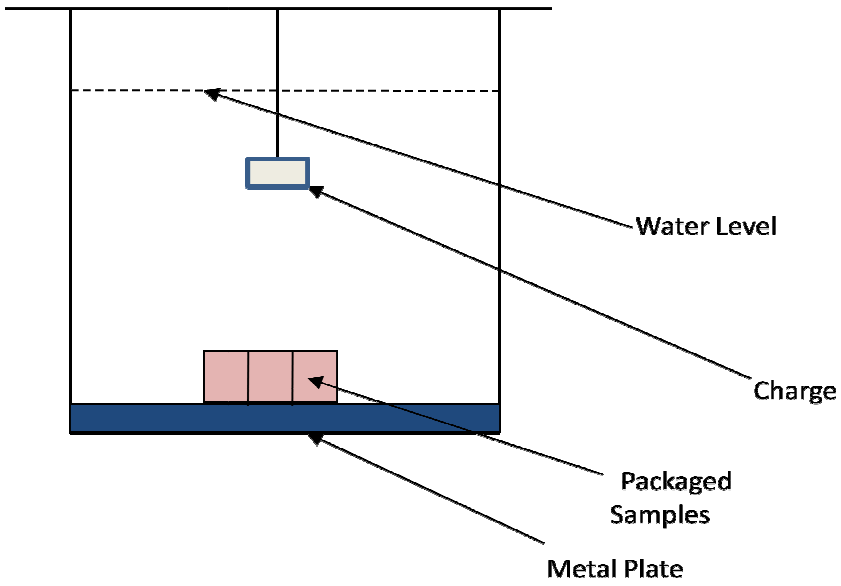

Figure 3.1: Set-up of the performed HDP procedure

Figure 3.2: Image acquisition of beef loins

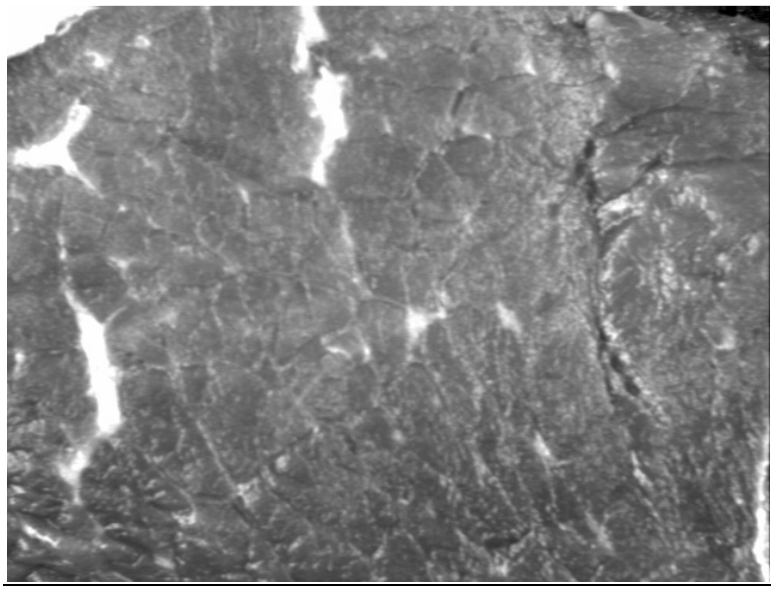

Figure 3.3: Close-up gray-scale image of beef loin

Figure 3.4: Acquisition of ultrasound data

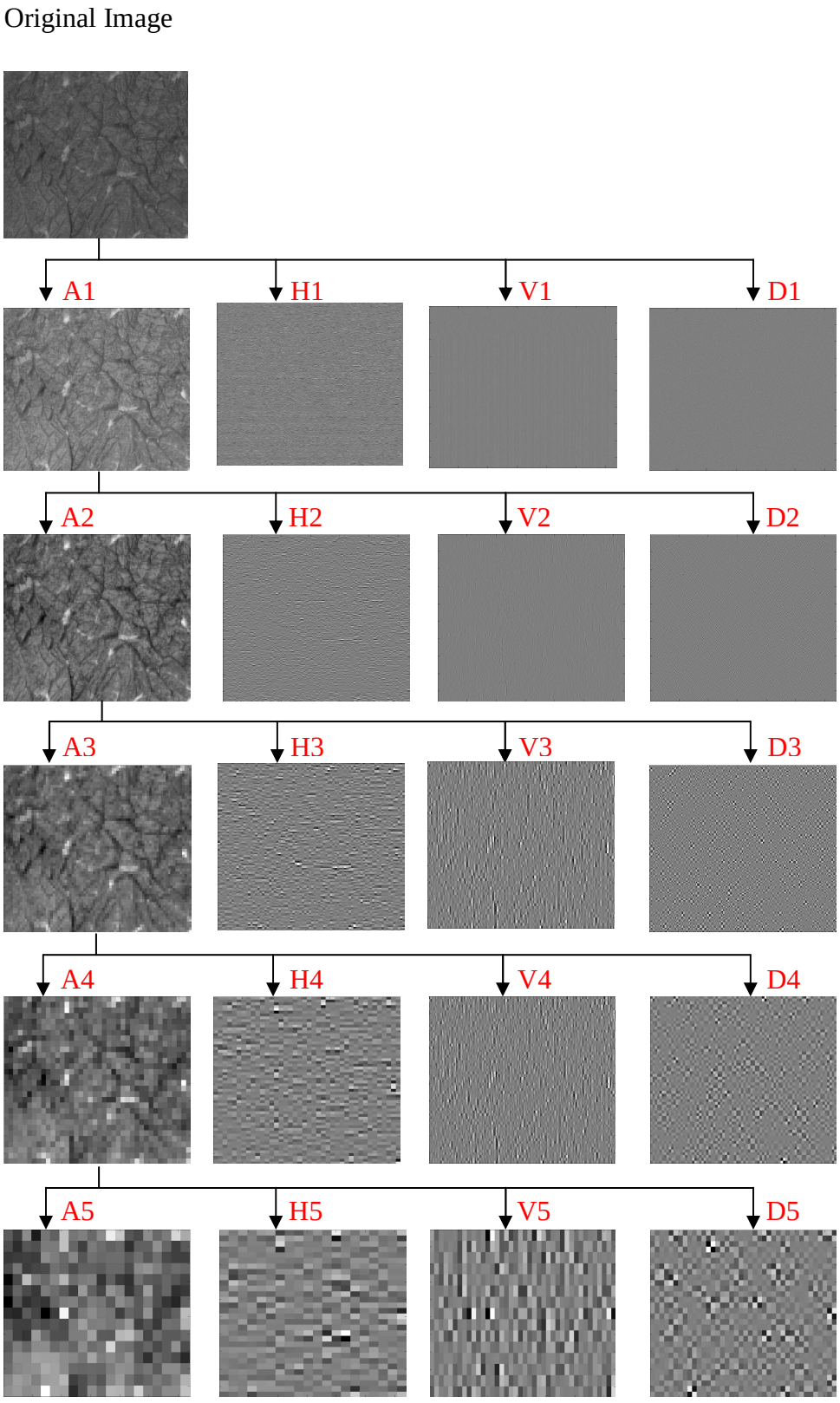

Figure 3.5: Five-level wavelet decomposition using Haar wavelets. A- approximation details; H- horizontal details; V- vertical details; D- diagonal details, from levels 1 to 5

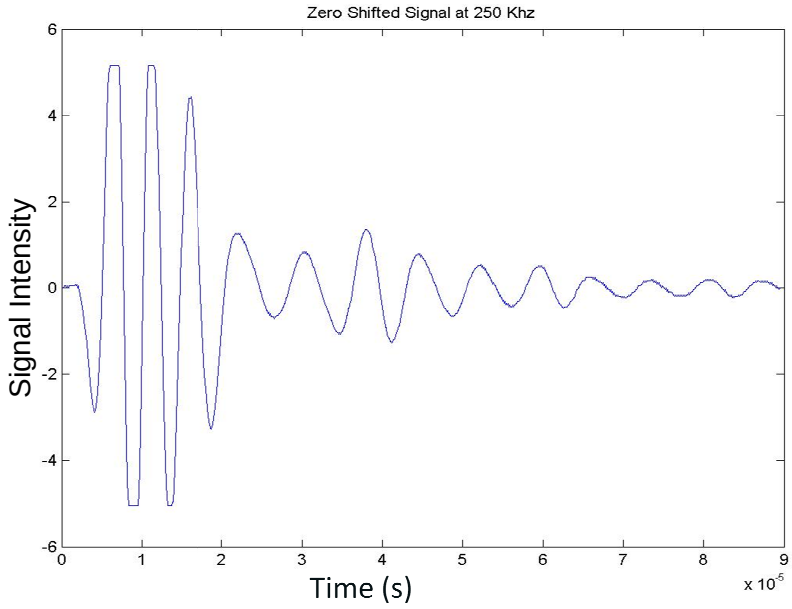

Figure 3.6: Ultrasound signal at 250 kHz

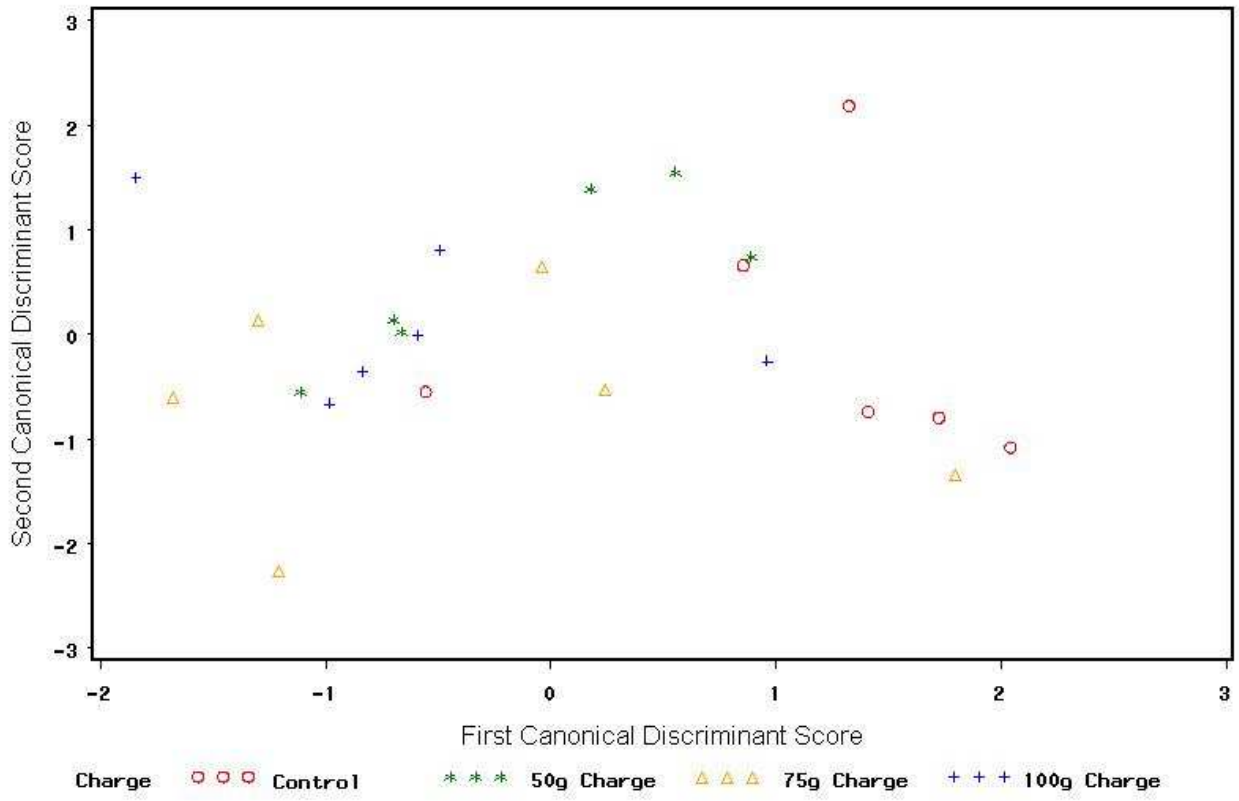

Figure 3.7: Distribution of samples in the canonical space based on charge amounts used in HDP-treatment using WBS and TPA scores as variables

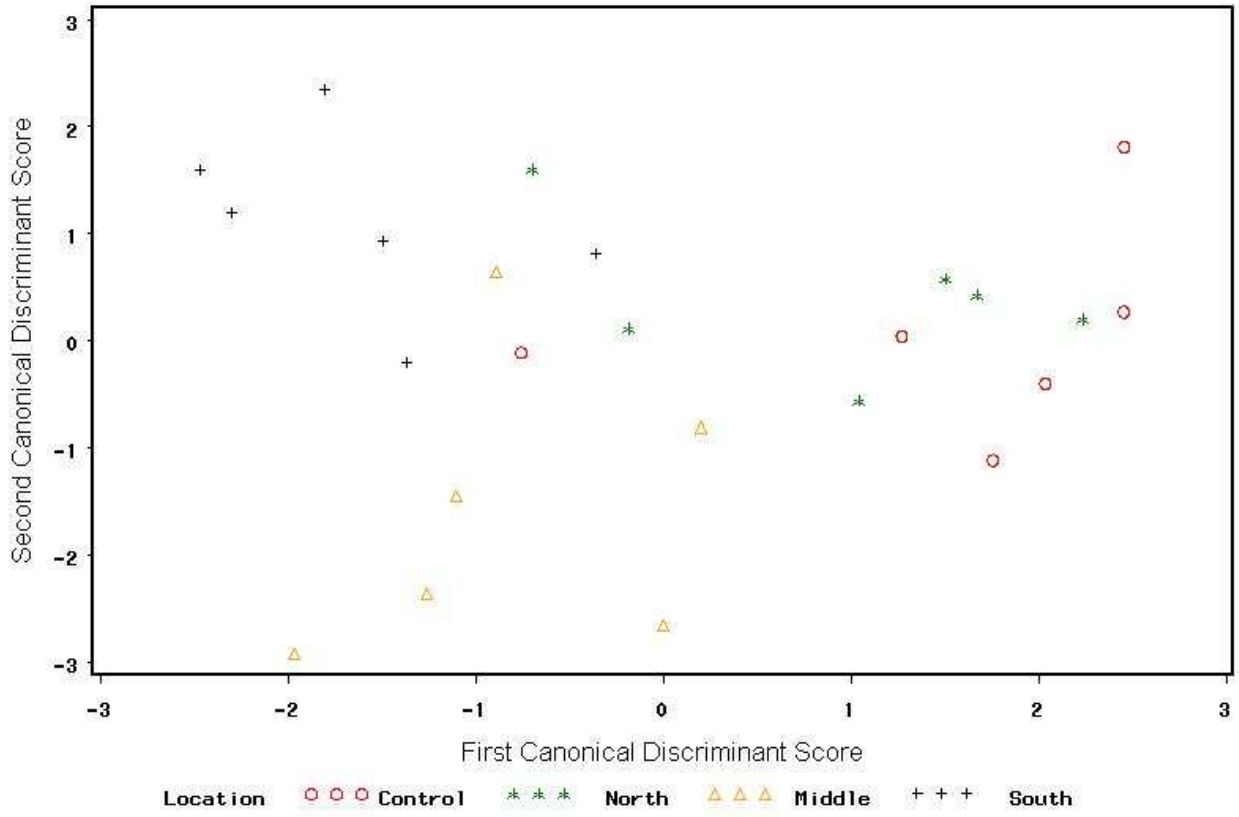

Figure 3.8: Distribution of samples in the canonical space based on sample location during HDP-treatment using WBS and TPA scores as variables

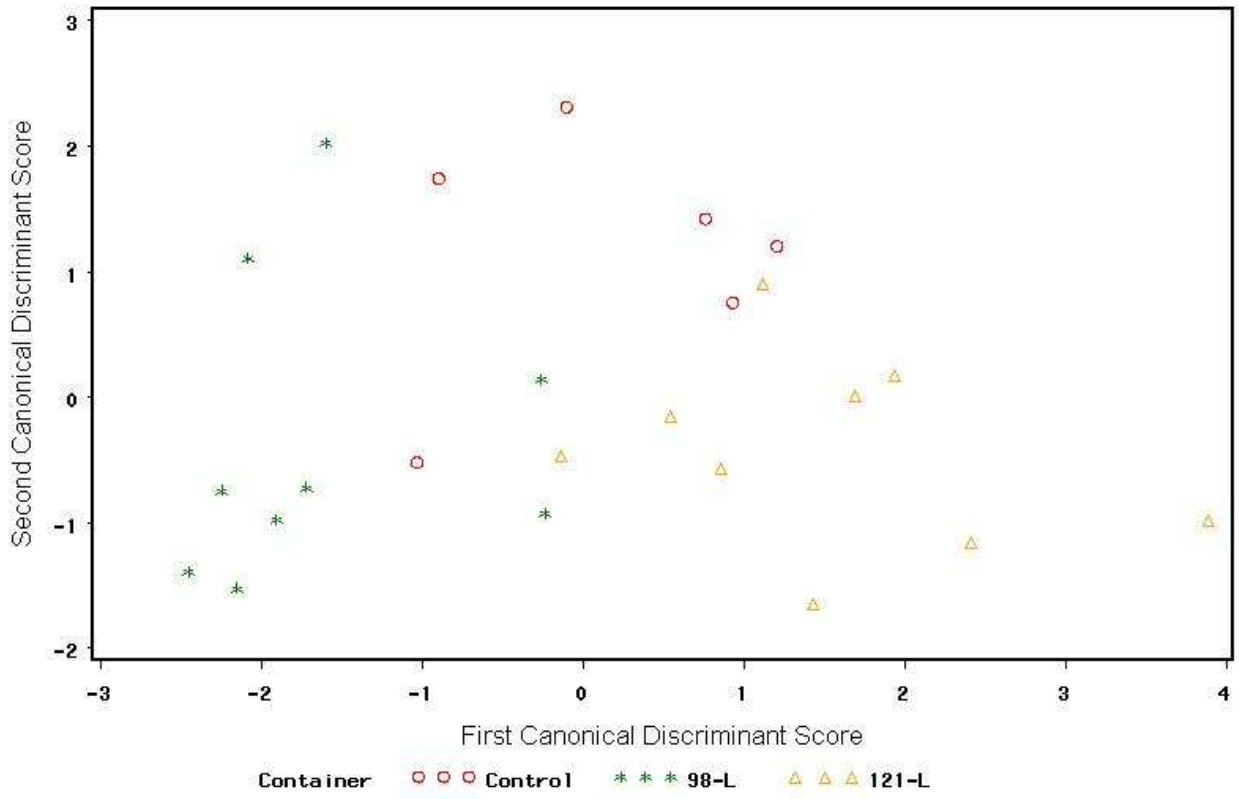

Figure 3.9: Distribution of samples in the canonical space based on container size used in HDP-treatment using WBS and TPA scores as variables

LIST OF TABLES

Table 3.1: Correlation coefficients and P- values (in parenthesis) for WBS and TPA features with ultrasound velocity (α =0.05)

	Velocity (250 kHz) m/s	*Velocity (500 kHz) m/s*	*Velocity (1000 kHz) m/s*
WBS (kg-f)	-0.00 (0.999)	-0.0812 (0.704)	0.21 (0.326)
Hardness (kg-f)	0.24 (0.256)	0.03 (0.879)	0.29 (0.168)
Cohesiveness	0.18 (0.410)	0.06 (0.780)	-0.23 (0.283)
Springiness	0.22 (0.293)	0.07 (0.759)	-0.16 (0.471)
Chewiness	0.25 (0.239)	0.07 (0.732)	0.24 (0.250)
Resilience	-0.26 (0.220)	0.06 (0.769)	-0.20 (0.337)

Table 3.3: R^2 values for regression fit of WBS and TPA features with imaging features (α = 0.05)

	R^2 *values*
WBS (kg-f)	0.15
Hardness (kg-f)	0.09
Cohesiveness	0.44
Springiness	0.45
Chewiness	0.18
Resilience	0.15

Table 3.2: Correlation coefficients and P-values (in parenthesis) for WBS and TPA features with imaging features ($\alpha = 0.05$)

	VarFT[a]	*EH3*[b]	*EH1*[b]	*EV3*[c]	*WED5*[d]	*VarH4*[e]	*VarV1*[e]	*SkA5*[f]	*KH5*[g]	*KH3*[g]	*KH2*[g]	*KH1*[g]	*KV1*[h]
WBS (kg-f)	-0.34 (0.095)	-0.25 (0.230)	-0.38 (0.0635)	-0.32 (0.121)	-0.40 (0.056)	-0.25 (0.234)	-0.35 (0.095)	0.22 (0.294)	0.04 (0.868)	0.20 (0.342)	-0.01 (0.962)	-0.15 (0.483)	0.08 (0.722)
Hardness (kg-f)	-0.21 (0.332)	-0.27 (0.198)	-0.36 (0.082)	-0.23 (0.284)	-0.35 (0.093)	-0.29 (0.174)	-0.26 (0.213)	0.18 (0.401)	-0.00 (0.992)	0.31 (0.136)	0.24 (0.266)	0.12 (0.575)	0.11 (0.605)
Cohesiveness	-0.26 (0.210)	-0.52 (0.009)	-0.51 (0.010)	-0.27 (0.194)	-0.34 (0.107)	-0.43 (0.034)	-0.41 (0.050)	0.04 (0.841)	0.22 (0.299)	-0.19 (0.380)	-0.06 (0.788)	-0.14 (0.501)	-0.10 (0.624)
Springiness	-0.23 (0.271)	-0.52 (0.010)	-0.57 (0.004)	-0.35 (0.098)	-0.32 (0.121)	-0.44 (0.033)	-0.50 (0.013)	0.03 (0.894)	0.15 (0.473)	-0.12 (0.583)	0.03 (0.882)	-0.07 (0.736)	-0.04 (0.869)
Chewiness	-0.25 (0.247)	-0.33 (0.116)	-0.46 (0.025)	-0.25 (0.233)	-0.3 (0.106)	-0.33 (0.117)	-0.37 (0.072)	0.12 (0.584)	-0.03 (0.872)	0.22 (0.292)	0.22 (0.305)	0.09 (0.662)	0.04 (0.852)
Resilience	0.01 (0.970)	0.04 (0.861)	0.09 (0.662)	0.07 (0.735)	0.19 (0.377)	0.03 (0.904)	0.05 (0.799)	-0.20 (0.342)	0.14 (0.520)	-0.40 (0.051)	-0.37 (0.076)	-0.32 (0.125)	-0.28 (0.188)

[a] Variance of Fourier-Tranform
[b] Wavelet energy from horizontal images at levels 3 and 1
[c] Wavelet energy from vertical images at levels 3 and 1
[d] Wavelet edge density from diagonal image at level 5
[e] Variance from horizontal and vertical images at levels 4 and 1
[f] Skewness from approximation image at level 5
[g] Kurtosis from horizontal image at levels 5, 3, 2, and 1
[h] Kurtosis from horizontal image at level 1

Table 3.4: Percentage reduction (+ve values) or increase (-ve values) in values of WBS scores and TPA features in treated samples when compared to controls

Sample ID	*Charge Amount (g)*	*Container Size (L)*	*Location*	*% WBS (kg-f)*	*% Hardness (kg-f)*	*% Cohesivenesss*	*% Chewiness*	*% Springiness*	*% Resilience*
AC1	50	121	North	7.84	15.04	-1.84	16.08	0.60	-5.60
	75	121	North	32.89	40.45	-0.21	44.96	3.19	-17.13
	100	121	North	7.67	30.81	0.42	31.33	1.46	-7.60
BBE	50	121	Middle	6.51	18.85	12.51	25.64	10.12	-7.66
	75	121	Middle	-2.57	2.23	-4.52	-11.72	-6.63	-0.84
	100	121	Middle	29.35	46.95	-10.29	34.52	-7.84	-21.69
AC4	50	121	South	-25.00	45.30	-1.35	44.76	-0.23	-16.01
	75	121	South	11.09	38.26	-2.33	35.28	-2.94	-10.19
	100	121	South	2.20	14.12	-5.01	8.23	-4.10	-1.44
AC3	50	98	North	24.09	-0.85	-10.35	-24.35	-12.42	-9.03
	75	98	North	30.44	31.27	-5.25	24.09	-5.05	-13.11
	100	98	North	28.51	-5.99	-4.05	-16.71	-6.11	2.88
FM3	50	98	Middle	4.90	-19.00	-0.67	-22.49	-3.43	8.53
	75	98	Middle	22.09	26.52	-3.52	26.60	1.45	-8.15
	100	98	Middle	-8.80	17.90	17.93	27.53	18.16	-0.79
AC6	50	98	South	14.33	27.12	-5.66	17.98	-5.68	-7.71
	75	98	South	-0.59	30.85	-5.81	21.26	-6.94	-5.05
	100	98	South	-6.89	30.48	-5.83	22.49	-6.70	-10.97

n = 24 total samples, 18 HDP-treated and 6 controls.

Table 3.5: Average percentage change in WBS scores and TPA features with changing HDP-treatment variables (+ve values = reduction, -ve values = increase)

HDP Treatment Variable	*Average % change in WBS*	*Average % change in Hardness*	*Average % change in Cohesiveness*	*Average % change in Chewiness*	*Average % change in Springiness*	*Average % change in Resilience*
50 g	5.44	14.41	-1.23	9.60	-1.84	-6.25
75 g	15.56	28.26	-3.61	23.41	-2.82	-9.08
100 g	8.68	22.38	-1.14	17.90	-0.85	-6.60
121 L	7.77	28.00	-1.40	25.45	-0.71	-9.80
98 L	12.01	15.37	-2.58	8.49	-2.97	-4.82
North	21.91	18.45	-3.55	12.57	-3.06	-8.26
Middle	8.58	15.58	1.91	13.35	1.97	-5.10
South	-0.81	31.02	-4.33	25.00	-4.43	-8.56

Table 3.6: P>F values for test of significance for separate and combinatorial effects of variables of HDP-treatment on WBS scores and TPA features

HDP variable	*Test Statistic*	*P>F*
Charge Amount (g)	Wilk's Lambda	0.7852
	Pillai's Trace	0.7456
	Hotelling-Lawley Trace	0.7918
	Roy's Greatest Root	0.2184
Container size (L)	Wilk's Lambda	0.0048[a]
	Pillai's Trace	0.0067[a]
	Hotelling-Lawley Trace	0.0062[a]
	Roy's Greatest Root	0.0015[a]
Location	Wilk's Lambda	0.0134[a]
	Pillai's Trace	0.0276[a]
	Hotelling-Lawley Trace	0.0177[a]
	Roy's Greatest Root	0.0023[a]

[a] Indicates significant differences due to treatment effects

CHAPTER 4

RHEOLOGICAL METHOD FOR MODELING DEFORMATION BEHAVIOR OF A VISCOELASTIC PROTEIN GEL UNDERGOING HIGH HYDRODYNAMIC PRESSURE TREATMENT

ABSTRACT: High hydrodynamic pressure (HDP) has been considered as a new novel food processing technique to impart favorable textural changes in meat, especially tenderizing 'tough' cuts of meat. The only objective measurement of tenderness accepted by USDA is the Warner-Bratzler shear-force (WBS) testing procedure, which involves destructive testing, is laborious and time intensive. In addition, some samples indicate reduction in tenderness after HDP-treatment, which is not consistent with the claims of tenderization. A mathematical model simulating behavior of meat undergoing HDP treatment, accounts for different treatment parameters involved in the technology and also eliminates the need to carry out WBS testing.

In this study, a mathematical rheological model was developed for predicting the deformation history of a protein gel under cyclic loading of a shear stress was developed. A four-element Burger model was used as reference and expanded to consider stress and strain responses in the product under a varying pressure. Values for the storage and loss modulus of the product were taken from behavioral studies of β-lactogloublin protein gels. Creep recovery and stress relaxation response of the gel was used for prediction of the deformation in each element of the model, from which the overall deformation was estimated. Sensitivity analysis of the model indicated that low frequency oscillations and decreased storage modulus values dominated deformation behavior. The model was entirely non-sensitive to frequency changes above 30,000

rads/s. Values for deformation of the gel were calculated for a spectrum of frequencies between 30,000 rads/s and 300,000 rads/s, under very low pressures (50 kPa). There appeared to be some harmonic resonance between the applied pressure frequency and the loss tangent of the gel, resulting in a family of frequencies that caused the greatest deformation. The resulting deformation under very low pressures of 50 kPa indicated that the model was not valid for the high pressures in the order of MPa which HDP-treatments utilize. In addition, the viscous elements of the model played no role in predicting the rheological behavior of the model, which requires future studies be limited to numerical simulations of elastic behavior only.

INTRODUCTION

High hydrodynamic pressure processing (HDP) is a novel food processing technique that has gained significant interest in the food industry due to its non-thermal approach. The technology has been the focus of various studies due to the beneficial effects of the process on the texture of food products, especially beef, with minimal microbial inactivation.

Current literature has focused more on the effects of HDP-treatment on texture of foods because of its inconsistent microbial inactivation characteristics (Lorca et al., 2002 and 2003, Patel et al., 2004). The effects of HDP have been found to disrupt living cells (Delius et al., 1988 and 1998), indicated via studies in lithotripsy, which also utilizes shock waves for treatment of kidney stones. The disruptive effects of shock waves have enabled researchers to extend the HDP-treatment process to improving textural quality of food products, especially meats.

The importance of tenderness and favorable texture in the meat industry is paramount, considering the financial implications of good tender cuts and consumer satisfaction (NCBA, 2009). Tenderness and texture of meat and meat products are difficult characteristics to define considering the complexities of chemical and organoleptic properties of these products and the intricacies involved in human sensory perception during the chewing process. Instrument-based objective detection methods of tenderness and texture, viz. Warner-Bratzler shear-force testing (WBS) and texture profile analysis (TPA) involve destructive testing on cooked meat samples and are labor and time intensive. The application of a large-strain measurement such as WBS scores or TPA features to describe small-strain changes occurring in raw meat products undergoing HDP-treatment has been the focus of many studies, but there is a need to describe

these small-strain changes occurring during the treatment process that can eliminate the need for laborious destructive testing methods.

Currently, there exists almost very little literature clearly outlining the actual reason for the changes in textural effects after HDP-treatment. Studies of HDP-treatment on muscle structure have reported myofibrillar fragmentation in the Z-lines of bovine *longissimus dorsi* muscle in beef at 150 MPa (Zuckerman and Solomon, 1998). A result of this fragmentation has been speculated to result in a significant increase in tenderness. Studies by Bowker et al. (2007 and 2008) tried to establish a correlation between the effects of HDP-treatment on protein and on WBS scores in beef strip loins. The second study established a better correlation between MFI and WBS scores with *r*-value of -0.75.

Mathematical models offer a better alternative to lengthy laboratory methods by simulating different process parameters and provide information on optimum conditions to enable efficient processing and better quality of the products. This study involves modeling the process as a cyclic load on a protein matrix, comprised of viscoelastic elements, and evaluating the strains and deformations that the elements undergo upon loading. Understanding the cyclic loading response of a viscoelastic system is a preliminary study to effectively describe textural changes in food systems subjected to HDP-treatment. Mathematical predictions of rheological behavior of a viscoelastic model under constant shear stress is well established (Rao et al. 2005; Steffe 1996), but under a cyclic loading, the viscous and elastic elements become a function of the frequency and time history of the other elements in the system (Ma et al., 1998). Understanding these behaviors and dependencies will help optimize the hydrodynamic pressure treatment process in terms of achieving optimal textural changes in the food product.

MODEL DEVELOPMENT

Deformation of protein gels can be characterized as a complex viscoelastic response. Depending on the composition of the product, the material will exhibit a combination of liquid-like and solid-like behavior in which the stress-strain relationship is time dependant (Rao et al., 2005). There are several well established rheological models for determining the strain response of a product for an applied constant stress, such as the Kelvin model for elastic relaxation or the Maxwell model for creep (Mohsenin, 1986). When the applied stress is not constant, but varies sinusoidally, the strain response is dependent on both the shear frequency and rate of shear strain. In such cases the material will absorb some amount of the shear stress, and dissipate it over a period of time. This absorption and dissipation of energy is characterized by the material's storage modulus and loss modulus (Mohsenin, 1986).

For a viscoelastic material, the ratio of the amplitude between the applied shear stress and the strain response is the complex shear modulus, which characterizes both the elastic storage modulus and viscous loss modulus. This is illustrated in figure 4.1, showing how an applied oscillating stress causes a strain response. The phase shift of the response represents the delay from the time when the system absorbs the shear energy till it dissipates it. The limiting parameters that determine the deformation history with respect to time are defined by the conceptual arrangement of viscous and elastic elements in the system. This conceptual arrangement can be represented through different rheological models (Mohsenin, 1986).

Simple systems can be modeled as Maxwell bodies or Kelvin bodies that represent viscous and elastic elements in series or parallel respectively. More complex systems combine these bodies in circuits the same way electric circuits are drawn to illustrate current flow through

several resistive and capacitive elements. Though the exact arrangement of elements cannot be predicted in even simple viscoelastic materials, an approximation of the system can be made knowing the complex viscous and elastic responses.

In this study, a generalized Burger model was considered to provide an excellent starting point for understanding the underlying rheological behavior of the model system, since it can provide an excellent description of both the elastic relaxation and creep seen in rheological tests of protein gel. Over long periods of constant stress the Burger model converges into Newtonian type flow behavior, which does not accurately express the deformation of certain protein gels which display non-Newtonian behavior (Hickson et al., 1980). However for this study it was assumed that the frequency of the oscillating pressure wave restricts material behavior to a complex viscoelastic response.

The starting Burger model was modified by adding more viscous and elastic element terms until the model fitted empirical data. The simplest, four-element Burger model is shown (fig. 4.2) with G_0 and G_1 representing the elastic (storage) elements of the system, and η_1 and η_N representing the viscous (resistive) elements in the system. For the purposes of this model, the protein gel was considered to be analogous to an electric circuit composed of resistive and capacitive elements, representing the viscous and elastic elements of the system, respectively. The flow of electric current is defined as the rate of electrical charge passing through any given element in the system. Likewise, in a protein gel the flow behavior of the system is represented by the deformation in any given element at a given time. The current flowing in the system results from a potential difference in charge of the system, such that equilibrium is achieved. The analogy of voltage driving a current across a resistive element in electric circuits is

considered analogous to a force driving the deformational response across viscoelastic elements in the rheological model.

Since this model is considering an oscillating pressure wave to impart force to the system, analysis of a periodic voltage source is considered. The general form representing a sinusoidal voltage is given by:

$$v(t) = v_0 \cos(\omega t + \varphi) \quad (1)$$

where, v(t) = Sinusoidal voltage (volts) at any given time t,

v_0 = Initial value of sinusoidal voltage (volts),

ω = Angular frequency (rads/s), and

φ = Phase difference.

For purposes of simplicity, it is easier to work with the normal force exerted on the material. In this case, it was assumed that the pressure wave was entirely unidirectional, and impacted the gel normal to the material's surface. Using an Euler transformation, the function can be rewritten as a vector in complex notation, and in terms of the normal stress by:

$$\bar{\sigma}(t) = \sigma_0 e^{(\omega t|\phi)} \quad (2)$$

where, σ(t) = the applied stress function (Pa),

σ_0 = the maximum normal stress exerted on the surface of the material,

ω = the wave frequency of the applied stress (rads/s),

t = amount of time after the stress has been applied (s), and

φ = phase shift between normal stress and strain response (radians).

The material was assumed to behave as a Hookean body, so that the applied shear stress causes a linear deformation in the gel. Higher order relationships exist for non-linear deformations, but are based off of empirical relationships for specific materials under defined conditions. The assumption of linear deformation is valid for a protein gel up to the yield stress of the material, where the material begins to undergo a plastic or non-recoverable deformation. In the linear region of operation, the shear stress and strain can be written as:

$$\gamma(\omega t) = \gamma_0 e^{i\omega t} \tag{3}$$

$$\tau(\omega t) = \tau_0 e^{i(\omega t+\phi)} \tag{4}$$

where, $\gamma(\omega t)$ = oscillatory strain response (dimensionless),

γ_0 = the amplitude of strain in the system (dimensionless),

$\tau(\omega t)$ = the oscillatory applied shear stress (Pa), and

τ_0 = the amplitude of stress in the system (Pa).

The relationship defined by Ohm's law describes the linear flow of current in respect to the driving force and resistance in the system. A similar relationship is defined for the physical rheological system, except the deformation of the gel (flow) is multi-dimensional; a deformation in one axis of the material will cause a proportional deformation in the other two axes. It was assumed for the purposes of this model that the protein gel is incompressible, and therefore the dimensional deformations can be related by Hooke's Law. The general form of Hooke's Law states:

$$\varepsilon_x = (1/E)[\sigma_x - \nu(\sigma_y + \sigma_z)] \quad (5)$$

$$\gamma_{xy} = \tau_{xy} / G^* \quad (6)$$

$$\varepsilon_y = (1/E)[\sigma_y - \nu(\sigma_z + \sigma_x)] \quad (7)$$

$$\gamma_{yz} = \tau_{yz} / G^* \quad (8)$$

$$\varepsilon_z = (1/E)[\sigma_z - \nu(\sigma_x + \sigma_y)] \quad (9)$$

$$\gamma_{zx} = \tau_{zx} / G^* \quad (10)$$

where, ε_x, ε_y, ε_z = normal strain (dimensionless),

σ_x, σ_y, σ_z = normal stress (Pa),

γ_{xy}, γ_{yz}, γ_{zx} = shear strain (dimensionless),

τ_{xy}, τ_{yz}, τ_{zx} = shear stress (Pa),

E = modulus of elasticity (Pa),

G* = complex shear modulus (Pa), and

υ= Poisson's ratio.

As it has already been assumed that the normal stress is unidirectional,

$$\sigma_y = \sigma_z = 0 \quad (11)$$

and therefore,

$$\sigma_x = E\varepsilon_x \tag{12}$$

The deformation in any given element of the model can then be defined by:

$$\delta_n = \frac{\sigma_n L}{2G_n^*(1+\upsilon)} \tag{13}$$

where, δ_n = the deformation of the n^{th} element in the system (m),

σ_n = the normal stress exhibited in the n^{th} element of the system (Pa),

G_n^* = the complex shear modulus of the n^{th} element in the system (Pa),

L = the total length of the product tangential to the shear stress (m), and

υ = Poisson's ratio of the protein gel (dimensionless).

The $\frac{G_n^*}{L}$ term acts as the impedance to deformation in a viscoelastic model. Impedance should be considered separately from resistance since G* contains both capacitive and dissipative elements. The capacitive and dissipative elements of G* are $\pi/2$ radians out of phase from each other, although they may have different magnitudes. Therefore G* can be written as a phasor, and represented as below (fig. 4.3).

$$G^* = G' + iG'' \tag{14}$$

where, G' = shear storage modulus (Pa), and

G" = shear loss modulus (Pa).

After the impedance in each element is known, the total normal force exerted in each element can be calculated as a function of time. In general, the normal stress can be represented as:

$$\sigma_N = G^* \gamma + \eta^* \dot{\lambda} \tag{15}$$

G* and η* are the complex shear and viscous modulus, respectively, and are defined by the material properties as explained above. The complex viscous modulus is completely analogous to the complex shear response, consisting of both a storage and loss modulus component. In the linear viscoelastic range, the complex shear modulus and complex viscous modulus relate to each other as given below (Rao, 2007):

$$\eta' = \frac{G''}{\omega} \tag{16}$$

$$\eta'' = \frac{G'}{\omega} \tag{17}$$

The normal strain response, γ, for a viscoelastic material is defined as:

$$\gamma = \frac{P_0}{G^*}(1 - e^{-\frac{t}{\lambda_{ret}}}) \tag{18}$$

where, λ_{ret} = relaxation time of the material (sec)

The relaxation time of any material is a unique constant dependant on material properties, and can be thought of as similar to a time constant in an electrical circuit. The relaxation time in a viscoelastic material is defined as:

$$\lambda_{ret} = \frac{\eta^*}{G^*} \tag{19}$$

For the purely viscous elements in the Burger model, the strain response simplifies to:

$$\gamma_{vis} = \dot{\eta}_{vis} * t \tag{20}$$

The rate of strain response is difficult to solve mathematically in this situation, since it is a partial differential with respect to time, and is therefore approximated numerically as:

$$\frac{\partial \gamma}{\partial t} \approx \frac{\Delta \gamma}{\Delta t} \tag{21}$$

As the pressure wave travels through the protein gel, some energy will be lost to causing deformations in the product, frictional losses, and elastic collisions within the product, causing an attenuation of force throughout the product. This attenuation can be empirically described as (NDT, 2009):

$$P = P_0 e^{-\alpha L} \cos(\omega t) \tag{22}$$

where, P_0 = original pressure level at a source (Pa),

P = pressure level at second reference location (Pa),

α = attenuation coefficient, and

L = distance from original source to second reference location (m)

Although the pressure waves considered for this model are not strictly ultrasonic, it is assumed that the equation is still valid over a wide spectrum of frequencies.

RESULTS AND DISCUSSION

All cuts of meat are complex matrices of bone, connective tissues, fibers, and fat which are difficult to accurately characterize in a viscoelastic system. In addition to the analytical simplifications made in the model development, properties of the material being tested were also simplified to fit the model. Beef muscle or beef products is comprised of many types of proteins for structural, motor, and enzymatic functions, and other components such as intramuscular fat, connective tissue, etc., whereas the product considered for this modeling study was considered to be a simple β-lactogloublin protein gel with transglutaminase cross-linkages. This was thus modeled as a simple protein matrix that exhibits complex viscoelastic response considering objective measurements for tenderness and texture are made on cooked muscle tissue cores, which are devoid of any fat or connective tissue.

Dickinson and Yamamoto (1996) performed oscillatory shear stress testing on protein-stabilized emulsion gels and determined values for the storage and loss modulus for these systems up to 14% protein content by weight. A meat product for commercial utilization typically is composed of 20%-30% protein by weight (Hoagland et al., 1949). The values reported by Dickinson and Yamamoto (1996) were plotted, and a simple linear regression used to extrapolate appropriate shear modulus values at 23% protein content by weight (fig. 4.4).

An expanded four-element Burger model was used to approximate the rheological behavior of the protein gel and additional elements were added to this model to match empirical behavior of any protein gel or more complex systems such as meat products. As more elements were introduced, there were interactions between the additional elements and the resultant

behavior of the model was characterized by increasing resistance to deformation as more elements were added.

Complex viscous modulus terms were calculated from the shear modulus terms, under the assumption of linear viscoelastic behavior (Eqs. 16 and 17). Values for the attenuation coefficient (α) and Poisson's ratio (υ) were more difficult to estimate for a protein gel. The Non-Destructive Testing Resource Center (NDT, 2009) gives an empirical relationship for estimating the attenuation coefficient of any material, but a detailed knowledge of the entire composition of the product is necessary. To a large extent, rigorous testing of any material is necessary to estimate the rheological parameters to fit an accurate model, since the shear modulus, viscous modulus, and attenuation coefficient will all be strongly affected by water content, protein content and composition, degree of cross-linking of proteins, and fat content and distribution. Attenuation in κ-carrageenan gels of different concentrations have been reported was found to vary with variations in temperature (Wang et al., 2005). However there were no reported values on attenuation coefficient for β-lactogloublin gels and so the attenuation coefficient was assumed as a random variable in the mathematical model to be examined while conducting sensitivity analysis. Table 4.1 summarizes the material properties of a 23% β-lactogloublin protein gel used for baseline tests of the model.

The values for Poisson's ratio were more strictly defined, since in the linear viscoelastic behavior range Poisson's ratio must be defined between 0 and 1.0. A value of 0 represents a product that does not undergo deformation in any primary axis when subjected to an applied stress, whereas a value of 1.0 represents a material that completely translates an applied stress as deformation in a plane normal to the applied force, though no stable and linear isotropic solid material exhibits a Poisson's ratio value of 1.0. There are known materials with values for

Poisson's ratio outside these bounds, typically novel polymers and ceramics or auxetic materials with negative Poisson's ratio, but these material properties violated assumptions for this model. As with the attenuation coefficient, a value for Poisson's ratio of this protein gel was initially assumed as 0.3 (Segars et al., 1977), but also used as a variable in sensitivity analysis based on the study by Segars et al. (1977) who used Poisson's ratio as a small-strain parameter to correlate with large-strain measurements of sensory attributes. Since both Poisson's ratio and the attenuation coefficient were user-defined, a sensitivity analysis of the input variables to the model was necessary to determine what local boundaries would need to be imposed.

The values for the storage and loss modulus for the protein gel indicated that β-lactoglobulin gels were strongly dominated by elastic deformations, and that very little shear energy was dissipated by viscous forces. Alternatively, the extrapolated relationship assumed for the storage modulus may not be valid at high protein concentrations, since the relationship was established assuming linearity and this would require experimental testing.

As the pressure wave passes through the protein gel, elastic discontinuities cause energy losses and decrease the maximum deformation. The pressure response of the system versus time is given in figure 4.5. This plot is based on an assumed α value of 55.0 After approximately 10 seconds, a single pulse applied to the gel was completely attenuated, given the above material properties, assuming a gel thickness of 0.10 m. It was found that assuming the thickness of sample to be approximately 1" or 2.54 cm thick, like that of a beef loin, the attenuation coefficient needed to be at least 1 magnitude higher than the assumed value of 55 in order for the wave to attenuate in 10 seconds. First principle wave physics predicts that lower wave frequencies carry more energy, and will therefore take longer to attenuate, however this was not accurately reflected in this model due to the empirical attenuation relationship assumed. It was

assumed that the empirical relationship was valid for all wave frequencies, but the model was run using high frequency waves. As the applied pressure was increased, the amplitude of the wave and the length of time for the wave to completely attenuate, both increased. In practical applications, the wave pressure generated from the shockwave front would be in the order of MPa (fig. 4.8), but this is not represented for the material considered for purposes of simplicity. This amount of pressure caused complete mechanical failure of the β-lactogloublin gel, with the model predicting deformations many times larger than total thickness of the gel. Additionally, the amount of pressure acting on the system was not noticeably attenuated in this product over a realistic period of time.

Deformation of the protein gel was considered at 50 kPa and excitation frequency of 120,000 rads/s for a baseline calculation, and is represented in figure 4.6. In this test, the product reached a mechanical failure point, even when assuming a 0.10 m thickness of the gel, where the pressure wave caused a complete deformation of the product. The maximum deformation achieved being the same as the total thickness of the gel. This maximum deformation occurs after approximately 0.7 seconds post-wave impact. The plot shows that the gel completely relaxed after each oscillation, which was a result of the negligible viscous interactions. An increase in the loss tangent will result in the viscous interactions playing more of a role in the deformation of the product and as a result, the material will not be able to recover completely between oscillations.

Sensitivity Analysis

Sensitivity analysis included all the material properties defined in Table 4.1, in addition to the process conditions– the applied pressure wave and the frequency of the pressure wave. Material and process parameters were varied from an initial value and increased to 200% of the initial value in steps of 10%. Initial value for the applied pressure was chosen to be $1/4^{th}$ of 50 kPa, the value at which the material underwent complete deformation, so that the sensitivity analysis did not exceed this limit and to keep the observations within the elastic limit. Initial values for the material parameters were taken from numerically derived estimates as given in table 4.1. Percent change in deformation response with percentage change in the material and process parameters are shown in figures 4.9-4.11.

Effects of Material Parameters

Sensitivity analysis performed on the material parameters indicated that deformation response of the model was highly sensitive to changes in values of the storage modulus as indicated in figure 4.9, compared to the other material parameters, with the relationship indicating an exponential decay. Based on this observation, it can also be inferred that elastic interactions dominate over the viscous interactions, which implies a low level of dissipation of the impacted wave. The effects of storage moduli however have reduced influence on the deformation response after a 100% increase in value which could be attributed to dissipation of energy as the pressure wave progresses down the layers of the material.

Poisson's ratio and attenuation coefficient for the material contributed very negligibly to the deformation response of the product compared to the storage modulus of the material (fig.

4.9). Since the treatment due to HDP is considered a small-strain deformation and values of Poisson's ratio cannot realistically exceed 0.50 (Mohsenin, 1986), within the constraints, Poisson's ratio of the material indicated a linear relationship with the changes in deformation and in accordance with Hooke's law.

A linear relationship was also observed with attenuation coefficient, though its effects on deformation response were less pronounced than that of the material's Poisson's ratio (fig. 4.9). In contrast, changes in values of loss modulus were found to have no effects on deformation response of the material and this could be due to the fact that the estimated values of storage and loss moduli for the protein gel differed in values by a magnitude. It can also be inferred that this could be due to the high initial value of attenuation coefficient (α) of the material which might have contributed more to the dissipation of the pressure wave than the loss modulus. However, when the values for the loss modulus approached those of the storage modulus, a similar sensitivity response would be observed based on the noted observation of sensitivity of the gel's deformation to storage modulus values.

Effects of Process Conditions

Sensitivity analysis of the process parameters in the model indicated that a very high sensitivity was displayed in terms of percent change in deformation to changes in the frequency of applied pressure wave (fig. 4.10), with the relationship indicating an exponential decay. It can be inferred that varying the frequency of the pressure wave causes changes in the deformation of the product due to harmonic oscillations between the applied pressure wave and the loss tangent. Sensitivity of the material's deformation to the applied pressure intensity was comparatively low

when compared to pressure wave frequency, however a steady linear increase in sensitivity was observed in accordance with the relation of strain response to applied pressure equation 18 and with Hooke's law, since the 50 kPa limit was not exceeded. In comparison, a very high sensitivity of the deformation response to the change in pressure wave frequency was observed initially up to a 20% increase in value, after which the sensitivity was less pronounced and negligible after 80% increase in pressure wave frequency. It was observed thereafter that any increase in the frequency of the pressure wave caused no noticeable effect on the deformation history of the gel, except for the material deforming at a rate proportional to increase in frequency (fig. 4.7).

CONCLUSIONS

Results of this study indicated that the proposed rheological model did not explain the behavior of a substrate undergoing HDP treatment considering a complete deformation at 50 kPa, well below operating pressures exceeding 800 MPa. Utilization of an oscillating sinusoidal wave as a representative of HDP treatment is not an exact representation of an impinging shock wave and a protein gel is a much less complicated substrate that does not represent beef muscle/loin, whose texture is a complicated parameter and has been a subject of various studies over the years. This study also indicated that the material behavior of the model completely relied on elastic interactions and completely negated the role of viscous elements in the model.

Sensitivity analysis of material and process parameters indicated that storage modulus, pressure wave intensity and frequency contributed to the change in deformation response, whereas the effects due to Poisson's ratio, attenuation coefficient were negligible and that of loss

modulus was none. Since material properties are constants and cannot be changed, they cannot be used for optimization of the HDP treatment process. Applied frequency of the pressure wave can be considered a process variable, and can be examined at specific values to optimize which values of oscillation will produce the greatest deformation. Bounding the applied frequencies to a maximum and minimum value allows optimizing which values of frequencies will cause the greatest deformations, but in practical applications using explosion, the generated waves will not conform to a single frequency nor can their frequency be controlled.

Considering a large amount of research work computational studies in high hydrostatic processing (HHP) methods, there currently exists none in HDP technology and hence this was a pioneering study that allowed an initial analysis in understanding the technology that has shown inconsistencies in its effects on texture. Since this study indicated the lack of viscous elements in predicting deformation behavior of the model, the next approach is to model mechanical behavior of the system. A finite element method is proposed for future studies which shall model deformation behavior of beef muscle based on constitutive relationships between elastic properties of beef muscle for better understanding of the behavior of the muscle undergoing HDP-treatment and help optimize the process.

REFERENCES:

Bowker, B.C., M.N. Liu, M.B. Solomon, T.M. Fahrenholz, and J.S. Eastridge. 2007. Effects of hydrodynamic pressure processing and blade tenderization on intramuscular collagen and tenderness-related protein characteristics of top rounds from Brahman cattle. *J. Muscle Foods* 18, 35-55.

Bowker, B.C., T.M. Fahrenholz, E.W. Paroczay, J.S. Eastridge, and M.B. Solomon. 2008. Effect of hydrodynamic processing and aging on the tenderness and myofibrillar proteins of beef strip loins. *J. Muscle Foods* 19, 74-97.

Delius, M., M. Jordan, H. Eizenhoefer, E. Marlinghaus, G. Heine, H.-G. Liebich, and W. Brendel. 1988. Biological effects of shock waves: Kidney haemorrhage by shock waves in dogs-administration rate dependence. *Ultrasound in Med. & Biol.* 14(8), 689-694.

Delius, M., F. Ueberle, and W. Eisenmenger. 1998. Extracorporeal shock waves act by wave-gas bubble interaction. *Ultrasound in Med. & Biol.* 24(7), 1055-1059.

Dickinson, E., and Y. Yamamoto. 1996. Rheology of milk protein gels and protein-stabilized emulsion gels cross-linked with transglutaminase. *J. Agric. Food Chem.* 44, 1371-1377.

Hickson, D.W., C.W. Dill, R.G. Morgan, D.A. Sutter, and Z.L. Carpenter. 1980. A comparison of heat-induced gel strengths of bovine plasma and egg albumin proteins. *J. Ani. Sci.* 51, 69-73.

Hoagland, R., O. G. Hankins, N. R. Ellis, and G. G. Snider. 1949. Nutritive properties of protein in different cuts of beef. *J. Nutr*. 38, 381 - 393.

Lorca, T.A., M.D. Pierson, J.R. Claus, J.D. Eifert, J.E. Marcy, and S.S. Sumner. 2002. Penetration of surface-inoculated bacteria as a result of hydrodynamic shock wave treatment of beef steaks. *J. Food Prot.* 65, 616-620.

Lorca, T.A., J.R. Claus, J.D. Eifert, J.E. Marcy, and S.S. Sumner. 2003. Penetration of surface-inoculated bacteria as a result of electrically generated hydrodynamic shock wave treatment of boneless skinless chicken breasts. *J. Poultry Sci.* 82, 1205-1210.

Ma, L., D. C. Davis, L. G. Obaldo, and G.V. Barbosa-Canovas. 1998. *Engineering Properties of Foods and Other Biological Materials*. American Society of Agricultural Engineers.

NCBA. 2009. Research shows one of the keys to tender beef. Available at http://www.beefusa.org/NEWSResearchShowsOneoftheKeystoTenderBeef3451.aspx. Accessed April 10, 2009.

NDT. 2009. Non Destructive Testing Resource Center. Available at http://www.ndt-ed.org. Accessed on April 10, 2009.

Mohsenin, N. 1986. *Physical properties of plant and animal materials*. Gordon and Breach Science Publishers, New York, NY.

Patel, J.R., Williams-Campbell, A., Liu, M.N., and M.B. Solomon. 2004. Effect of hydrodynamic pressure processing on inactivation of *Escherichia coli* O157:h7 in blade tenderized beef steaks. *American Meat Science Association 57th Reciprocal Meat Conference*. 57-66.

Podolak, R., M.B. Solomon, J.R. Patel, and M.N. Liu. 2006. Effect of hydrodynamic pressure processing on the survival of *Escherichia coli* O157:H7 in ground beef. *Innov. Food Sci. & Emerg. Tech.* 7, 28-31.

Rao, M.A., S.S.H. Rizvi, and A.K. Datta. 2005. *Engineering properties of foods- 3rd Edition*. CRC Press, Boca Raton, FL.

Rao, M.A. 2007. *Rheology of fluid and semisolid foods: Principles and applications*. Springer Science Publication, New York, NY.

Segars, R., R.G. Hamel, and J.G. Kapsalis. 1977. Use of Poisson's ratio for objective-subjective texture correlations in beef: An apparatus for obtaining the required data. *J. Texture Studies* 8, 433-447.

Wang, Q., B. Rademacher, F. Sedlmeyer, and U. Kulozik. 2005. Gelation behaviour of aqueous solutions of different types of carrageenan investigated by low-intensity-ultrasound measurements and comparison to rheological measurements. *Innov. Food Sci. & Emerg. Technol.* 6, 465-472.

LIST OF FIGURES

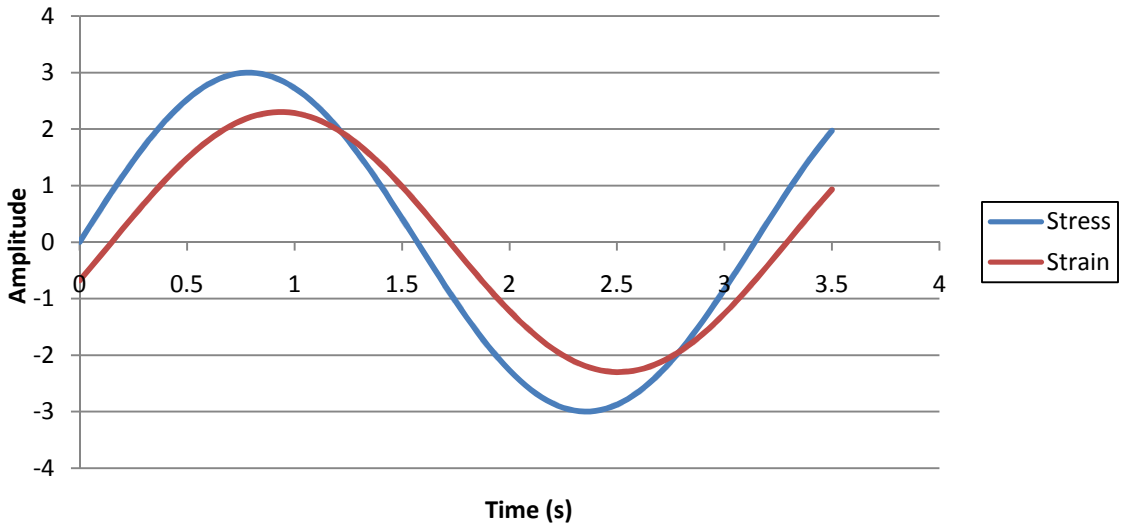

.

Figure 4.1: Strain response to an applied sinusoidal shear stress

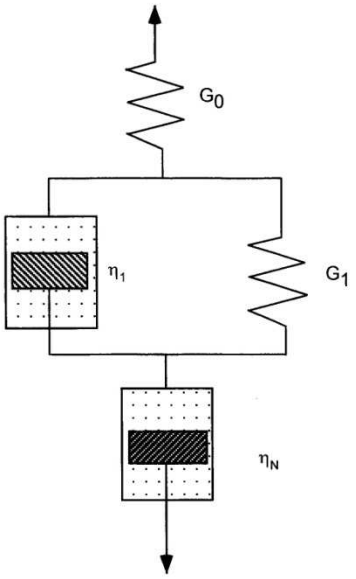

Figure 4.2: Four-element Burger model (Mohsenin, 1986)

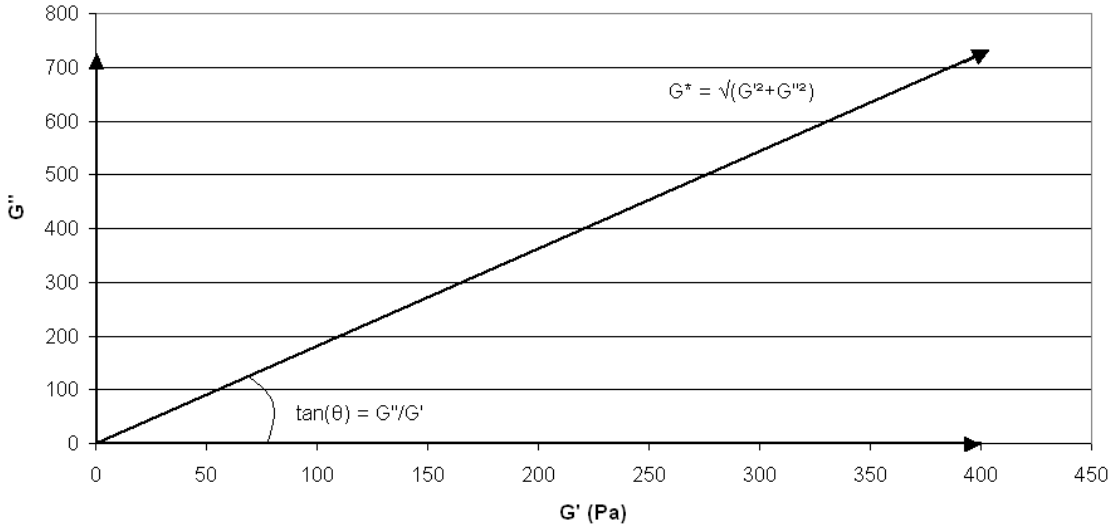

Figure 4.3: Phasor diagram of the complex shear modulus, G*

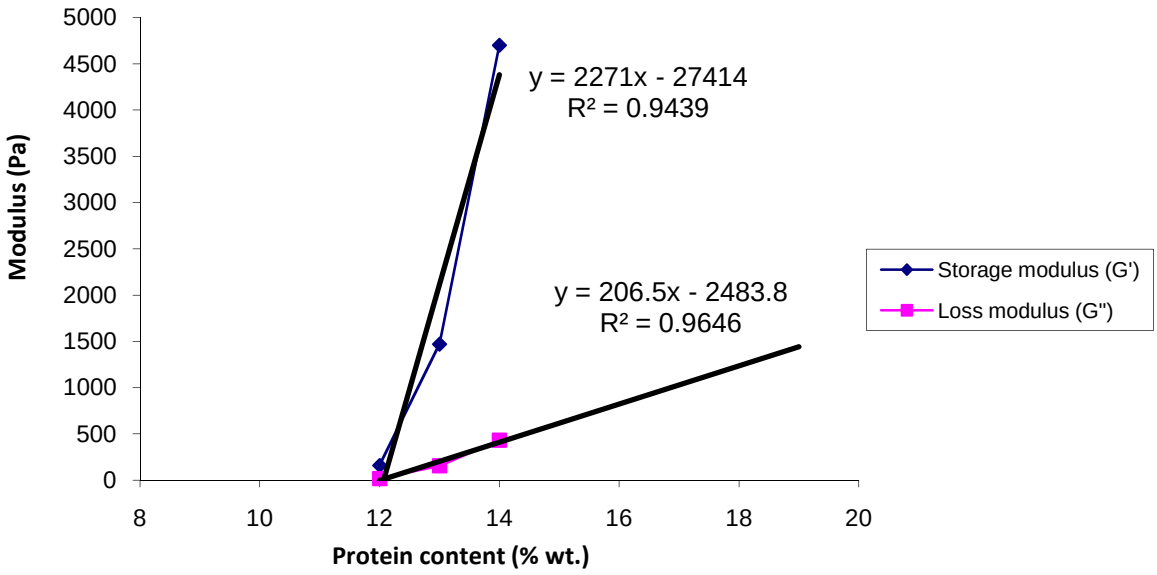

Figure 4.4: Shear modulus vs protein content in a protein-stabilized emulsion gel

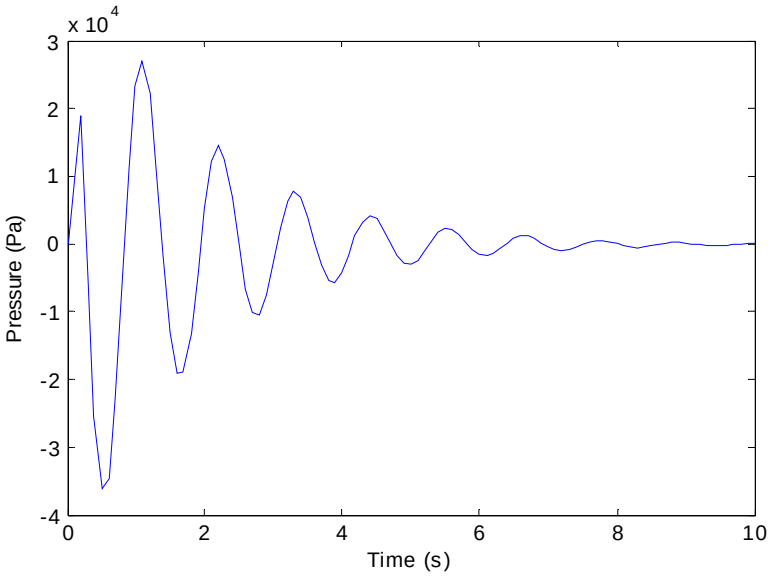

Figure 4.5: Pressure response of protein gel vs time

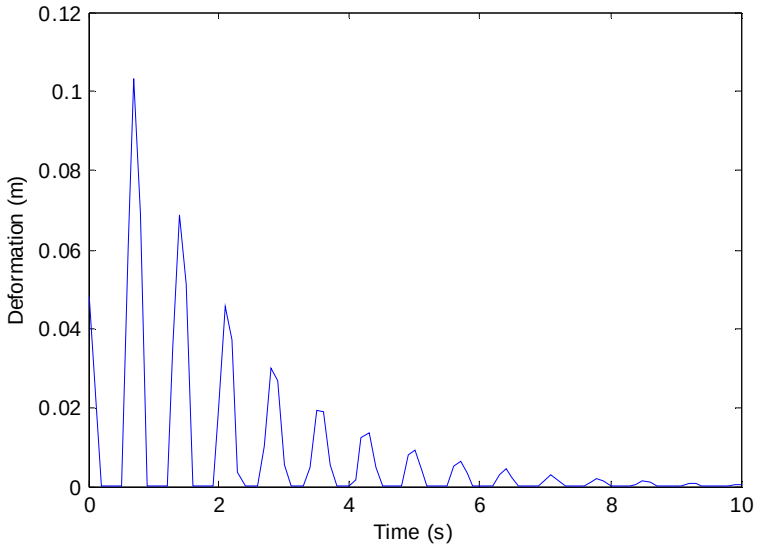

Figure 4.6: Deformation of a protein gel impacted by an oscillating pressure wave (P_{max}=50KPa, ω=120,000 rads/s)

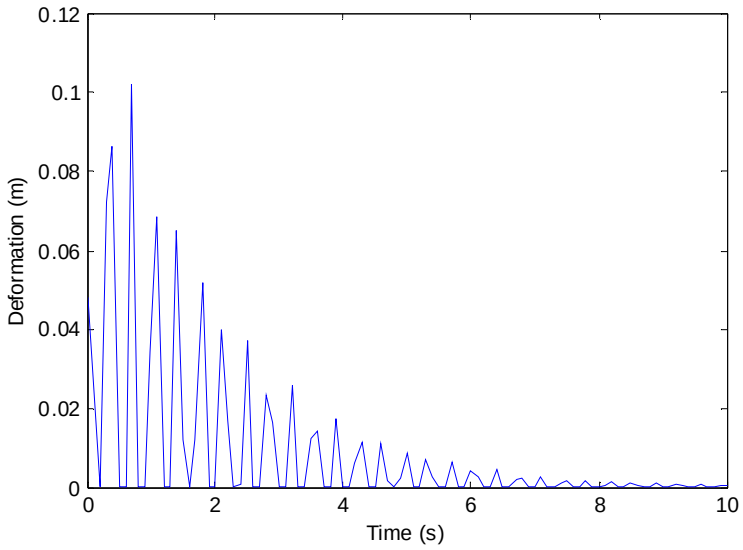

Figure 4.7: Deformation of a protein gel impacted by an oscillating pressure wave (P_{max}=50KPa, ω=240,000 rads/s)

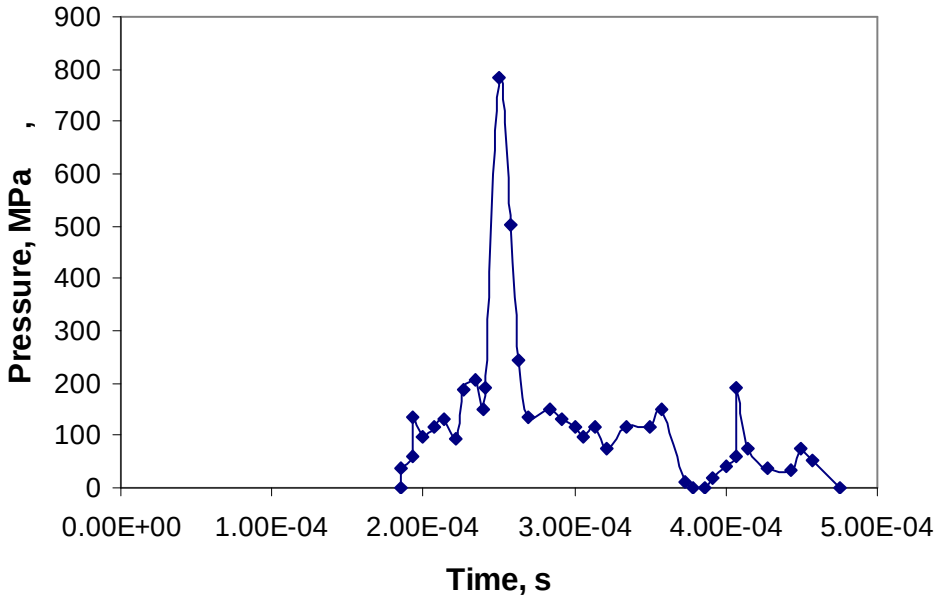

Figure 4.8: Time-pressure graph of incident shock wave during HDP-treatment (USDA-ARS proprietary information)

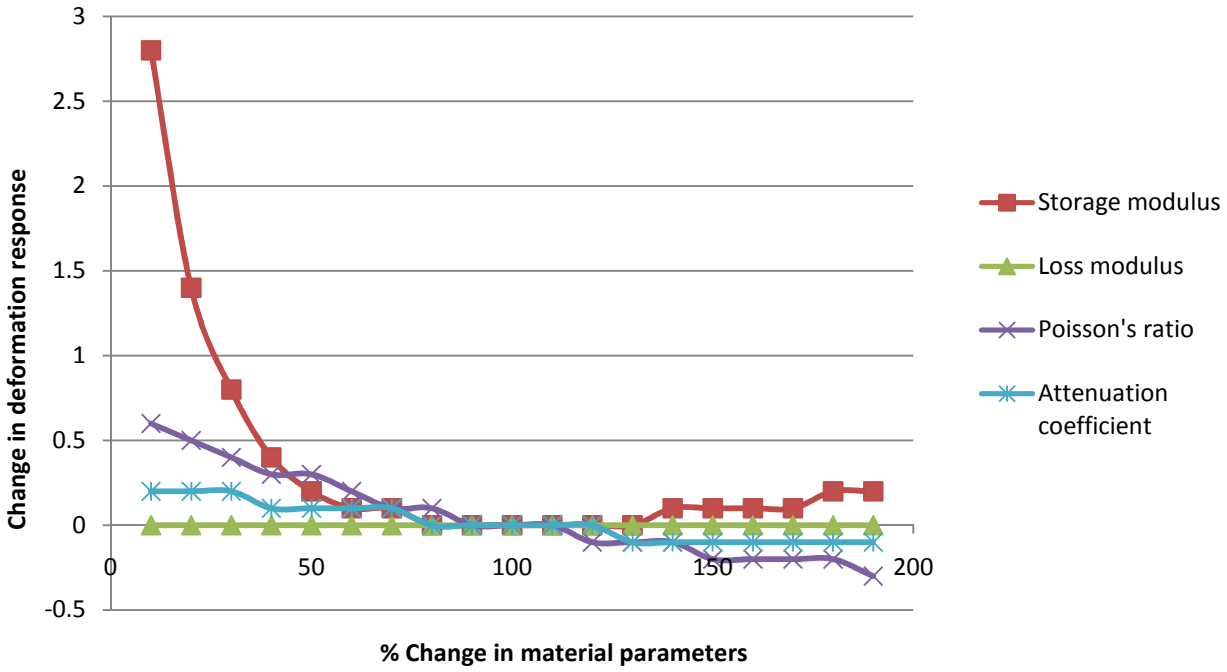

Figure 4.9: Sensitivity analysis of material parameter inputs for rheological model

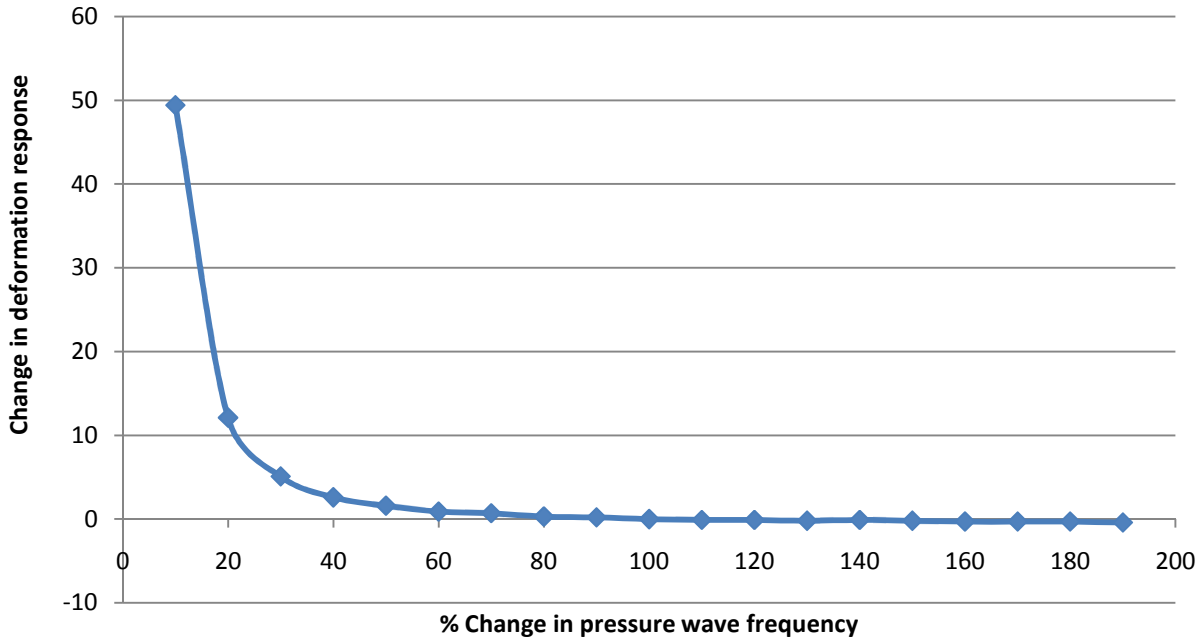

Figure 4.10: Sensitivity analysis of process parameter inputs (pressure wave frequency) for rheological model

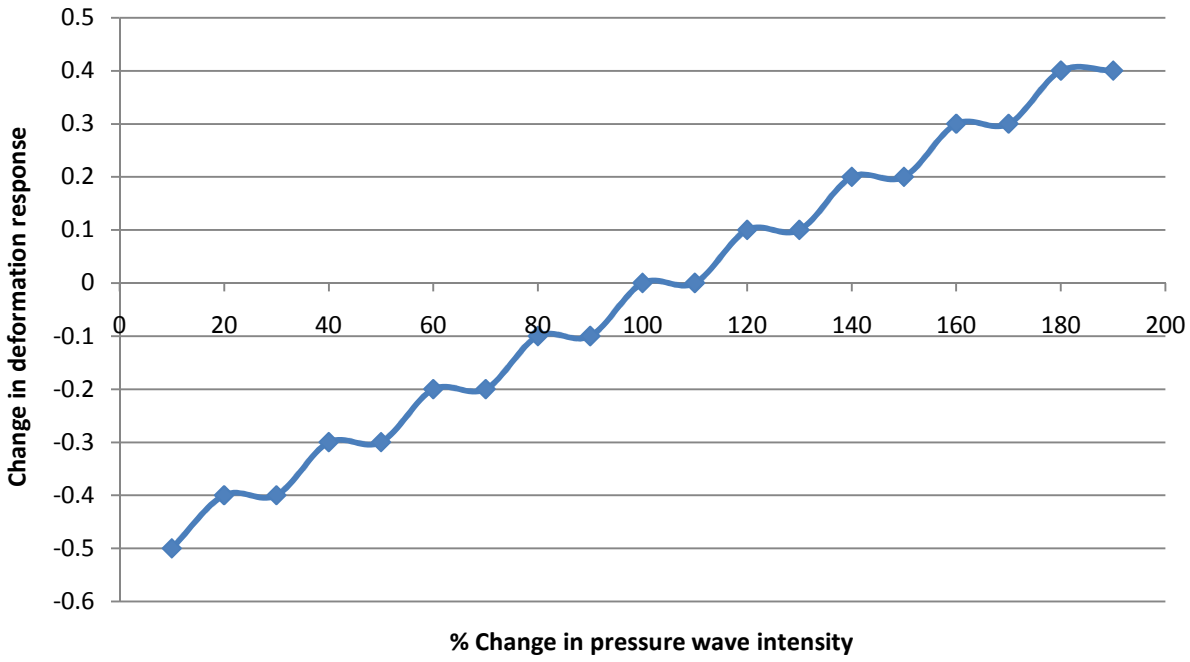

Figure 4.11: Sensitivity analysis of process parameter inputs (pressure wave intensity) for rheological model

LIST OF TABLES

Table 4.1: Material properties of β-lactogloublin protein gel with transglutaminase cross-linkages

Protein content of modeled material	23%
Shear storage modulus, G_1' (Pa)	42987[a]
Shear loss modulus, G_1" (Pa)	3917[a]
Shear storage modulus, G_2' (Pa)	38445[a]
Shear loss modulus, G_2" (Pa)	3505[a]
Shear storage modulus, G_3' (Pa)	40716[a]
Shear loss modulus, G_3" (Pa)	3711[a]
Poisson's ratio	0.3[b]
Attenuation coefficient, α	Assumed

[a] Values estimated mathematically from study by Dickinson and Yamamoto (1996) using protein content data from Hoagland et al. (1949)

[b] Estimated from Segars et al. (1977)

MATLAB CODE

```
max_value = 0;
omega = 120000; %(rads/s)

%Definition of material viscoelastic properties for 23% protein gel
G1_prime = 42987; %(Pa)
G1_2prime = 3917; %(Pa)
G2_prime = 38445; %(Pa)
G2_2prime = 3505; %(Pa)
G3_prime = 40716; %(Pa)
G3_2prime = 3711; %(Pa)
G4_prime = 33903; %(Pa)
G4_2prime = 3091; %(Pa)

n_poisson = 0.3; % Poisson's ratio
alpha = 55.7; % Attenuation Coefficient
L = 0.1; % Thickness of the product (m)

P_0 = 50000; %(Pa)
run_time = 10; %(s)
time_inc = 100;
del_t = run_time/time_inc;
del_L = L/time_inc;
```

```
%Calculation of complex viscoelastic elements
G1_complex = (G1_prime^2+G1_2prime^2)^0.5;
theta1 = atan(G1_2prime/G1_prime);
n1_complex = 0;

G2_complex = (G2_prime^2+G2_2prime^2)^0.5;
n2_prime = G2_2prime/omega;
n2_2prime = G2_prime/omega;
n2_complex = (n2_prime^2+n2_2prime^2)^0.5;
t2_relax = n2_complex/G2_complex;

G3_complex = (G3_prime^2+G3_2prime^2)^0.5;
n3_prime = G3_2prime/omega;
n3_2prime = G3_prime/omega;
n3_complex = (n3_prime^2+n3_2prime^2)^0.5;
t3_relax = n3_complex/G3_complex;

G4_complex = (G4_prime^2+G4_2prime^2)^0.5;
n4_prime = G4_2prime/omega;
n4_2prime = G4_prime/omega;
n4_complex = (n4_prime^2+n4_2prime^2)^0.5;

%Calculate shear stress and strain in product
i = 1;
t(i) = 0;
```

```
strain1(i) = (P_0(i)/G1_complex);
strain2(i) = (P_0(i)/G2_complex)*(1-exp(-t(i)/t2_relax));
strain3(i) = (P_0(i)/G3_complex)*(1-exp(-t(i)/t3_relax));
strain4(i) = (n4_complex*del_t*i);

shear1(i) = (G1_complex*strain1(i));
shear2(i) = (G2_complex*strain2(i));
shear3(i) = (G3_complex*strain3(i));
shear4(i) = 0;

def_1(i) = (shear1(i)*L)/(2*G1_complex*(1+n_poisson));
def_2(i) = (shear2(i)*L)/(2*G2_complex*(1+n_poisson));
def_3(i) = (shear3(i)*L)/(2*G3_complex*(1+n_poisson));
def_4(i) = (shear4(i)*L)/(2*G4_complex*(1+n_poisson));

strain_total(i)=strain1(i)+strain2(i)+strain3(i)+strain4(i);
def_total(i) = def_1(i)+def_2(i)+def_3(i)+def_4(i);

for i=2:time_inc;
   t(i) = del_t*i;
   P(i) = P_0*exp(-alpha*del_L*i)*cos(omega*t(i));

   strain1(i) = (P(i)/G1_complex);
   del_strain1(i) = 0;
```

```
strain2(i) = (P(i)/G2_complex)*(1-exp(-t(i)/t2_relax));
del_strain2(i) = (strain2(i)-strain2(i-1))/(t(i)-t(i-1));

strain3(i) = (P(i)/G3_complex)*(1-exp(-t(i)/t3_relax));
del_strain3(i) = (strain3(i)-strain3(i-1))/(t(i)-t(i-1));

strain4(i) = (n4_complex*t(i));
del_strain4(i) = (strain4(i)-strain4(i-1))/(t(i)-t(i-1));

strain_total(i)=strain1(i)+strain2(i)+strain3(i)+strain4(i);

shear1(i) = (G1_complex*strain1(i));
shear2(i) = (G2_complex*strain2(i))+(n2_complex*del_strain2(i));
shear3(i) = (G3_complex*strain3(i))+(n3_complex*del_strain3(i));
shear4(i) = (n4_complex*del_strain4(i));

def_1(i) = (shear1(i)*L)/(2*G1_complex*(1+n_poisson));
    if def_1(i) < 0
        def_1(i) = 0;
    end
def_2(i) = (shear2(i)*L)/(2*G2_complex*(1+n_poisson));
    if def_2(i) < 0
        def_2(i) = 0;
    end
def_3(i) = (shear3(i)*L)/(2*G3_complex*(1+n_poisson));
```

```
        if def_3(i) < 0
                def_3(i) = 0;
        end
    def_4(i) = (shear4(i)*L)/(2*G4_complex*(1+n_poisson));
        if def_4(i) < 0
                def_4(i) = 0;
        end
    def_total(i) = def_1(i)+def_2(i)+def_3(i)+def_4(i);

    if def_total(i) > max_value
       max_value = def_total(i);
    end

end
```

CHAPTER 5

FINITE ELEMENT METHOD FOR MODELING MECHANICAL BEHAVIOR IN BEEF LOINS UNDERGOING HIGH HYDRODYNAMIC PRESSURE-TREATMENT

ABSTRACT: A 3-D numerical model assuming transversely isotropic behavior of beef loins subjected to high hydrodynamic pressure treatment using the finite element method was studied under different pressure conditions. Ten samples with 2 controls and 8 treated samples using 50 g, 75 g and 100 g charges were chosen for this study and were used to experimentally estimate the diagonal elastic coefficients of the stiffness matrix, C_{ij} of beef loins were estimated from ultrasound longitudinal and shear wave speeds. Average values of the experimentally derived diagonal elastic coefficients c_{11}, c_{22}, c_{33}, c_{44}, c_{55}, and c_{66} were estimated to be 1.03 GPa, 2.14 GPa, 1.45 GPa, 0.715 MPa, 0.316 MPa, and 0.24 MPa, respectively. Results indicated that many values of the elastic coefficients indicated an increase after HDP-treatment. Highest values of reduction for c_{44} and c_{66} at 1.58% and 44.2%, respectively were observed when samples were treated with the 75 g charge where as the highest reduction for c_{55} at 36.2% was observed when the sample was treated with a 100 g charge. Treatment with the 75 g and 100 g charges were found to be most effective in reduction of these coefficients.

The experimentally estimated coefficients were used in the finite-element model where the sample beef loin's mechanical behavior as an elliptical 3-D plate was simulated under different pressure conditions generated by shock waves described by the Euler's equation and Tammann Equation of States (EOS). Results of the simulation indicated no deformational

response of the model to the shock wave and thus a sensitivity analysis of the model could not be conducted. When the model was implemented assuming a unidirectional linear propagation of shock wave, deformation characteristics of the model assuming transversely isotropic indicated more realistic values indicating that the high values of estimated and assumed elastic coefficients were able to impede deformation as a result of the incident pressure wave. Isotropic behavior of the model did not indicate realistic results of deformation, which could be attributed to the low values of Young's modulus in the model.

INTRODUCTION

HDP in food processing has been primarily used for tenderizing unacceptably tough cuts of beef, and allow them to be used in more valuable products. However, the experimental study conducted in chapter 1 indicated that certain samples underwent an increase in Warner-Bratzler shear (WBS) and indicated inconsistencies in values of texture profile analysis (TPA) features after HDP-treatment, which required a detailed modeling study of the technology.

Much of reported literature in the field of high pressure treatment has been reported in the field of high hydrostatic pressure (HPP) and its effects on microbial inactivation and chemical and physical properties of foods. Works have been reported in inactivation of *E. coli* and *S. aureus* in whole milk under isothermal conditions (Guan et al., 2006), non-log-linear inactivation kinetics of *E. coli* in tryptic soy broth (Klotz et al., 2007), recovery of *L. monocytogenes* on sliced cooked ham (Koseki et al., 2007), survival of *L. innocua* in exponential and stationary growth phases (Saucedo-Reyes et al., 2009), etc.. There currently exists no literature in the field of mathematical modeling in high hydrodynamic pressure treatment (HDP) that provides information on textural changes occurring in food products subjected to HDP treatment.

Studies in underwater shock wave modeling in the field of lithotripsy in 2-D and 3-D have been reported. Saito et al (2003) used a finite-volume method (FVM) to numerically model attenuation of underwater shock waves, generated via a lithotripter, through a porous media. Finite-volume method using Riemann solvers were used by Fagnan et al. (2008) model 3-D shock wave propagation in tissue and bone in human body. Cleveland and Sapozhnikov (2005) utilized a finite-difference method (FDM) to model 2-D propagation of shock waves in and its effects on the shear and tensile stress and strain on kidney stones. Numerical finite-element

method (FEM) was used by Mihradi et al. (2004) to study stress generation in kidney stones due to direct pulse impingement and Tham et al. (2007) used FEM to model mechanical behavior of kidney stones using tandem pulses of shock .

The previous chapter dealt with modeling using a 4-element Burger model to describe rheological changes by means of deformation in a protein slab. This attempt was not successful because of the medium undergoing complete deformation at a very low pressure of 50 kPa, which is very inconsistent with the high hydrodynamic pressure (HDP) treatment process. In this attempt, the sample was assumed to be a beef loin instead of a protein matrix and the behavior of the beef loin was modeled using a 3-D finite-element-based, constitutive relationship model incorporating shockwave propagation and elastic behavior, in order to understand textural and structural changes on beef samples subjected to HDP treatment.

MODEL DEVELOPMENT AND GOVERNING EQUATIONS

Constitutive Relationships for Mechanical Properties

Linear elastic materials obey the Hooke's law which states that the stress (σ) is proportional to strain within the elastic limit and the general form is expressed as (Ophir et al., 1997):

$$\sigma_i = C_{ij}\varepsilon_j \quad (1)$$

where, ε = strain, and

C_{ij} = stiffness matrix of elastic coefficients.

In the case of isotropic materials where elastic properties are same in all the directions, response of to an acting load can be characterized by 2 independent elastic constants viz., Young's modulus (E) and Poisson's ratio (ν), since the material response to loads in all directions is the same (Shull, 2002). Examples of isotropic materials primarily include metals such as, iron, aluminum, etc. However, many materials of practical interest, especially biological materials, do not exhibit homogeneity and thus the response of the materials varies along each directions (Bonet and Burton, 1998). Such materials exhibit anisotropic behavior which implies that the material exhibits different physical properties and responses to applied load along different directions (Kaw, 1997).

In the case of anisotropic materials, 21 independent elastic constants are needed to characterize the response of the material (Kaw, 1997) and the relationship between stress and strain using stiffness matrix for such materials is represented in the matrix form as (Kaw, 1997):

$$\begin{bmatrix} \sigma_{11} \\ \sigma_{22} \\ \sigma_{33} \\ \sigma_{23} \\ \sigma_{31} \\ \sigma_{12} \end{bmatrix} = \begin{bmatrix} c_{11} & c_{12} & c_{13} & c_{14} & c_{15} & c_{16} \\ c_{21} & c_{22} & c_{23} & c_{24} & c_{25} & c_{26} \\ c_{31} & c_{32} & c_{33} & c_{34} & c_{35} & c_{36} \\ c_{41} & c_{42} & c_{43} & c_{44} & c_{45} & c_{46} \\ c_{51} & c_{52} & c_{53} & c_{54} & c_{55} & c_{56} \\ c_{61} & c_{62} & c_{63} & c_{64} & c_{65} & c_{66} \end{bmatrix} * \begin{bmatrix} \varepsilon_{11} \\ \varepsilon_{22} \\ \varepsilon_{33} \\ \varepsilon_{23} \\ \varepsilon_{31} \\ \varepsilon_{12} \end{bmatrix} \quad (2)$$

where c_{ij} = material's elastic coefficients.

The relationship in equation 2 can be expressed using the compliance matrix, S_{ij} as:

$$\begin{bmatrix} \varepsilon_{11} \\ \varepsilon_{22} \\ \varepsilon_{33} \\ \varepsilon_{23} \\ \varepsilon_{31} \\ \varepsilon_{12} \end{bmatrix} = \begin{bmatrix} s_{11} & s_{12} & s_{13} & s_{14} & s_{15} & s_{16} \\ s_{21} & s_{22} & s_{23} & s_{24} & s_{25} & s_{26} \\ s_{31} & s_{32} & s_{33} & s_{34} & s_{35} & s_{36} \\ s_{41} & s_{42} & s_{43} & s_{44} & s_{45} & s_{46} \\ s_{51} & s_{52} & s_{53} & s_{54} & s_{55} & s_{56} \\ s_{61} & s_{62} & s_{63} & s_{64} & s_{65} & s_{66} \end{bmatrix} * \begin{bmatrix} \sigma_{11} \\ \sigma_{22} \\ \sigma_{33} \\ \sigma_{23} \\ \sigma_{31} \\ \sigma_{12} \end{bmatrix} \quad (3)$$

Many anisotropic or non-homogeneous materials do possess material symmetry and can be classed as monoclinic materials, where there is one plane of material symmetry or orthotropic materials, which exhibit three mutually perpendicular planes of material symmetry (Kaw, 1997). Monoclinic materials require 13 independent elastic constants and orthotropic materials need 9 independent elastic constants to characterize their responses. Stiffness matrices C_{ij}, of monoclinic and orthotropic materials are given in equations 4 and 5 as:

$$[C] = \begin{bmatrix} c_{11} & c_{12} & c_{13} & 0 & 0 & c_{16} \\ c_{21} & c_{22} & c_{23} & 0 & 0 & c_{26} \\ c_{31} & c_{32} & c_{33} & 0 & 0 & c_{36} \\ 0 & 0 & 0 & c_{44} & c_{45} & 0 \\ 0 & 0 & 0 & c_{45} & c_{55} & 0 \\ c_{16} & c_{26} & c_{36} & 0 & 0 & c_{66} \end{bmatrix} \quad (4)$$

$$[C] = \begin{bmatrix} c_{11} & c_{12} & c_{13} & 0 & 0 & 0 \\ c_{21} & c_{22} & c_{23} & 0 & 0 & 0 \\ c_{31} & c_{32} & c_{33} & 0 & 0 & 0 \\ 0 & 0 & 0 & c_{44} & 0 & 0 \\ 0 & 0 & 0 & 0 & c_{55} & 0 \\ 0 & 0 & 0 & 0 & 0 & c_{66} \end{bmatrix} \quad (5)$$

Some biological materials such as wood, human cortical bone (Rho, 1996), have been found to exhibit orthotropic behavior. Compliance matrix for orthotropic material can be expressed in terms of Young's moduli, Poisson's ratio, and shear moduli

$$[S]=\begin{bmatrix} \frac{1}{E_1} & -\frac{\nu_{21}}{E_1} & -\frac{\nu_{31}}{E_3} & 0 & 0 & 0 \\ -\frac{\nu_{12}}{E_1} & \frac{1}{E_2} & -\frac{\nu_{32}}{E_3} & 0 & 0 & 0 \\ -\frac{\nu_{13}}{E_1} & -\frac{\nu_{23}}{E_2} & \frac{1}{E_3} & 0 & 0 & 0 \\ 0 & 0 & 0 & \frac{1}{G_{23}} & 0 & 0 \\ 0 & 0 & 0 & 0 & \frac{1}{G_{31}} & 0 \\ 0 & 0 & 0 & 0 & 0 & \frac{1}{G_{12}} \end{bmatrix} \quad (6)$$

where, E_i = Young's moduli in the *i* direction,

ν_{ij} = Poisson's ratios for strain in the *j* direction with stress in the applied *i* direction, and

G_{ij} = shear moduli in the *i-j* plane.

Materials where there is a principal fiber direction and the material exhibits isotropic properties along directions orthogonal to this fiber or the material is symmetric about an axis normal to the plane of isotropy are termed as transversely isotropic materials (Bonet and Burton, 1998). In such materials, 5 independent elastic constants are needed to characterize the response of the material. Examples of transversely isotropic materials include piezo electric crystals, fiber-reinforced composites, and some biological materials, like marine nacre aragonite (Barthelat and Espinosa, 2003). For a transverse-isotropic material, the following conditions apply (Bonet and Burton, 1998) as given below:

$$E_1 = E_2 = E \neq E_3 \tag{7}$$

$$\nu_{12} = \nu_{23} = \nu_{13} = \nu \tag{8}$$

$$G_{13} = G_{23} = G_3 \tag{9}$$

$$G_{12} = \frac{E}{2(1+\nu)} \tag{10}$$

In the compliance matrix form S_{ij} of a transversely-isotropic material, equations 7-10 reduce the compliance matrix of orthotropic materials, given in equation 6, to the form:

$$[S] = \begin{bmatrix} \frac{E(1-n\nu^2)}{m(1+\nu)} & \frac{E(\nu+n\nu^2)}{m(1+\nu)} & \frac{E\nu}{m} & 0 & 0 & 0 \\ & \frac{E(1-n\nu^2)}{m(1+\nu)} & \frac{E\nu}{m} & 0 & 0 & 0 \\ & & \frac{E_3(1-n\nu^2)}{m(1+\nu)} & 0 & 0 & 0 \\ & (sym.) & & \frac{E}{2(1+\nu)} & 0 & 0 \\ & & & & G_3 & 0 \\ & & & & & G_3 \end{bmatrix} \tag{11}$$

where, $n = E_3/E$ and $m = 1-\nu-2n\nu^2$

In the stiffness matrix form, the following additional conditions also apply for transversely isotropic materials (Rho, 1996)

$$c_{31} = c_{13} = c_{23}$$

(12)

$$c_{66} = \frac{1}{2}(c_{11} - c_{12}) \tag{13}$$

Constitutive Relationships for Shock Wave Propagation

A shock wave passing through a material has an appreciable effect on the nature of the behavior of the material (Stepanov, 1970). Shock waves are often characterized by a sudden rise from ambient pressure to the maximum pressure in the system, with the velocity of the sound waves and wave components at higher pressure moving faster than those at lower pressure (Fagnan et al., 2006). Shock wave equations in a medium can be described by Euler's equations of gas dynamics as a compressible flow in a medium, that obey nonlinear conservation laws of mass, momentum, and energy and by Rankine-Hugoniot relations (Stepanov, 1970 and Isbell, 2005).

The system of equations governing Eulerian gas dynamics is given below (Yin, 2004)

$$\begin{cases} \partial_t \rho + \nabla(\rho U) = 0, \\ \partial_t (\rho U) + \nabla(\rho U \otimes U + pI) = 0, \\ \partial_t (\rho e + \frac{1}{2}\rho U^2) + \nabla\left\{\left(\rho e + \frac{1}{2}\rho U^2 + p\right)U\right\} = 0, \\ \rho_{t=0} = \overline{\rho} + \xi\rho_0(x), U_{t=0} = \xi u_0(x), S_{t=0} = \overline{S} \end{cases} \tag{14}$$

where, U = velocity of wave in x, y, and z directions,

ρ = density of the material,

p = pressure of the shock wave ,

e = internal energy,

I = unit 3x3 matrix,

S = specific entropy, and

$\xi > 0$.

Speed of sound (α) in Eulerian gas dynamics is given by the relation:

$$\alpha^2 = \gamma * \frac{p}{\rho} \tag{15}$$

where, γ = Ratio of specific heats of medium at constant pressure to constant volume.

Rankine-Hugoniot relations help describe the state of the material behind the shock from the measured velocities of propagation and assume equilibrium conditions on either side of the shock front zone (Isbell, 2005). Rankine-Hugoniot conservation of momentum and energy relations can be simplified as:

$$\sigma - \sigma_0 = \rho_0(\alpha - U_0)(U - U_0) \tag{16}$$

$$e - e_0 = \frac{1}{2}(\sigma + \sigma_0)\left\{\frac{1}{\rho_0} - \frac{1}{\rho}\right\} \tag{17}$$

where, U_0 and U = wave velocities of propagation waves ahead and behind the wave front, respectively, and

σ_0, ρ_0, and e_0 = stress, density, and internal energy of propagating medium ahead of the wave front, respectively.

In this study, the Euler's system of equation was modified using Tammann equation of states (EOS), which can be applied for flows with entropy changes (Saito et al., 2003). The Tammann EOS was used by Saito et al. (2003) in their study on underwater shock wave attenuation. Speed of sound in terms of Tammann EOS is written as:

$$\alpha^2 = \frac{n}{\rho}(p + P_c) \tag{18}$$

where, P_c = pressure constant, and

n = polytropic constant, depending on medium of propagation.

Generally, two types of waves propagate in an elastic solid. These are P-waves (pressure or primary waves) and S-waves (shear or secondary waves) which are a result of compression or normal stresses and shear stresses, respectively (Fagnan et al., 2006). The system of equations of wave motion in terms of elasticity equations is given below. The stress (σ) and strain (ε) terms are expressed here as σ

$$\begin{aligned}
&\varepsilon_t^{11} - u_x = 0 \\
&\varepsilon_t^{22} - v_y = 0 \\
&\varepsilon_t^{33} - w_z = 0 \\
&\varepsilon_t^{12} - 0.5(v_x + u_y) = 0 \\
&\varepsilon_t^{23} - 0.5(w_y + v_z) = 0 \\
&\varepsilon_t^{13} - 0.5(u_z + w_x) = 0 \\
&\rho u_t - \sigma_x^{11} - \sigma_y^{12} - \sigma_z^{13} = 0 \\
&\rho v_t - \sigma_x^{12} - \sigma_y^{22} - \sigma_z^{23} = 0 \\
&\rho w_t - \sigma_x^{13} - \sigma_y^{23} - \sigma_z^{33} = 0
\end{aligned} \tag{19 a-i}$$

where, u,v,w = components of velocity,

ε^{ij} = components of the strain tensor

Using the above equations of motion and the linear relationship for Hooke's law, the constitutive relationship given by the following system of equations for an isotropic solid:

$$\sigma_t^{11} - c_{11}u_x - c_{12}v_y - c_{12}w_z = 0$$
$$\sigma_t^{22} - c_{21}u_x - c_{22}v_y - c_{23}w_z = 0$$
$$\sigma_t^{11} - c_{31}u_x - c_{32}v_y - c_{33}w_z = 0$$
$$\sigma_t^{12} - (\frac{c_{11} - c_{12}}{2})(v_x + u_y) = 0$$
$$\sigma_t^{23} - (\frac{c_{11} - c_{12}}{2})(v_z + w_y) = 0 \qquad \text{(20 a-i)}$$
$$\sigma_t^{31} - (\frac{c_{11} - c_{12}}{2})(w_x + u_z) = 0$$
$$\rho u_t - \sigma_x^{11} - \sigma_y^{12} - \sigma_z^{13} = 0$$
$$\rho v_t - \sigma_x^{12} - \sigma_y^{22} - \sigma_z^{23} = 0$$
$$\rho w_t - \sigma_x^{13} - \sigma_y^{23} - \sigma_z^{33} = 0$$

For a transversely isotropic material, the system of equations then becomes:

$$\sigma_t^{11} - c_{11}u_x - c_{12}v_y - c_{13}w_z = 0$$
$$\sigma_t^{22} - c_{21}u_x - c_{22}v_y - c_{13}w_z = 0$$
$$\sigma_t^{11} - c_{31}u_x - c_{32}v_y - c_{33}w_z = 0$$
$$\sigma_t^{12} - c_{44}(v_x + u_y) = 0$$
$$\sigma_t^{23} - c_{55}(v_z + w_y) = 0 \qquad \text{(21 a-i)}$$
$$\sigma_t^{31} - c_{66}(w_x + u_z) = 0$$
$$\rho u_t - \sigma_x^{11} - \sigma_y^{12} - \sigma_z^{13} = 0$$
$$\rho v_t - \sigma_x^{12} - \sigma_y^{22} - \sigma_z^{23} = 0$$
$$\rho w_t - \sigma_x^{13} - \sigma_y^{23} - \sigma_z^{33} = 0$$

where, σ^{ij} = components of the stress tensor

Modeling on FEMLAB 2.3

A multi-physics approach was implemented using FEMLAB 2.3 (COMSOL Inc., Burlington, MA) utilizing the structural mechanics and variable coefficient form modes. Structural mechanics module was used to assess the effects of the shock-wave generation, which were created using the equations in the general form module, by evaluating stresses and deformation on the sample.

Spadaro et al. (2002) described beef tissues as composite material with myofibers regularly distributed in a matrix of collagen and such behavior is responsible for transversely isotropic nature of the muscle. Therefore all myofiber rods display identical behavior with the same cross sectional area and length. Based on this observation, treatment, the following assumptions were considered for the beef loin:

- beef loin displays a transversely-isotropic behavior
- elastic behavior of the beef loin is linear
- beef loin structure is considered a continuum that allows propagation of waves
- beef loin is modeled as a 3-D elliptical plate of 2.54 cm thickness (fig. 5.3) and major axis of 20 cm and minor axis of 10 cm.
- Density of the loin 1100 kg/m^3 (Gennisson et al., 2003) and isotropic Young's modulus of 3.0 kPa (Chen et al., 1994) and Poisson's ratio of 0.26 (Segars et al., 1977)

The following assumptions were considered for the process conditions

- beef is assumed to be placed along the z-direction on a flat surface
- force of wave impacts along the z-direction of beef loin (fig. 5.2)
- there is no reflection of the pressure wave from the bottom of beef loin

Balance of force can be formulated in terms of the deformation components formulating a system of equations called Navier's equations of equilibrium, whose general form is given by (FEMLAB, 2003):

$$\rho \frac{\partial^2 \varepsilon_k}{\partial t^2} - \nabla . c * \nabla \varepsilon_k = K \qquad (22)$$

where, ε_k = deformation components in all 3 directions,

K = body forces, and

c^* = 3 x 3 matrix, comprised of 9 sub-matrices, given by (Hosten and Castaings, 2006):

$$c^*_{11} = \begin{bmatrix} c_{11} & 0 & 0 \\ 0 & c_{22} & 0 \\ 0 & 0 & c_{33} \end{bmatrix} \quad c^*_{12} = \begin{bmatrix} 0 & c_{12} & 0 \\ c_{12} & 0 & 0 \\ 0 & 0 & 0 \end{bmatrix} \quad c^*_{13} = \begin{bmatrix} 0 & 0 & c_{13} \\ 0 & 0 & 0 \\ c_{13} & 0 & 0 \end{bmatrix}$$

$$c^*_{21} = \begin{bmatrix} 0 & c_{12} & 0 \\ c_{12} & 0 & 0 \\ 0 & 0 & 0 \end{bmatrix} \quad c^*_{22} = \begin{bmatrix} c_{22} & 0 & 0 \\ 0 & c_{33} & 0 \\ 0 & 0 & c_{44} \end{bmatrix} \quad c^*_{23} = \begin{bmatrix} 0 & 0 & 0 \\ 0 & 0 & c_{23} \\ 0 & c_{23} & 0 \end{bmatrix}$$

$$c^*_{31} = \begin{bmatrix} 0 & 0 & c_{13} \\ 0 & 0 & 0 \\ c_{13} & 0 & 0 \end{bmatrix} \quad c^*_{32} = \begin{bmatrix} 0 & 0 & 0 \\ 0 & 0 & c_{23} \\ 0 & c_{23} & 0 \end{bmatrix} \quad c^*_{33} = \begin{bmatrix} c_{66} & 0 & 0 \\ 0 & c_{55} & 0 \\ 0 & 0 & c_{44} \end{bmatrix} \qquad (23\ a\text{-}i)$$

For a traction force $\boldsymbol{t}$ acting on a region S_2 on a bounded region S, the displacements e_k will occur on the remaining portion S_1 (fig. 5.1), for which the boundary conditions are:

$\varepsilon_k = \varepsilon_k^{*}$ on ∂S_1

$\sigma^{ij}n - \boldsymbol{t_i} = 0$ on ∂S_2

and $\varepsilon_z = 0$, based direction of incident pressure wave. (24 a-c)

Elastic coefficients c_{11}-c_{66} in equations 23 (a-i) were estimated from ultrasound. Methods and materials employed to estimate the elastic coefficient of the stiffness matrix are described in the next section.

MATERIALS AND METHODS

Ultrasound Velocity and Material Constants

Ultrasound techniques are widely used in non-destructive testing and to estimate mechanical properties of isotropic, transverse-isotropic, and anisotropic materials (Shull, 2002). Material stiffness for small deformations can be non-destructively measured based on the principle that velocity of sound in a homogeneous continuum or non-porous material is proportional to the square root of its elastic modulus (Martin et al., 2004).

Upon application of a mechanical wave pulse to an isotropic and homogeneous solid, shear and compression waves are generated in the medium (Gennisson et al., 2003) whose speeds are related to the elastic Lame' constants- Lame's first parameter (λ) and shear modulus (G) by the equations:

$$V_c = \sqrt{\frac{\lambda + 2G}{\rho}} \quad \text{and} \qquad V_s = \sqrt{\frac{G}{\rho}}, \tag{25}$$

where, ρ = density of the material, and

ν = Poisson's ratio.

Young's modulus, E is given by the relation:

$$E = \frac{G(3\lambda + 2G)}{\lambda + G} \tag{26}$$

In the case of a transversely isotropic solid, the elastic moduli in the stiffness matrix can be solved by estimating the speeds of the compression and shear waves along the *z* direction, which is perpendicular to the fibers in the *x* directions, and also by estimating the speed for the shear wave with a polarization perpendicular and parallel to the fibers. Determination of the elastic coefficients of the C_{ij} matrix for a transverse-isotropic material can be determined based on the following relations (Rho, 1996):

$$c_{11} = \rho v_1^2 \tag{27}$$

$$c_{22} = \rho v_2^2 \tag{28}$$

$$c_{33} = \rho v_3^2 \tag{29}$$

$$c_{44} = \rho v_{23}^2 \tag{30}$$

$$c_{55} = \rho v_{13}^2 \tag{31}$$

$$c_{66} = \rho v_{12}^2 \quad (32)$$

$$c_{12} = c_{11} - 2 * c_{66} \quad (33)$$

where, ρ = density of the material,

v_i = velocity of the longitudinal wave in the direction *i*, and

v_{ij} = velocity of a shear/transverse wave in the direction *i* and particle motion along *j*.

In this study, the elastic coefficients of the C_{ij} matrix for beef muscle were determined using longitudinal and shear transducers, which were then implemented in the model. The sample preparation and testing procedure is described in detail.

Sample Testing and Preparation

Beef loins, control (non HDP-treated) and HDP-treated loins (with 50, 75, and 100g) charges were acquired from USDA-ARS, Beltsville, MD. A total of 30 samples were received, from which 10 samples were used for estimating elastic constants out of which. Four among the 10 samples were treated with 75 g charges, and two each for 50 g and 100 g charge treatments and controls.

Raw beef loins were thawed and then cut into rectangular blocks along the direction of fibers. These rectangular blocks were then frozen again to -4 ºC to arrest aging of beef, which occurs between 1 to -1 ºC (Epley, 2009, Hedrick et al., 1993). From these sections, square to rectangular shaped sections of thicknesses ranging from 0.3-0.5 cm and dimensions ranging from 1.5-2.0 cm were cut along the prescribed 1, 2, and 3 directions. Figure 5.4 indicates a schematic

representation of a rectangular block of beef loin and how each section was cut from it. This extraction of sample sections for measuring elastic constants was followed as per the procedure described in detail by Kriz and Stinchomb (1979).

Approximately 2-4 sections for each direction were cut out from the samples and then frozen again to -4 ºC prior to testing in freezer bags. In addition to preventing aging, freezing allowed propagation of shear waves since they get highly attenuated in fluid-rich medium like animal tissue. Freezing also prevented damage to the specimens during ultrasound acquisition since the cross sectional area and thickness of the samples being tested were very small (figs. 5.5 and 5.6). Dimensions of the frozen sections (length, width, and thickness) were measured using calipers and each sample was weighed to estimate the density of the material which was used in estimation of the diagonal elastic coefficients (c_{11}-c_{66}) of the C_{ij} matrix.

Ultrasound velocity in the frozen sections in the prescribed 1, 2, and 3 directions were determined using longitudinal and shear wave transducers. A 250 kHz Ultran W-series standard miniature contact transducer (The Ultran Group, State College, PA) was used for estimating the longitudinal wave velocities and for estimation of shear wave velocities, a 2 MHz Ultran SWC50, 0° shear wave transducer (The Ultran Group, State College, PA) was used. Both longitudinal and shear wave transducers were set to analyze in through-transmission mode to prevent attenuation in the sample. An Ultran BP-9400A signal transducer was used to generate acoustic pulses, which were received by an Ultran BR-640A broadband receiver (The Ultran Group, State College, PA). The received pulses were sent to a 100 MHz Tektronix® oscilloscope, model 2230 with a GPIB interface (Tektronix Inc., Richardson, TX), connected to a computer which was used to acquire the signal.

Ultrasound time of flight through the sample was calculated using a fast Fourier transform method, as explained in chapter II, using a reference signal (without any medium in between transducers) and the signal acquired for the samples. The calculated time of flight was converted to velocity by dividing it by the sample thickness (l) using the following equation (Antonova et al., 2003)

$$v_{sample} = \frac{l}{(TOF - TOF_0)} \tag{34}$$

where, v_{sample} = ultrasound velocity through the beef sample (m/s)

l = thickness of the sample (m)

TOF = time of flight with the sample between the transducers (m/s)

TOF_0 = time of flight without the sample between the transducers (m/s)

RESULTS AND DISCUSSION

Estimation of Elastic Coefficients using Ultrasound Velocity

The elastic coefficients of the diagonal of the stiffness matrix C_{ij} were estimated using ultrasound methods as described. Only the diagonal coefficients of the matrix could be estimated via experimental methods due to the fact that

- estimation of c_{23}, c_{13}, and c_{12} require extraction of samples in the 2/3, 1/3, and 1/2 orthogonal directions

- wave motion of the shear transducer must propagate in the $(i+j)/\sqrt{2}$ direction with particle motion in the i-j plane for estimating the above 3 elastic constants (Rho, 1996)

This was very difficult to achieve with the nature of the biological material in beef, which does not possess a rigid structure to enable precise cutting in the given directions. In addition, wave motion in the $(i+j)/\sqrt{2}$ direction involves estimation of the wave's quasi-longitudinal (Q_L) and quasi-transverse (Q_T) components and the sample thickness must be cut sufficiently thick to allow the separation of these components (Kriz and Stinchomb, 1979), which could not be achieved.

Speed of the longitudinal wave in the frozen beef muscle ranged from 1000-1950 ms^{-1}. Gennisson et al. (2003) reported speed of longitudinal waves in beef muscle at room temperature at around 1500 ms^{-1} and Park and Chen (1997) reported it around 1618 ms^{-1}. Higher values of longitudinal velocity reported in this study can be attributed to freezing the sample. Miles and Cuttin (1974) reported that speed of longitudinal waves were about 70% higher at -5 ºC than the speed of waves in water (1402 ms^{-1}). Sigfusson et al. (2004) in their study in monitoring freezing in blocks of biological materials- beef, chicken, and gelatin, also reported an approximate 43% reduction in ultrasonic TOF, and hence an increase in wave velocity, from 18 ºC to -5 ºC.

Shear wave velocity in the frozen beef muscle ranged from 15 ms^{-1} (perpendicular to fibers) to 40 ms^{-1} (parallel to the fibers) which were in accordance with the values reported by Gennisson et al. (2003) in their experiments in characterizing shear wave speeds in muscle (10 ms^{-1} and 28 ms^{-1}, respectively). The increase could also be attributed to freezing, and is

corroborated by Lee et al. (2004) who reported an increase in shear wave velocity in frozen orange juice from 1700 ms^{-1} at -20 ºC to 2000 ms^{-1} at -50 ºC.

Table I gives the values of the diagonal elastic coefficients estimated using ultrasound. It can be inferred that the values for $c_{11,}$ c_{22}, and c_{33} were found to be much higher than the estimated values of isotropic moduli in beef muscle. Chen et al. (1994 and 1996) estimated isotropic Young's modulus values from 3.0 kPa to 6.0 kPa in beef muscle, undergoing small strains in the range of 1-5%, using ultrasound methods, lower than the reported values by a magnitude of 6. However, the reported values for the three elastic constants agree with the reported values of longitudinal wave speeds in beef muscle. Since there exists no other study on estimation of transverse isotropic elastic coefficients of the stiffness matrix on beef muscle, these estimated values were used in this study, combined with the off-diagonal elements of human cortical bone (Rho, 1996). The off-diagonal coefficients of cortical bone were derived from the compliance matrix reported by Rho (1996) and used in equations 23 (a-i) in FEMLAB 2.3.

Effect of HDP-treatment on elastic coefficients

Percentage change in the elastic coefficients was measured post-treatment for each amount charge (50, 75, and 100 g) when compared to the controls as given in Table II. Results indicated that many values of the elastic coefficients indicated an increase after HDP-treatment. Reduction of the coefficients c_{55} and c_{66} was observed in 6 and 5 samples from the HDP-treated set, respectively, but only one sample indicated a decrease in value for the coefficient c_{44}, out of the 8 treated samples. Highest values of reduction for c_{44} and c_{66} at 1.58% and 44.2%, respectively were observed when samples were treated with the 75 g charge where as the highest

reduction for c_{55} at 36.2% was observed when the sample was treated with a 100 g charge. Treatment with the 75 g and 100 g charges were found to be most effective in reduction of these coefficients. HDP-treatment led to an increase in these values or coefficients c_{11}, c_{22}, c_{33}, in 6, 7, and 5 samples out of the 8 treated samples. Highest values of increase for c_{11} and c_{33} 65.24% and 101.24%, respectively were observed when samples were treated with the 75 g charge and the highest value of increase for c_{22} was observed when the samples were treated with the 50 g charge.

Results of numerical modeling

Finite-element modeling of a transversely isotropic elliptical plate, simulating the beef muscle utilized off-diagonal elastic coefficients that were estimated from the compliance matrix for a cortical bone (Rho, 1996). The off-diagonal coefficient values estimated were c_{12} and c_{13} since from equation 11 it is established that $c_{13} = c_{23}$. These values were 1.03 GPa and 0.14 GPa, respectively for c_{12} and $c_{13}= c_{23}$. For the shock wave propagation through the material the polytropic constant (n) for the Tammann EOS was assumed to be 7.15 and the pressure constant (P_c) to be 300 MPa, as was used by Saito et al. (2003).

Stress Analysis

The von-Mises stress is a representation of the stress tensor and gives an idea of the load acting on the medium. It is expressed by:

$$\sigma_{VM} = \sqrt{\frac{(\sigma_{11} - \sigma_{22})^2 + (\sigma_{22} - \sigma_{33})^2 + (\sigma_{11} - \sigma_{33})^2 + 6 * (\sigma_{12}^2 + \sigma_{23}^2 + \sigma_{31}^2)}{2}} \quad (35)$$

The corresponding effective strain or deformation is expressed as:

$$\varepsilon_{VM} = \frac{2}{3} * \sqrt{\frac{(\varepsilon_{11} - \varepsilon_{22})^2 + (\varepsilon_{22} - \varepsilon_{33})^2 + (\varepsilon_{11} - \varepsilon_{33})^2}{2} + \frac{3}{4}(\varepsilon_{12}^2 + \varepsilon_{23}^2 + \varepsilon_{31}^2)} \quad (36)$$

Simulations were run with an initial load of 800 MPa (fig. 5.7), and two pressures at 800 MPa and 600 MPa were used to analyze the total deformation and von-Mises stresses on the material.

The issues with modeling involved predicting the values for the Dirichlet boundary conditions for the shock wave pressure through the continuum. While the initial value for pressure was based on the values for incident waves used in simulation, the final values of pressure and wave velocities at the boundaries was considered along the dimensions of the beef loin being simulated, i.e. the length, width (major and minor axis of the ellipse) and the thickness of the sample (NDT, 2009):

$$P_l = P_0 e^{-kL} \quad (37)$$

where, P_l = pressure of the shock wave front (Pa)

P_0 = Initial pressure (Pa)

k = attenuation coefficient

L= dimension length of the sample (m)

Figures 5.8-5.11 indicate that the finite-element simulation of the shock wave using non-linear Eulerian equation was not simulated very well through a continuum of beef muscle. The effective von-Mises stresses on the model were simulated to be negative and there was no deformation response in the material. Initially it was assumed that the lack of deformation behavior in the sample was due to the very high values (in the range of GPa) of the experimentally derived elastic constants of the beef muscle, but upon simulations assuming isotropic behavior of beef muscle, it was inferred that the elastic behavior of the beef loin, within the elastic limit, could not be described by the propagation of a shock wave described by a non-linear stationary simulation Euler's equation. As a result, a sensitivity analysis using different values of attenuation coefficient, polytropic constant, and pressure constant could not be performed and a correlation between experimentally derived WBS and TPA features and numerically simulated values of deformation and strains in the three directions could not be established.

Modeling Linear Shock Wave Propagation

Due to the failure of the Euler's equation to explain the stress and deformation behavior in the loin, the model was implemented based on linear response. A simpler approach was assumed, with the pressure wave acting on the beef loin and attenuating within the loin based on the relationship given in equation 37. The pressure wave was assumed to propagate along the z-direction alone, and the material was simulated for both isotropic and transversely isotropic behavior for the interaction of the attenuating pressure wave with the elastic components of the

beef loin. Operating pressures of 800 MPa and 600 MPa were utilized for this approach, and an attenuation coefficient value of 9.1×10^5 s^{-1} was adopted from Tham et al. (2007).

Isotropic Behavior

Results from this modeling approach indicated that the pressure behavior in the sample was of a completely compressive nature. The von-Mises stresses for 800 MPa pressure assuming isotropy of beef muscle is given in figure 5.12. It can be inferred that the beef model was subjected to a unidirectional force of 800 MPa. For simplicity, it was also assumed that the time period of propagation was along the z-axis. Since the thickness of the sample was only 2.54 cm or 1", there was not sufficient time or distance for the pressure wave to attenuate in the medium and therefore the von-Mises stress response was a direct function of the incident pressure wave. Deformation behavior of the beef model assuming isotropy of beef muscle at 800 MPa is given in figure 5.13. The figure clearly indicates that the beef model underwent an unrealistic minimum deformation of 800 m at the top of the beef model, with much larger values of deformation around 2000 m along the x and y axes. This however indicated that the pressure wave caused complete irreversible deformation which could be attributed to the isotropic constants of Young's modulus of 3.0 kPa (Chen et al., 1994) and Poisson's ratio of 0.3 (Segars et al., 1977) which were assumed for the model. The same behavior was observed with an initial pressure of 600 MPa, the only difference being the amount of deformation the model underwent which reported to be a maximum of 1650 m. deformation. This also indicated that the model behavior was similar to the rheological model in chapter 4, which saw complete deformations at pressures as low as 50 kPa

This deformation behavior however, contradicted the boundary conditions for the model given in equations 24 (a-c). According to the given boundary conditions, the lower values of deformation must occur at the base of the model, considering no reflecting surface and no displacement along the z-direction. The reason for this aberration could not be ascertained.

Transversely Isotropic Behavior

Diagonal coefficients of the stiffness matrix estimated from ultrasound velocity and off-diagonal coefficients assumed from human cortical bone (Rho, 1996) and were used in equations 23 (a-i) in FEMLAB. The von-Mises stresses for 800 MPa pressure assuming transversely isotropic behavior of beef muscle is given in figure 5.14. As in the model assuming isotropic behavior, the stress response acted on the entire sample, without having undergone complete attenuation. However, the resultant compression stress on the model was much lower than the incident pressure wave, ca. 100 MPa. This could be due to the high values of the elastic coefficients c_{11}, c_{22}, and c_{33} in the model, which were experimentally estimated in the order of gigapascals. This was also due to the high values of the off-diagonal coefficients assumed from study by Rho (1996). These high elastic coefficient values also resulted in much lower deformation of the beef model as indicated in figure 5.14. A maximum deformation of 0.2 m was seen at the top of the beef model and the lower values of 0.04 m were seen at the base of the model. It can be inferred that the transversely isotropic behavior of the beef model, due to its high values of elastic coefficients, was able to impede the incident pressure wave in the material and reported more realistic values of deformation, which also obeyed the boundary conditions as per equations 24 (a-c).

Since it was inferred from the previous study that the attenuation coefficient had no role in attenuating the pressure wave, due to the small thickness of the model, a sensitivity analysis using attenuation coefficient was not needed. High values of elastic coefficients for the transversely isotropic considerations for the model indicated that these values were positively correlated to resistance to stress. The model for this study was however very simple and did not simulate underwater shock wave behavior and its effects on a beef loin since only longitudinal compression waves were assumed. In order for wave propagation in different modes to occur, these waves need to be focused. HDP-treatment at the USDA-ARS, Beltsville facility use a metal plate to reflect shock waves onto the meat product, as indicated in chapter 3, but there is no method employed for focusing the incident wave. Future studies must account for modeling using the reflected component of the wave, which could give better results and realistically simulate propagation of shock waves in beef loins.

CONCLUSIONS

The FEM model used to simulate the effects of shock waves on the transversely isotropic behavior of beef muscle using Euler's equation and Tammann EOS was not successful in simulating the deformation response and stress behavior because of the non-linear nature of the Euler's equation describing wave propagation. Results from the model assuming linear propagation of shock wave indicated that the beef model assuming transversely isotropic behavior was found to resist deformation much better than the assumed isotropic behavior due to the estimated and assumed values of elastic coefficients.

The beef loin here was modeled as a transversely isotropic material, as per Spadaro et al. (2002). However, Weiss et al. (1996), Gennisson et al. (2003), and Fagnan et al. (2008) consider beef and soft tissue to display anisotropic nature requiring 21 elastic constants to describe their mechanical behavior. This poses a challenge for describing mechanical behavior considering the requirement to estimate all the elastic coefficients of the stiffness matrix C_{ij} and currently there is no published literature in estimation of all the elastic coefficients related to transverse isotropic behavior of muscle, although Gennisson et al. (2003) reported values for the coefficients c_{44}=110 kPa and c_{66} = 862 kPa. The values of c_{44} and c_{66} determined experimentally in this study corroborated very well with the values estimated by Gennission et al. (2003), but other values could not be corroborated. More studies are needed to standardize a method for estimating elastic coefficients from beef muscle, if modeling a more complicated anisotropic behavior of beef muscle is to be considered.

REFERENCES:

Barthelat, F. and H.D. Espinosa. 2003. Elastic properties of nacre aragonite tablets. *Proc. 2003 SEM Ann. Conf. and Expo on Exptl. And Appl. Mech.*, June 2-4, Charlotte, NC. Paper 187, Session 68.

Bonet, J. and A.J. Burton. 1998. A simple orthotropic, transversely isotropic hyperelastic constitutive equation computations. *Comput. Methods Appl. Engg.* 162, 151-164.

Chen, E.J., J. Novakofski, K. Jenkins, and W.D. O'Brien Jr.. 1994. Ultrasound elasticity measurements of beef muscle. *1994 Ultrasonics Symposium*, 1459-1462.

Chen, E.J., J. Novakofski, W.K. Jenkins, and W.D. O'Brien Jr.. 1996. Young's modulus measurements of soft tissues with application to elasticity imaging. *IEEE Trans. Ultrasonics, Ferroelectrics, and Freq. Control* 43 (1), 191-194.

Cleveland, R.O. and O.A. Sapozhnikov. 2005. Modeling elastic wave propagation in kidney stones with application to shock wave lithotripsy. *J. Acou. Soc. Am.* 118(4), 2667-2676.

Epley, R.J. 2009. Aging beef. University of Minnesota Extension. Available at http://www.extension.umn.edu/distribution/nutrition/DJ5968.html. Accessed May 23, 2009.

Fagnan, K., R.J. Leveque, T.J. Matula, and B. MacConaghy. 2008. High-resolution finite volume methods for extracorporeal shock wave therapy. *Proc. 11th Intl. Conf. Hyperbolic Problems*, June 17-21, 2006, Lyon, France. Springer Publication, New York, NY, 503-510.

FEMLAB. 2003. User's guide and introduction. *Version 2.3 by COMSOL*.

Gennisson, J-L, S. Catheline, S. Chaffai, and M. Fink. 2003. Transient elastography in anisotropic medium: Application to the measurement of slow and fast shear wave speeds in muscles. *J. Acoust. Soc. Am.*114(1), 536-541.

Guan, D., H. Chen, E. Y. Ting, and D. G. Hoover. 2006. Inactivation of *Staphylococcus aureus* and *Escherichia coli* O157:H7 under isothermal-endpoint pressure conditions. *J. Food Engg.* 77, 620-627.

Gulyaev, V.I., P.Z. Lugovoi, G.M. Ivanchenko, and E.V. Yakovenko. 1999. Interaction of shock-wave fronts with interface of transversely isotropic elastic media. *Intl. Appl. Mech* 35(4), 349-355.

Hedrick, H.B., Stringer, W.C., and C. Clarke. 1993. Recommendations for aging beef. University of Missouri Extension. Available at http://extension.missouri.edu/publications/DisplayPub.aspx?P=G2209. Accessed May 23, 2009.

Hosten, B. and M. Castaings. 2006. FE modeling of Lamb diffraction by defects in anisotropic viscoelastic plates. *NDT&E Intl.* 39, 195-204.

Isbell, W.M. 2005. *Shock waves: Measuring the dynamic response of materials*. Imperial College Press, London, UK.

Kaw, A.K. 1997. *Mechanics of composite materials- 2nd Edition*. CRC Press, Boca Raton, FL.

Klotz, B. D. L. Pyle, and B.M. Mackey. 2007. New mathematical modeling approach for predicting microbial inactivation by high hydrostatic pressure. *Appl. & Envtl. Microbiol.* 73(8), 2468-2478.

Koseki, S, Y. Mizuno, and K. Yamamoto. 2007. Predictive modelling of the recovery of *Listeria monocytogenes* on sliced cooked ham after high pressure processing. *Intl. J. Food Micro.* 119, 300-307.

Kriz, R. and W.W. Stinchomb. 1979. Elastic moduli of transversely isotropic graphite fibers and their composites. *Expt. Mech.* 19(2), 41-49.

Lee, S., L.J. Pyrak-Nolte, P. Cornillon, and O. Campanella. 2004. Characterization of frozen orange juice by ultrasound and wavelet analysis. *J. Sci. Food Agric.*84, 405-410.

Leveque, R.J. 2002. *Finite volume methods for hyperbolic problems*. Cambridge University Press, Cambridge, UK.

Martin, R.B., D.B. Burr, and N.A. Sharkey. 2004. *Skeletal tissue mechanics*. Springer Science, New York, NY.

Mihradi, S., H. Homma, and Y. Kanto. 2004. Numerical analysis of kidney stone fragmentation by short pulse impingement. *JSME Intl. Journal* 47(4), 581-590.

Miles, C.A. and C.L. Cutting. 1974. Changes in the velocity of ultrasound in meat during freezing. *J. Food Tech.* 9(1), 119–122.

Park, B.and Y.R. Chen. 1997. Ultrasonic shear wave characterization in beef *Longissimus* muscle. *Trans. ASAE* 40(1), 229-235.

Rho, J-Y. 1996. An ultrasonic method for measuring the elastic properties of human tibial cortical and cancellous bone. *Ultrasonics* 34, 777-783.

Reddy, J.N. 2006. *An introduction to the finite element method- 3rd edition*. McGraw Hill Inc, New York, NY.

Saito, T., M. Marumoto, H. Yamashita, S.H.R. Hosseini, A. Nagakawa, T. Hiranio, and K. Takayama. 2003. Experimental and numerical studies of underwater shock wave attenuation. *Shock Waves* 13, 139-148.

Saucedo-Reyes, D., A. Marco-Celdrán, M. C. Pina-Pérez, D. Rodrigo, and A. Martínez-López. 2009. Modeling survival of high hydrostatic pressure treated stationary- and exponential-phase *Listeria innocua* cells. *Innov. Food Sci. & Emerg. Tech.* 30, 135-141.

Segars, R.A., R.G. Hamel, and J.G. Kapsalis. 1977. Use of Poisson's ratio for objective-subjective texture correlations in beef: An apparatus for obtaining the required data. *J. Texture Studies* 8, 433-447.

Sigfusson, H., G.R. Ziegler, and J.N. Coupland. 2004. Ultrasonic monitoring of freezing. *J. Food Engg.* 62(3), 263-269.

Shull, P.J. 2002. *Non-destructive evaluation: Theory, techniques, and applications*. Marcel Dekker Inc., New York, NY.

Spadaro, V., Allen, D.H., Keeton, J.T., Moreira, R., and Boleman, R.M.. 2002. Biomechanical properties of meat and their correlation to tenderness. *J. Texture Studies* 33, 59-87.

Stepanov, G.V. 1971. Speed of propagation of elasto-platic shock waves in metals. *Str. Of Matls.*3(2), 229-232.

Tham, L-M., H.P. Lee, and C. Lu. 2007. Enhanced kidney stone fragmentation by short delay tandem conventional and modified lithotripter shock waves: A numerical analysis. *J. Urology* 178, 314-319.

Weiss, J.A., B.N. Maker, and S. Govindjee. 1996. Finite element implementation of incompressible, transversely isotropic hyperelasticity. *Comput. Methods Appl. Mech. Engg.* 135, 107-128.

Whittaker, A.D., B. Park, B.R. Thane, R.K. Miller, and J.W. Savell. 1992. Principles of ultrasound and measurement of intramuscular fat. *J. Ani. Sci* 70, 942-952.

Yin, H. 2004. Formation and construction of a shock wave for 3-D compressible Euler equations with the spherical initial data. *Nagoya Math. J.*, 175, 125-164.

LIST OF FIGURES

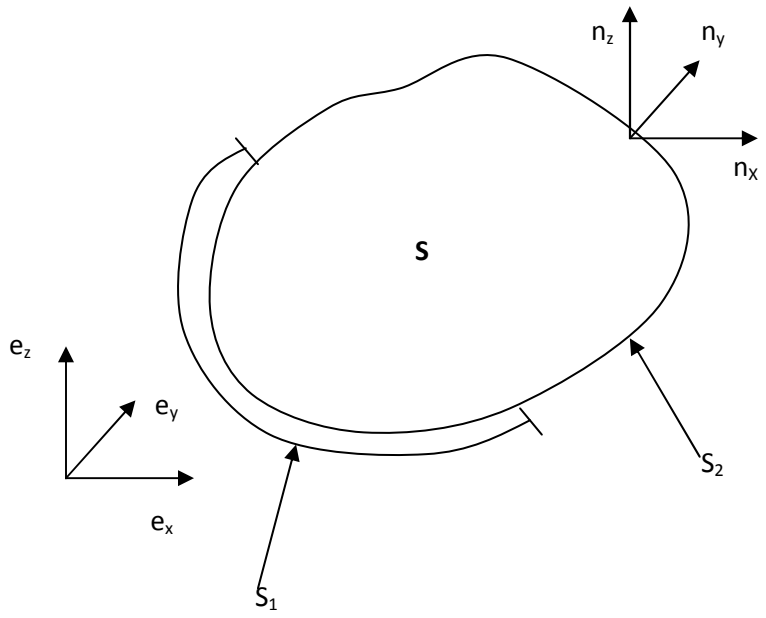

Figure 5.1: 3-D elastic body with displacements and forces (Reddy, 2006)

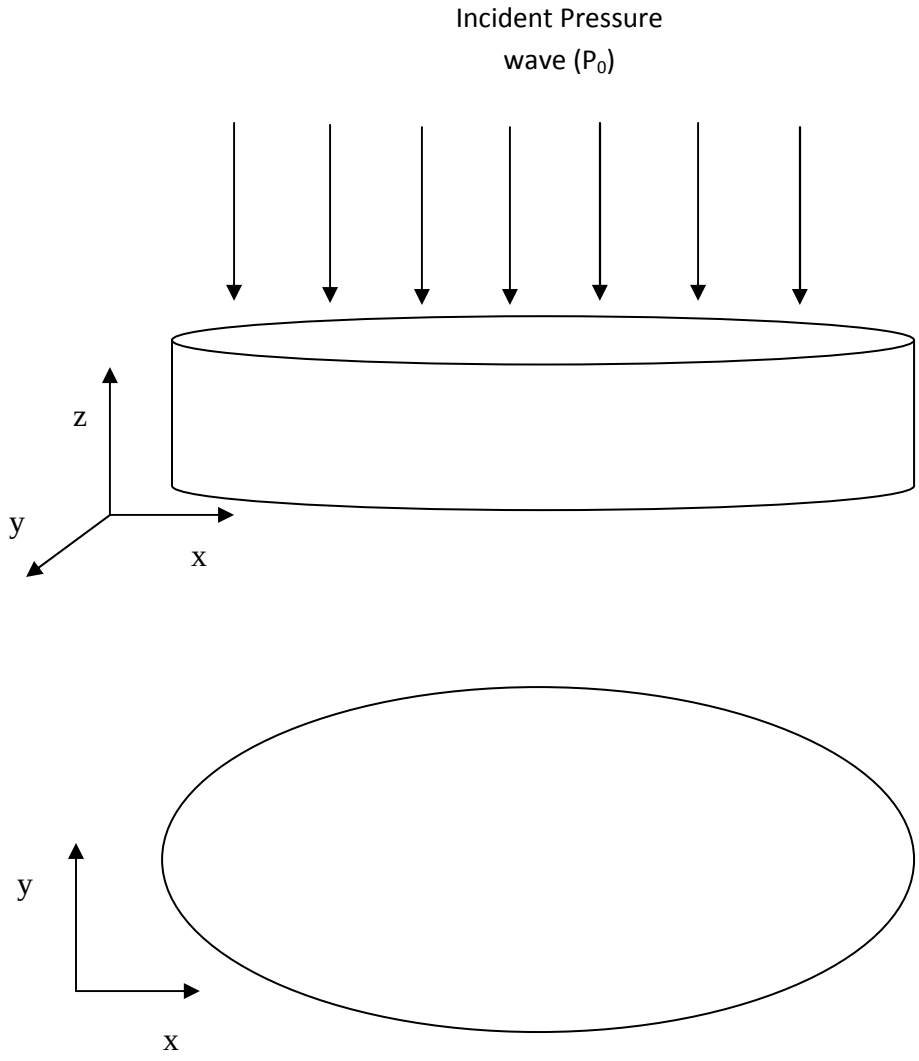

Figure 5.2: Schematic representation of incident shock wave (P_0) on sample

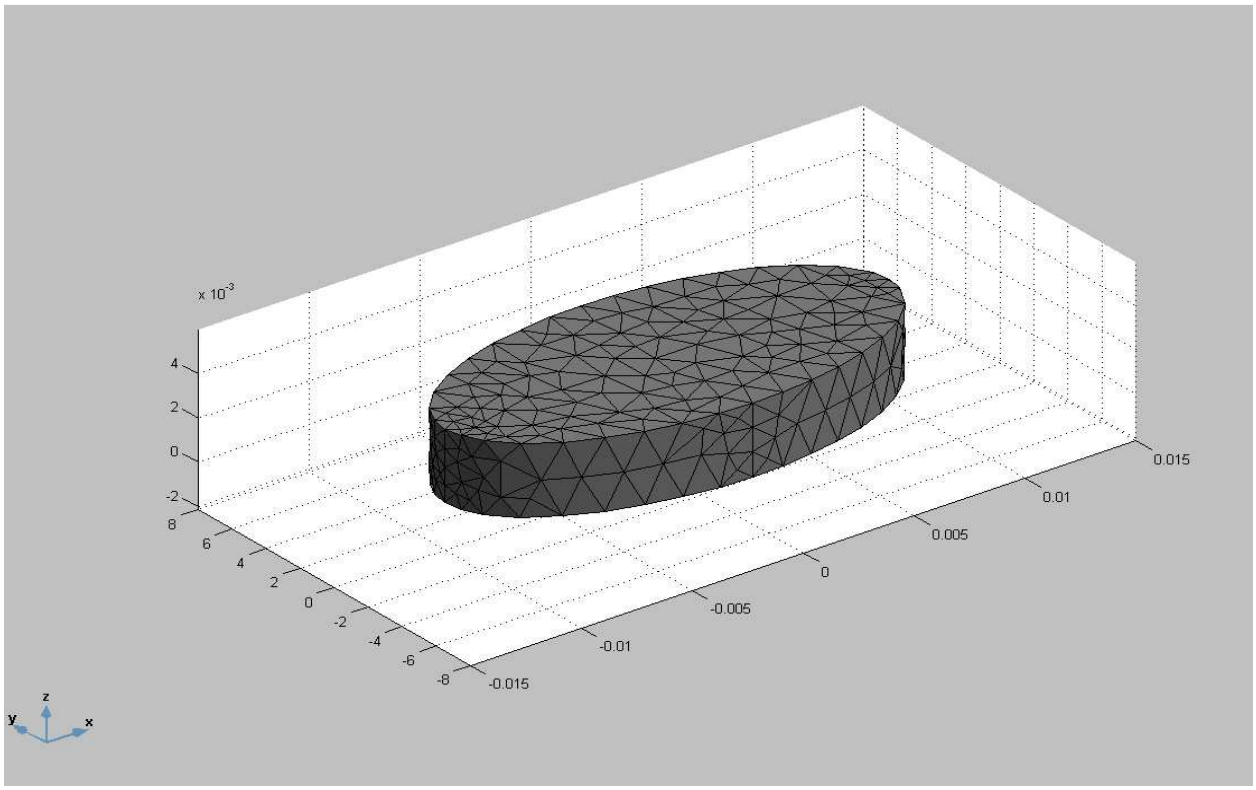

Figure 5.3: Elliptical plate model of beef with meshing

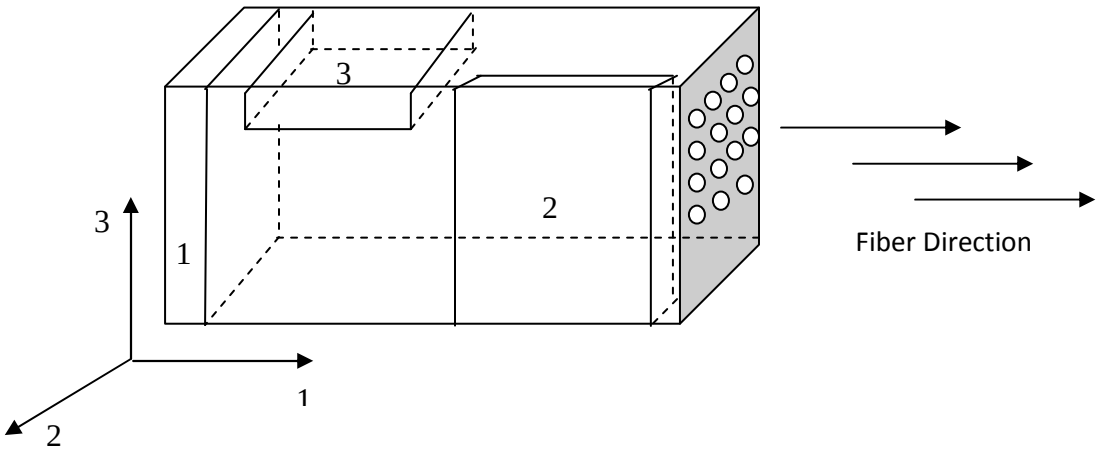

Figure 5.4: Extraction schematic for samples for elastic coefficient estimation using ultrasound

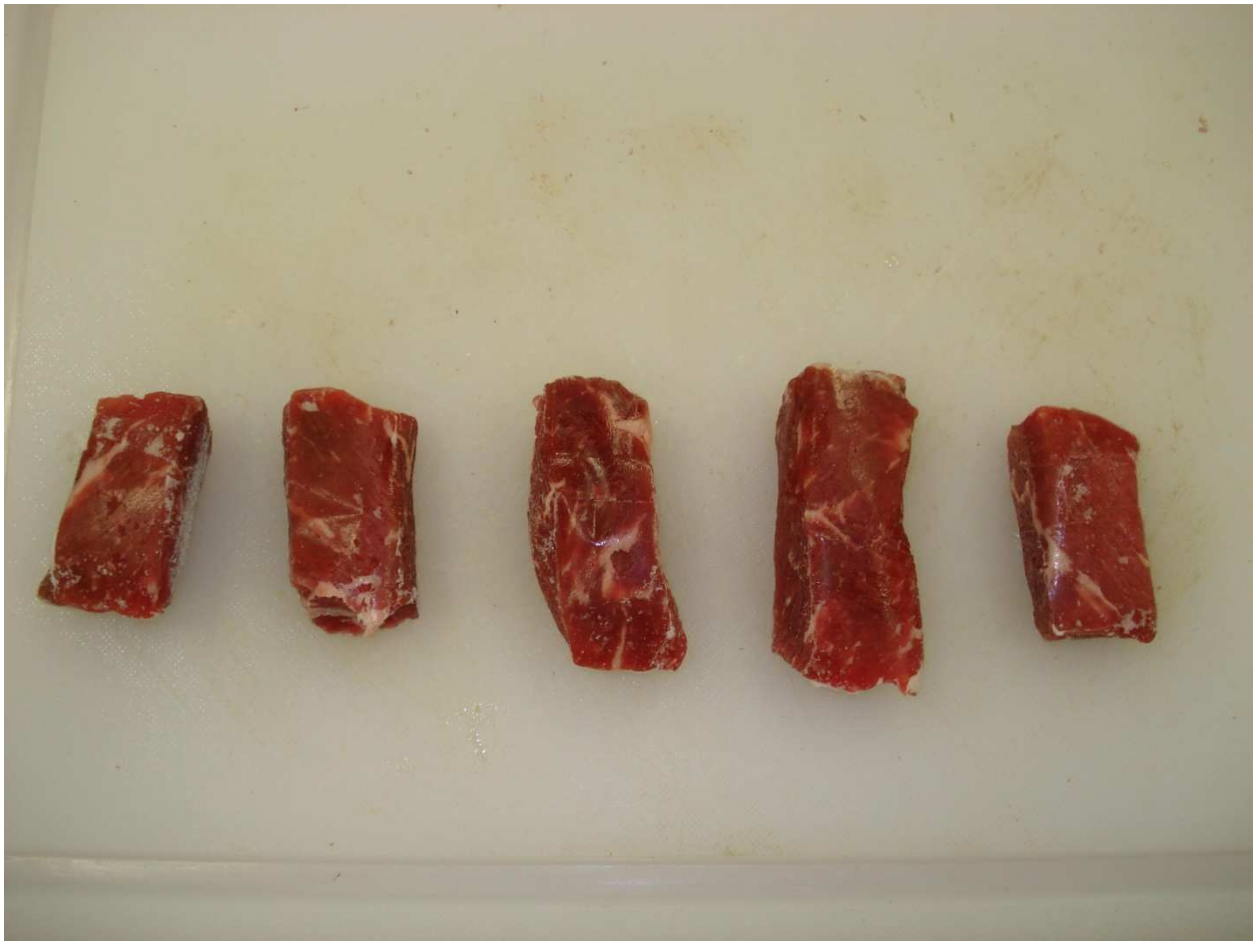

Figure 5.5: Frozen cylindrical segments of beef loins

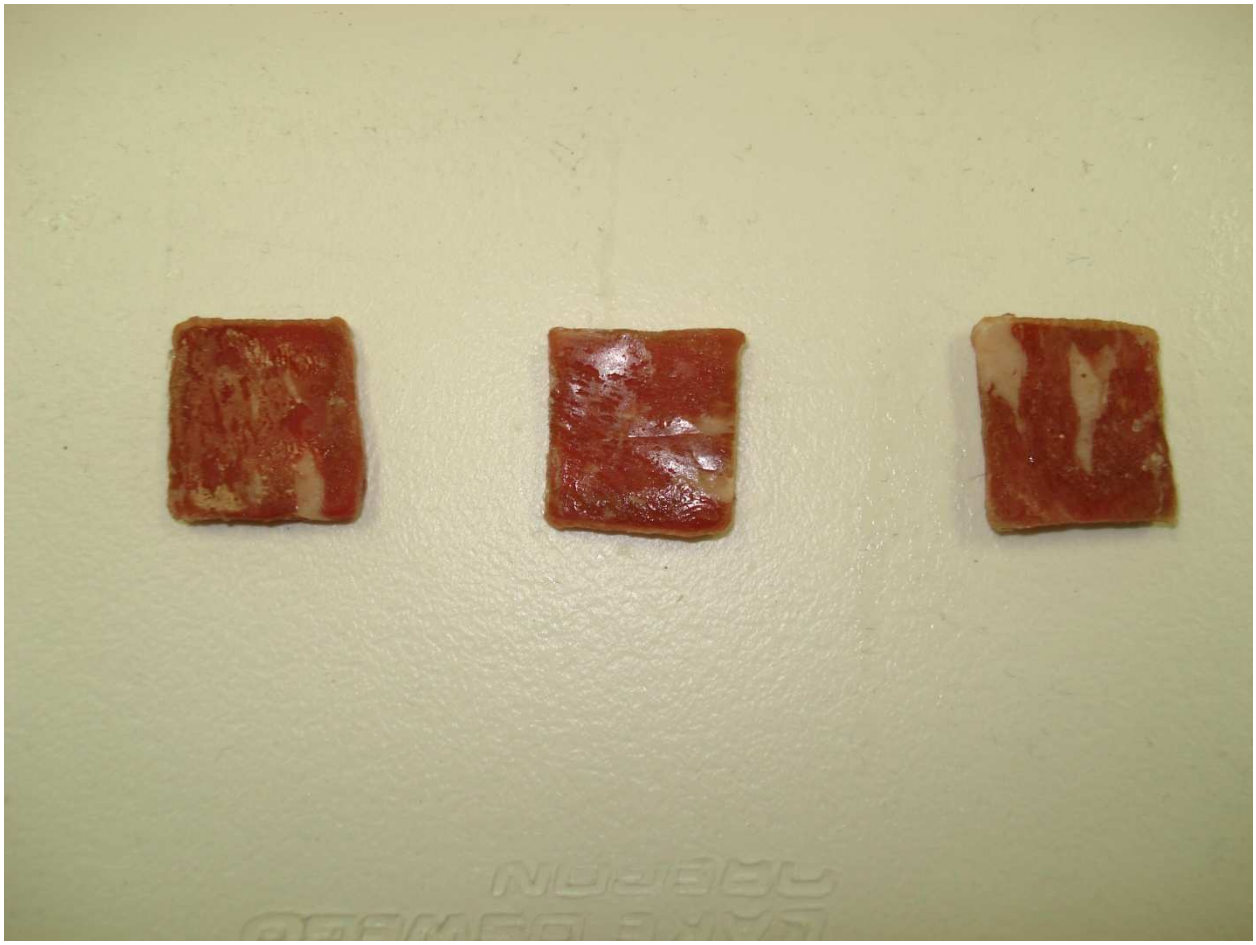

Figure 5.6: Frozen beef samples extracted for elastic coefficient estimation using ultrasound

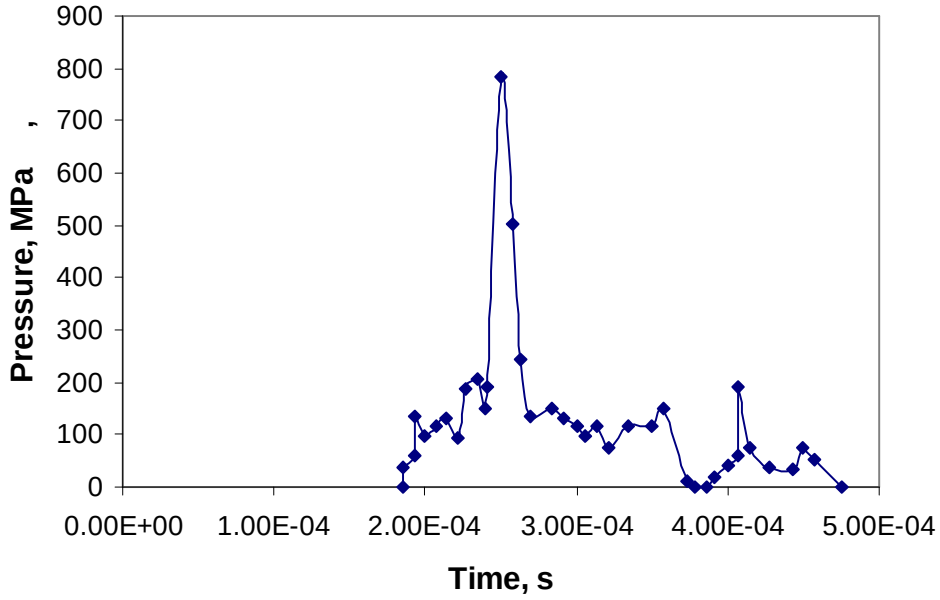

Figure 5.7: Time-pressure graph of incident shock wave during HDP-treatment (USDA-ARS proprietary information)

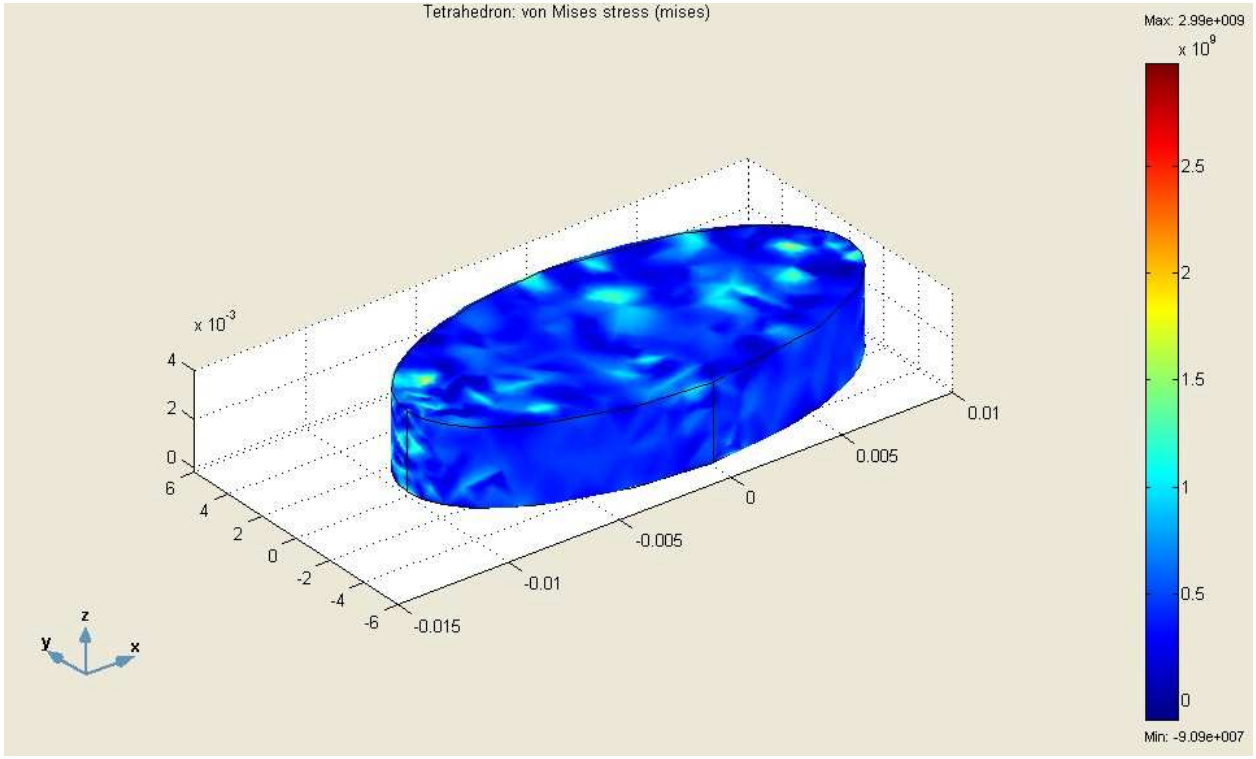

Figure 5.8: von-Mises stresses on beef model at 800 MPa for non-linear shock wave propagation

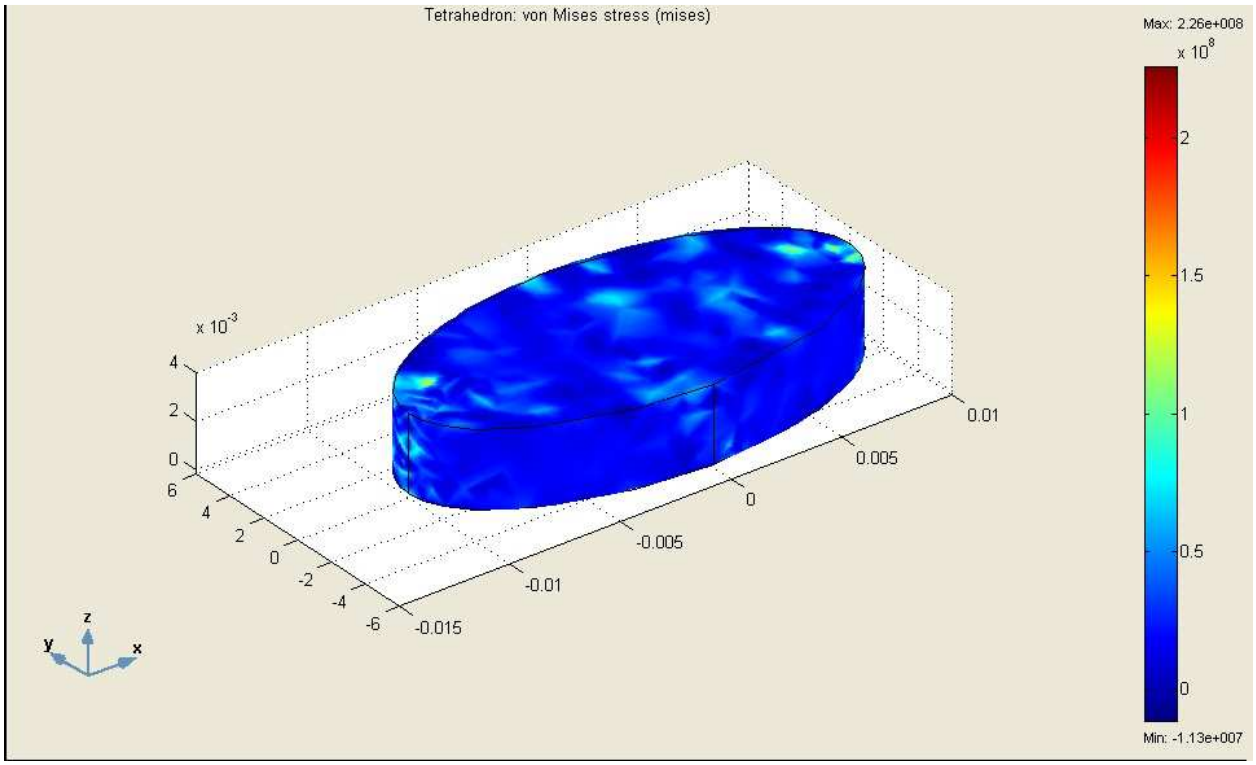

Figure 5.9: von-Mises stresses on beef model at 600 MPa for non-linear shock wave propagation

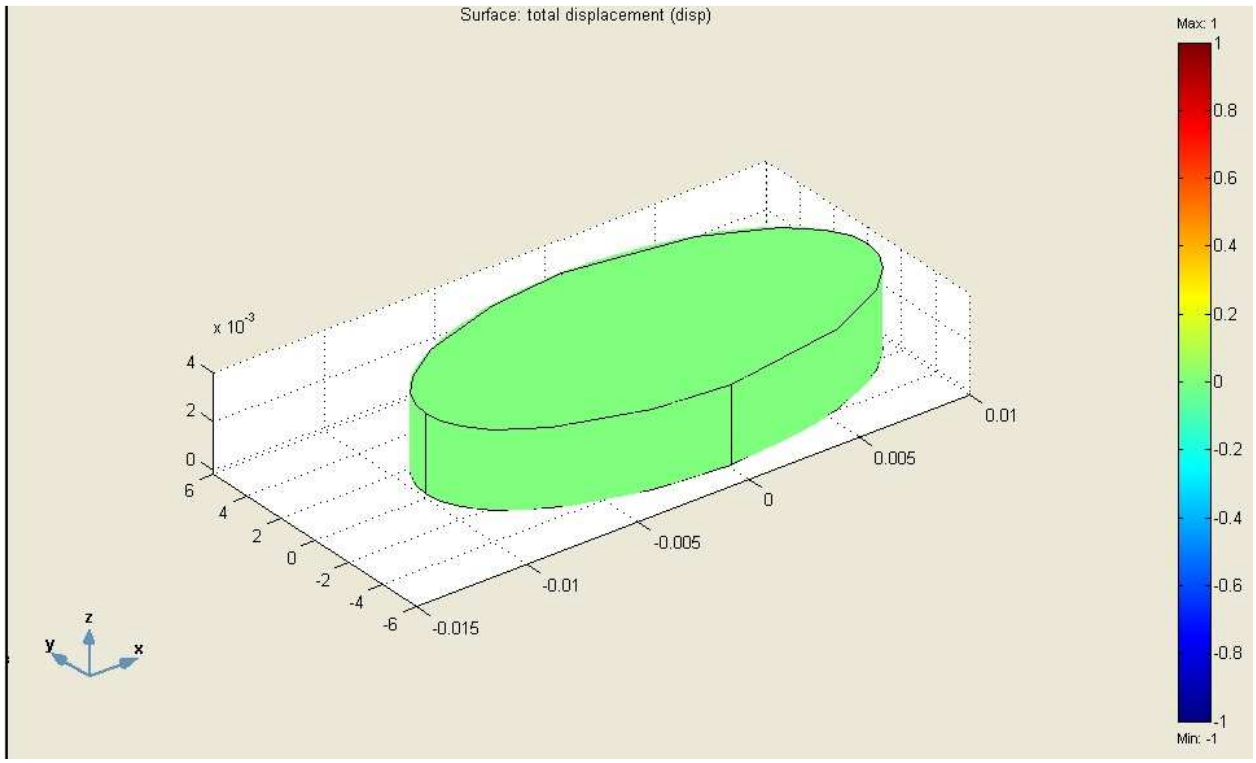

Figure 5.10: Deformation of beef model at 800 MPa for non-linear shock wave propagation

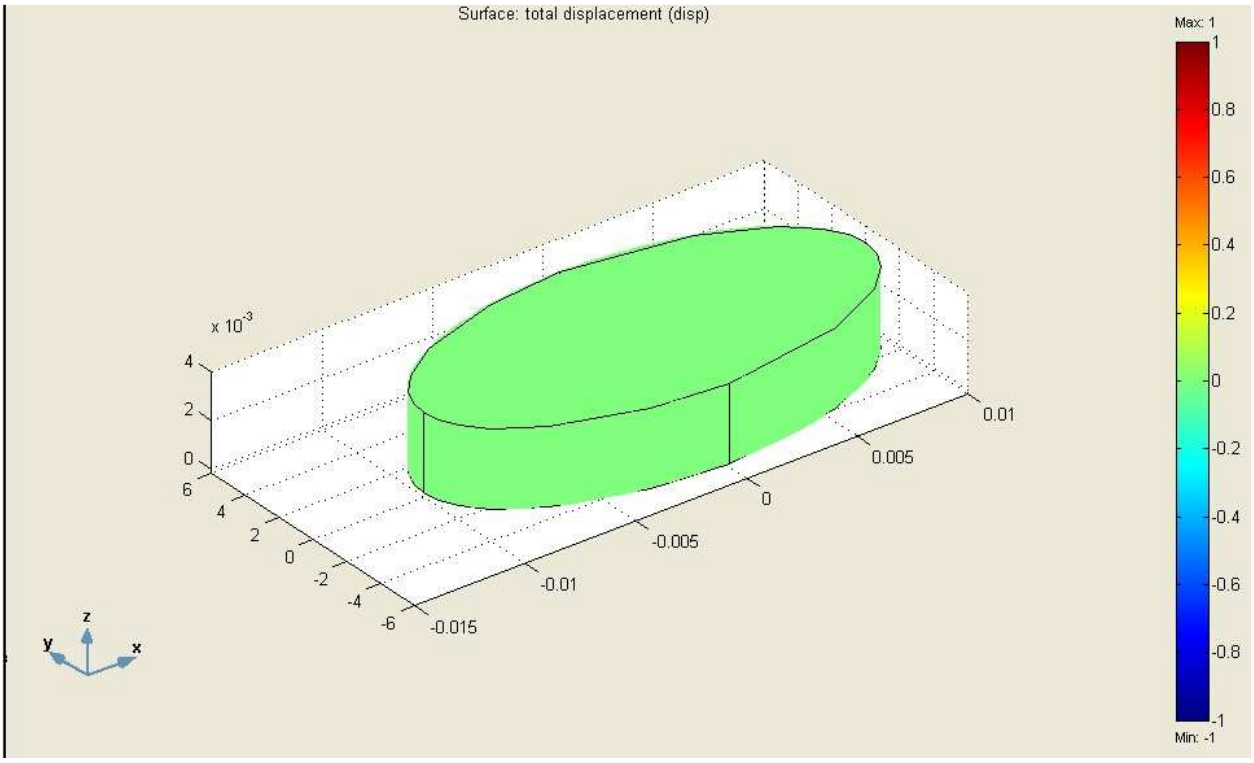

Figure 5.11: Deformation of beef model at 600 MPa for non-linear shock wave propagation

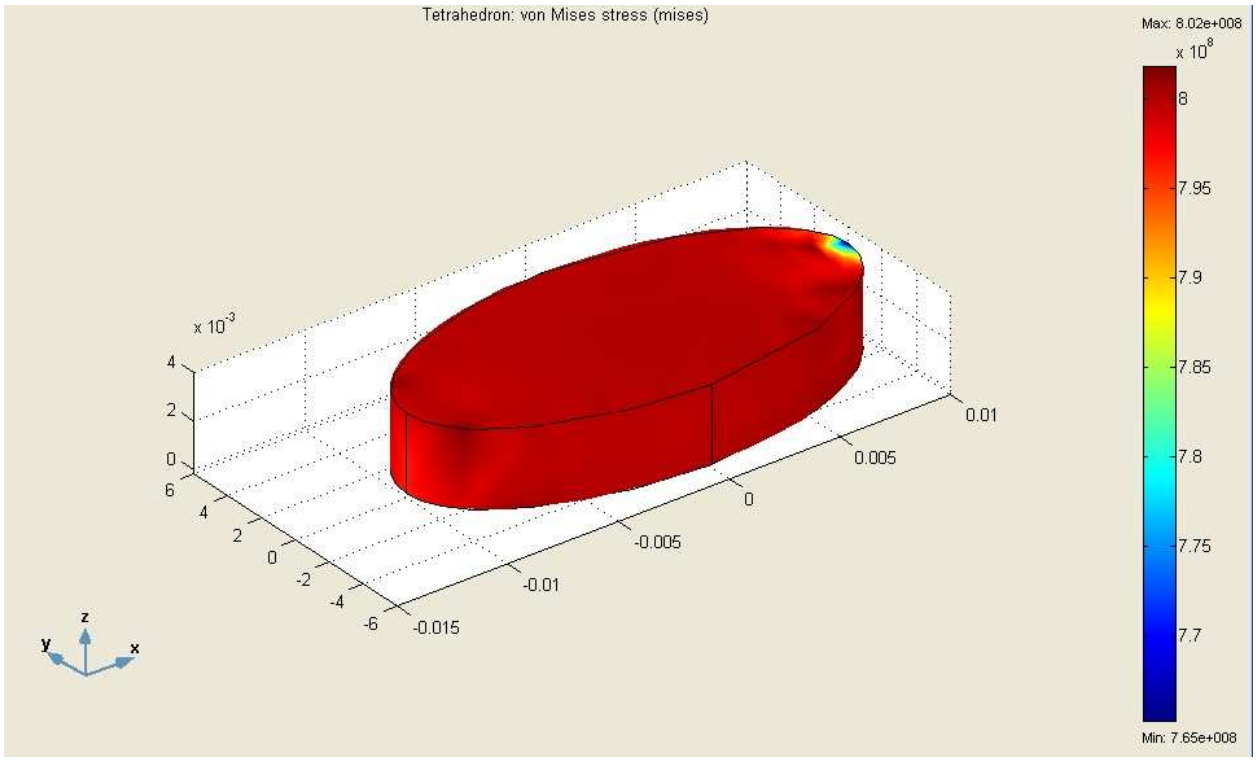

Figure 5.12: von-Mises stresses on beef model at 800 MPa for linear shock wave propagation assuming isotropy

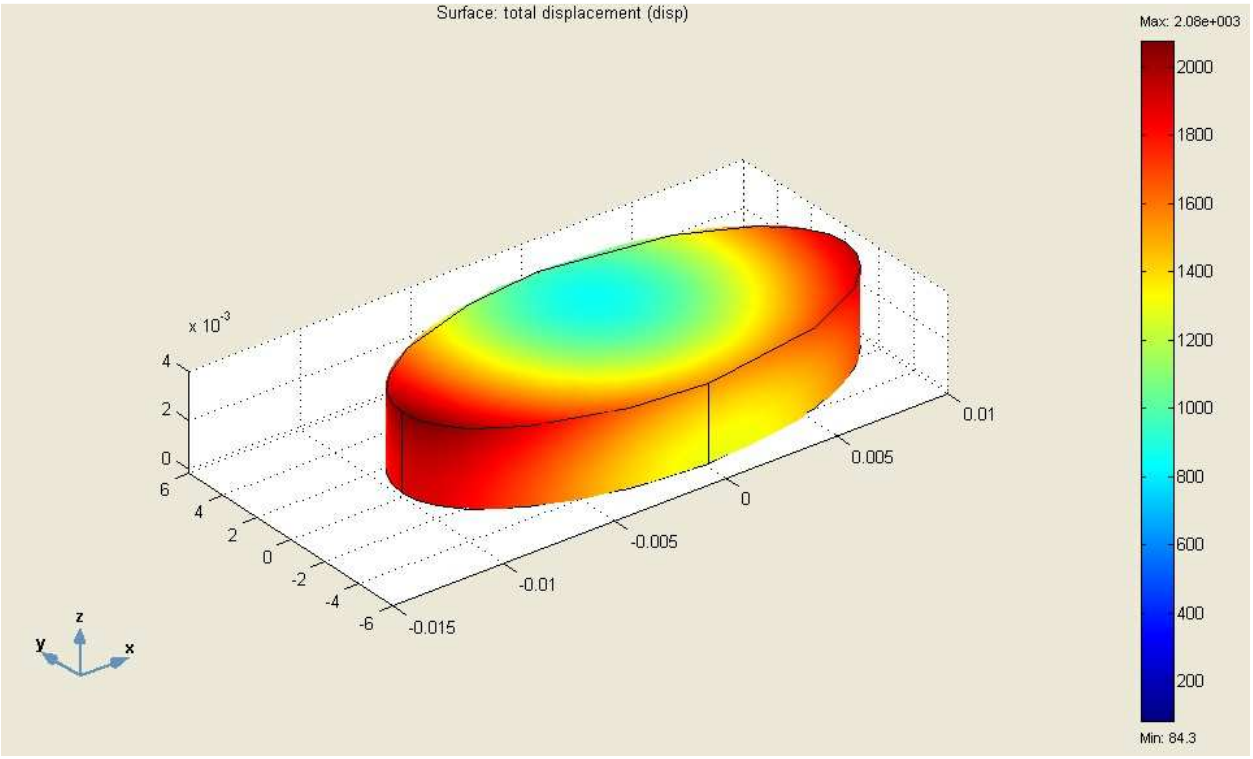

Figure 5.13: Deformation of beef model at 800 MPa for linear shock wave propagation assuming isotropy

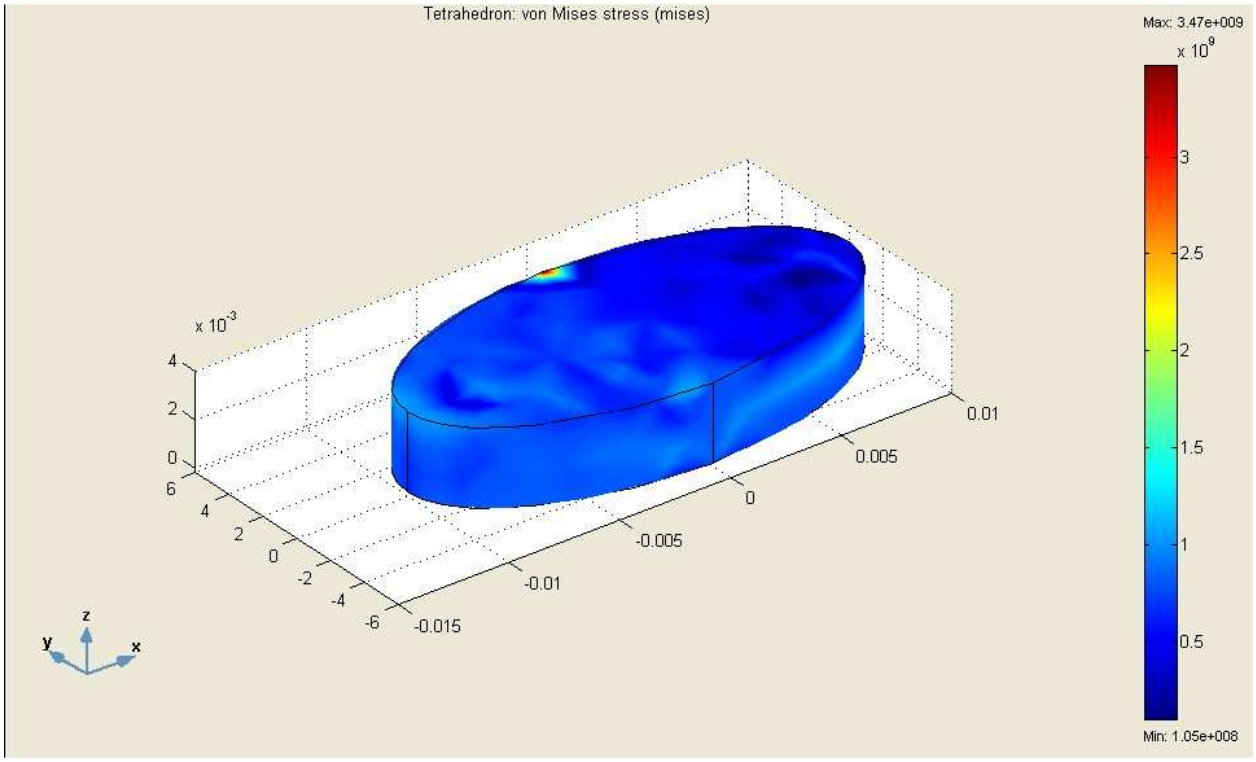

Figure 5.14: von-Mises stresses on beef model at 800 MPa for linear shock wave propagation assuming transverse isotropy

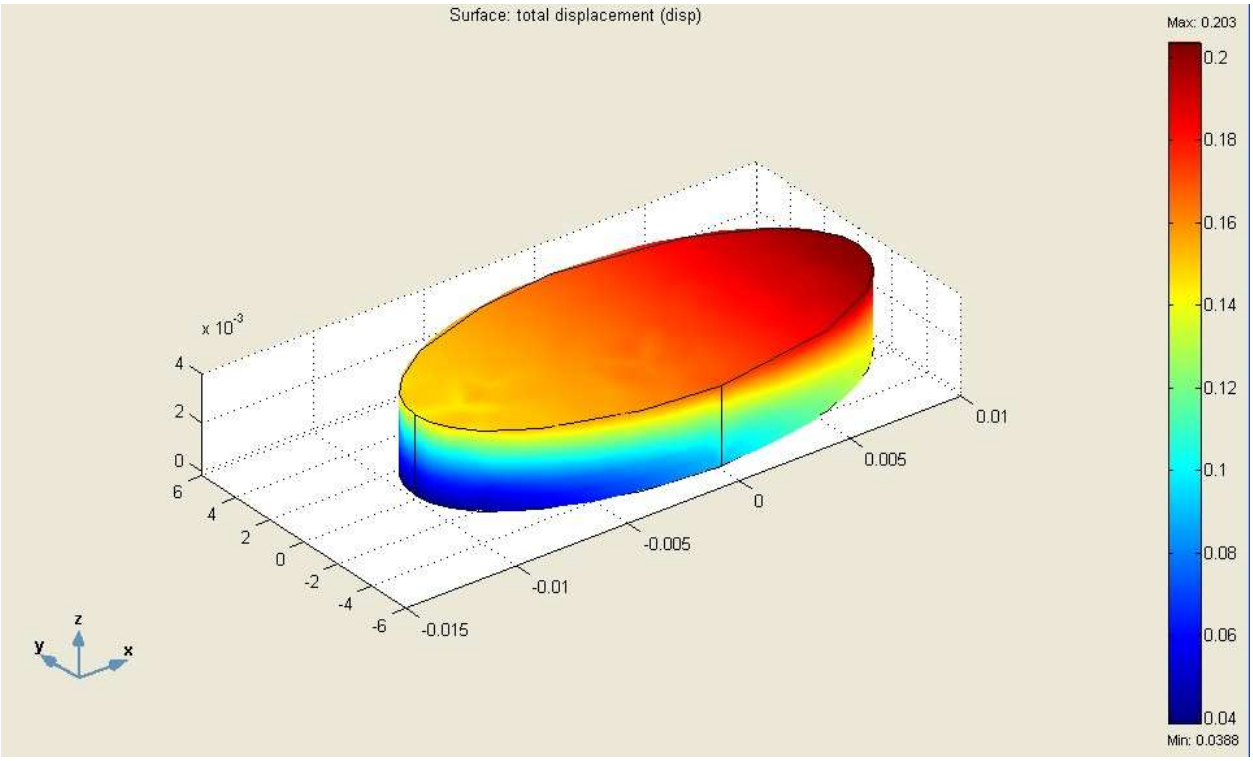

Figure 5.15: Deformation of beef model at 800 MPa for linear shock wave propagation assuming transverse isotropy

LIST OF TABLES

Table 5.1: Average values of diagonal coefficients of stiffness matrix C_{ij} estimated using ultrasound techniques

Beef Loin ID	*Charge Amount (g)*	C_{11} *(Pa)*	C_{22} *(Pa)*	C_{33} *(Pa)*	C_{44} *(Pa)*	C_{55} *(Pa)*	C_{66} *(Pa)*
2C	Control	9.8E+08	2.04E+09	1.60E+09	803161.40	279861.95	302418.09
1C	Control	1.1E+09	2.23E+09	1.3E+09	626493.53	352307.15	182641.84
2A1	50	1.3E+09	2.59E+09	1.27E+09	896814.41	276427.50	172506.35
2A2	50	1.6E+09	3.91E+09	1.59E+09	1217942.02	886102.84	245647.82
2B1	75	1.0E+09	2.03E+09	1.21E+09	703567.41	275958.94	275465.13
2B2	75	1.1E+09	2.21E+09	1.47E+09	982729.52	409051.39	135323.41
1B1	75	1.4E+09	2.79E+09	2.91E+09	804695.56	212853.07	285126.43
1B2	75	1.7E+09	3.01E+09	2.6E+09	1311486.91	315171.97	141710.62
1A1	100	1.5E+09	3.19E+09	1.14E+09	1267413.03	201789.73	145832.12
1A2	100	1.5E+09	3.22E+09	2.58E+09	1002194.60	298582.74	156661.03

n= 2-4 samples per average estimated value

Table 5.2: Percentage change in elastic coefficients post HDP-treatment (-ve values indicate increase post-treatment)

Beef Loin ID	*Charge Amount (g)*	*% change in* c_{11}	*% change in* c_{22}	*% change in* c_{33}	*% change in* c_{44}	*% change in* c_{55}	*% change in* c_{66}
2A1	50	-22.78	-21.43	12.00	-25.46	12.55	28.87
2A2	50	-59.52	-83.03	-9.50	-70.38	-180.34	-1.29
2B1	75	3.06	5.13	16.26	1.58	12.69	-13.58
2B2	75	1.19	-2.90	-1.61	-37.48	-29.41	44.20
1B1	75	-32.99	-30.46	-101.12	-12.57	32.66	-17.56
1B2	75	-65.24	-40.73	-79.81	-83.47	0.29	41.57
1A1	100	-44.06	-49.25	21.12	-77.30	36.20	39.87
1A2	100	-50.47	-50.91	-78.10	-40.20	5.54	35.41

CHAPTER 6

CORRELATING SMALL-STRAIN AND LARGE-STRAIN BEHAVIOR IN BEEF LOINS USING AGING AND HIGH HYDRODYNAMIC PRESSURE-TREATMENT STUDIES

ABSTRACT: Aging and high hydrodynamic pressure treatment processes are two known methods that have been reported to improve tenderness in beef cuts. This improvement has been indicated by using the Warner-Bratzler shear-force test procedure, performed on cooked beef muscle, subject to a large-strain shear-force perpendicular to the muscle fibers. In order to establish correlation between small- and large-strain behavior, two studies were conducted. The first one utilized aging to improve textural properties in beef loins and stress relaxation time, estimated using tensile creep test at 20% strain, was used as the small-strain measurement to correlate with texture profile analysis (TPA) measures of cohesiveness, springiness, resilience, hardness, and chewiness. The second study utilized high hydrodynamic processing (HDP) to improve textural properties in beef loins and elastic coefficients of the diagonal (c_{11}-c_{66}) of the stiffness matrix C_{ij}, estimated using ultrasound velocity, were correlated with TPA features and WBS scores. The first study indicated that TPA cohesiveness (r = 0.69), chewiness (r = *0*.65), and springiness (r = 0.55) showed a moderately good correlation with stress relaxation time. Statistical correlation in the HDP-treatment study between WBS and TPA features and the elastic coefficients of the C_{ij} matrix indicated TPA cohesiveness and springiness showed a very high correlation to c_{11}, c_{22}, and c_{44} with r-values > 0.85. This indicated that stress relaxation time and elastic coefficients of the stiffness matrix can be promising parameters for predicting textural properties in beef.

INTRODUCTION

Many textural attributes of foods are directly related to mechanical properties. In judging the overall quality of beef, tenderness plays a major role in a consumer's perception of beef quality (Koohmaraie et al., 1995). The Warner-Bratzler (WBS) shear testing method involves a process of compression, bending, and shearing of the sample and due to the structure of the WBS blade, the loading process is difficult to interpret (Lu and Chen, 1998). The WBS testing procedure subjects the sample to large deformations, but methods like aging (Hopkinson et al., 1985, Mies et al., 2009, Parish, 2009, etc.) and high hydrodynamic pressure (HDP) treatment process (Solomon et al., 1997, Schilling et al., 2003, Solomon et al., 2008, etc.), which are reported to improve tenderness, do not cause large deformations. Improvement in tenderness and texture using such methods is only ascertained through testing by subjecting the sample to cooking and large deformations, most notably WBS testing. Effects of heat treatment in muscle foods have been reported to cause increase in firmness (Martens et al., 1982) and reduction in hardness (Bertola et al., 1994) which could be attributed to denaturation of myofibrillar proteins, shrinkage in sarcomere length, and decrease in fiber diameter with increasing temperature (Palka and Daun, 1999, Wattanachant et al., 2005). There is therefore a need to establish a relationship between small-strain changes occurring in raw beef muscle due to tenderness improvement and large-strain estimations of tenderness.

Mohsenin and Mittal (1977) hypothesized that no correlation should exist between a large-strain/failure parameter and small-strain/non-failure parameter and descriptive terms like texture profile analysis (TPA) estimates of hardness, cohesiveness, springiness, etc. do not have to conform to rheological or mechanical principles. However, the rationale behind conducting experiments to determine such a relationship arises from strong correlation established between

the two parameters. Segars et al. (1977) reported that *r*-values for correlation between sensory attributes such as, chewiness, difficulty of cutting, and residue and a non-failure parameter, Poisson's ratio was around 0.90. Spadaro et al. (2002) also determined that biomechanical parameters of meat- initial and final stiffness and total energy dissipation, for parallel and perpendicular geometry, correlated very highly with sensory attributes such as, overall tenderness and fiber tenderness.

The purpose of this study was to establish a relationship between small-strain measurements in beef loins and correlate them with large-strain measures of WBS scores and TPA features. Two studies, one using aging as a textural improvement method and the other using HDP-treatment, were conducted. The former utilized measurement of stress relaxation time as the small-strain parameter and statistical relationship with large-strain measures of TPA features was established. The second study utilized measurement of elastic coefficients of the diagonal of the stiffness matrix C_{ij} as small-strain parameters and statistical relationships with large-strain measures of WBS scores and TPA features were established.

MATERIALS AND METHODS

Correlating Relaxation Time and TPA features

Aging of Samples

Eighteen loins, six each from sample sets Q, S, and T were acquired from USDA-ARS, Beltsville, MD for this study. Samples were vacuum-packaged and subjected to 1, 3, and 7 days of aging in a refrigerator (fig. 6.1). The aging temperature was maintained around 1°C. After the

prescribed aging period, two loins from each sample set, totaling six loins per aging period were chosen for stress relaxation and texture profile analysis (TPA) experiments.

Stress Relaxation Estimation

Raw loins from sample sets Q, S, and T, for every aging period of 1, 3, and 7 days (one loin each), were subjected to testing. Thin strips of beef loin of approximately 40-45 mm length and 10-15 mm width were cut with a thin-bladed knife from the raw loins to prevent any damage to the strips. Each sample had 3-4 replicates for testing. Each samples were fixed between two clamps on a Texture Analyzer TA-XT2 (Texture Technologies Corp., Scarsdale, NY) so that the effective length between the clamps was 30 mm. The beef strips were coated with a layer of ultrasound gel to prevent moisture loss.

Although studies in measurement of deformation behavior of muscle utilize have utilized compression methods (Segars et al., 1977 and Lepetit, 1991), tensile strain testing was employed in this test since meats undergo combinations of shear, tension, and compression during chewing (Berry, 1983). Creep experiments were performed based on tensile strain at 20% (Segars et al., 1997), with a test speed of 0.5mm/s using a data acquisition rate of 2 points per second. Even though the strain used in this study was in the non-linear region, it was within the elastic limit. This procedure was roughly adapted from experiments in estimating tensile properties of white muscle in Chinook Salmon by Jerrett et al. (1996).

Texture Profile Analysis

For every aging period of 1, 3, and 7 days, one loin each from Q, S, and T sample sets was chosen for TPA testing. Samples were cooked according to AMSA guidelines (AMSA, 1995) to an internal temperature of 71°C and 3 cores from each loin (20 mm diameter and 15 mm height) were extracted. Samples were tested at 50% compression at a crosshead speed of 1 mm/s. Hardness, springiness, cohesiveness, chewiness, and resilience were then extracted for further analysis.

Statistical Analysis

Statistical analysis of correlation between TPA features and stress relaxation time was conducted at $\alpha = 0.05$ and was performed on SAS 9.1 (SAS Institute Inc., Cary, NC).

Correlating Elastic Coefficients and WBS Scores and TPA Features

HDP-treatment of Samples

Beef loins, control (non HDP-treated) and HDP-treated loins (with 50, 75, and 100g) charges were acquired from USDA-ARS, Beltsville, MD. The HDP-treatments were assigned as follows:

- Loin 1: 1A=100g; 1B =75g; 1C= Control,
- Loin 2: 2A=75g; 2B = 50g; 2C = Control,

- Loin 3: 3A=50g; 3B = 100g; 3C = Control,
- Loin 4: 4A=50g; 4B = 100g; 4C = Control,
- Loin 5: 5A=75g; 5B = 100g; 5C = Control,
- Loin 6: 6A=50g; 6B = 75g; 6C = Control.

All samples were extracted from the anterior region of the loin and each set, e.g. 1A, 1B, 1C, were taken from adjacent sections of the same loin to minimize variation. Each HDP-treated sample had two replicates, to account for a total of 24 treated and 6 control samples for a total of 30 samples. Samples 1A, 1B, 2A, 2B, 1C, and 2C, numbering 10 samples were used for estimating elastic constants. This set had four samples treated with 75 g charge, two each with 50 and 100 g charges, and two control samples. Samples 4A, 4B, 6A, 6B, 4C, and 6C, numbering 10 samples were used for WBS testing. This set had four samples treated with 50 g charge, two each with 75 and 100 g charges, and two control samples. Samples 3A, 3B, 5A, 5B, 3C, and 5C, numbering 10 samples were used for TPA procedures. This set had four samples treated with 100 g charge, two each with 50 and 75 g charges, and two control samples.

Estimation of Elastic Coefficients Using Ultrasound

Determination of the elastic coefficients of the stiffness matrix (C_{ij}) for the beef loins were based on the assumption of transverse-isotropic behavior. In this study, the elastic

coefficients of the C_{ij} matrix for beef muscle were determined using longitudinal and shear transducers, based on the following relations (Rho, 1996):

$$c_{11} = \rho v_1^2 \quad (1)$$

$$c_{22} = \rho v_2^2 \quad (2)$$

$$c_{33} = \rho v_3^2 \quad (3)$$

$$c_{44} = \rho v_{23}^2 \quad (4)$$

$$c_{55} = \rho v_{13}^2 \quad (5)$$

$$c_{66} = \rho v_{12}^2 \quad (6)$$

where, ρ = density of the material,

v_i = velocity of the longitudinal wave in the direction *i*, and

v_{ij} = velocity of a shear/transverse wave in the direction *i* and particle motion along *j*.

Raw beef loins were thawed and then cut into rectangular blocks along the direction of fibers. These were frozen again to -4 ºC to arrest aging of beef, which occurs between 1 to -1 ºC (Epley, 2009, Hedrick et al., 1993). From these sections, square to rectangular shaped sections of thicknesses ranging from 0.3-0.5 cm and dimensions ranging from 1.5-2.0 cm were cut along the prescribed 1, 2, and 3 directions. Figure 6.3 indicates a schematic representation and procedure for the extraction of sections for estimation of elastic constants. This procedure was adopted from Kriz and Stinchomb (1979).

Approximately 2-4 square to rectangular sections for each direction were cut out from the samples and then frozen again to -4 ºC prior to testing in freezer bags. The freezing process prevented aging and also allowed propagation of shear waves since they get highly attenuated in water-rich medium like animal tissue. Freezing also prevented damage to the specimens during the ultrasound measurements since the cross sectional area and thickness of the samples being tested were very small. Dimensions of the frozen sections (length, width, and thickness) were measured using calipers and each sample was weighed to estimate the density of the material which was used in estimation of the diagonal elastic coefficients (c_{11}-c_{66}) of the C_{ij} matrix.

Ultrasound velocity in the frozen sections in the prescribed 1, 2, and 3 directions were determined using longitudinal and shear wave transducers. A 250 kHz Ultran W-series standard miniature contact transducer (The Ultran Group, State College, PA) was used for estimating the longitudinal wave velocities and for estimation of shear wave velocities, a 2 MHz Ultran SWC50, 0° shear wave transducer (The Ultran Group, State College, PA) was used. Both longitudinal and shear wave transducers were set to analyze in through-transmission mode to prevent attenuation in the sample. An Ultran BP-9400A signal transducer was used to generate acoustic pulses, which were received by an Ultran BR-640A broadband receiver (The Ultran Group, State College, PA). The received pulses were sent to a 100 MHz Tektronix® oscilloscope, model 2230 with a GPIB interface (Tektronix Inc., Richardson, TX), connected to a computer which was used to acquire the signal.

Ultrasound time of flight through the sample was calculated using a fast Fourier transform method, using a reference signal (without any medium in between transducers) and the signal acquired for the samples. The calculated time of flight was converted to velocity by dividing it by the sample thickness (l) using the following equation (Antonova et al., 2003)

$$v_{sample} = \frac{l}{(TOF - TOF_0)} \quad (7)$$

where, v_{sample} = ultrasound velocity through the beef sample (m/s)

l = thickness of the sample (m)

TOF = time of flight with the sample between the transducers (m/s)

TOF_0 = time of flight without the sample between the transducers (m/s)

Warner-Bratzler Shear and Texture Profile Analysis

Ten samples each were segregated for Warner-Bratzler shear (WBS) and texture profile analysis (TPA). Steaks were cooked according to American Meat Science Association (AMSA, 1995) guidelines to 71°C or medium doneness and chilled before coring. WBS and TPA analysis (50% compression) were carried out on a Texture Analyzer TA-XT2 (Texture Technologies Corp., Scarsdale, NY). TPA hardness, chewiness, springiness, cohesiveness, and resilience were measured.

Statistical Analysis

Statistical correlation between WBS scores and TPA features and experimentally determined elastic coefficients was conducted at $\alpha = 0.05$ and were performed on SAS 9.1 (SAS Institute Inc., Cary, NC).

RESULTS AND DISCUSSION

Aging Study: Correlation between Relaxation Time and TPA features

Stress relaxation time was calculated by a method of curve fitting using KaleidaGraph 4.0 (Synergy Software Inc., Reading, PA). The curve-fitted graph is indicated in figure 6.5, which was plotted using normalized data and the stress relaxation time was calculated based on the relationship given by:

$$\frac{\sigma}{\sigma_{max}} = \sigma_0 + \alpha * e^{-\left(\frac{t}{\tau}\right)} \quad (8)$$

where, σ = stress at any given time, t,

σ_{max}= maximum value of stress,

σ_0= initial value of stress at time t=0,

α= constant,

τ = relaxation time in s.

Results from this study indicated an increase in stress relaxation time from day 1 to day 3, but a reduction in stress relaxation time from day 3 to day 7 (fig. 6.6). Subsequently, values of hardness increased with days of aging, springiness and resilience showed decrease in values with days of aging, and chewiness and cohesiveness indicated increase from day 1 to day 3, but a decrease from day 3 to day 7 of aging (fig. 6.7). Overall time-constant from stress-relaxation showed a positive correlation with cohesiveness and chewiness, (r > 0.65) and with springiness

(r = 0.55) (Table 6.1), whereas hardness and resilience showed very poor correlation (r < 0.2), and were not used in the regression analysis.

Regression analysis of the three TPA features, viz. cohesiveness, springiness, and chewiness (figs. 6.8-6.10) was conducted on MS Excel. From table 6.1 it can be inferred that all three TPA features constituting large-strain measurements were estimated very well by small-strain measurements of stress relaxation time (τ) indicated by a low mean-squared error value (MSE). Cohesiveness and springiness were estimated more accurately using when compared to chewiness, although the differences in MSE values were very negligible.

Bertram et al. (2004) indicated an increase in sarcomere length between day 1 and day 3 of aging and then a reduction from day 3 and day 7. This indicates that the stress relaxation time would correlate positively with sarcomere length, which could have effects on tenderness attributes. In the same study, the variation in sarcomere length was also found in WBS scores, which indicates a positive correlation. Wheeler and Koohmaraie (1999) reported from their studies on the effects of sarcomere length in muscle on proteolysis, which occurs during aging, and tenderness that there was an indirect effect on tenderness due to sarcomere length, but it did not affect the extent of proteolysis. Wheeler and Koohmaraie (1999) were contradicted by Bowker et al. (2008) who concluded from their studies that sarcomere length played a major role in determining tenderization potential and that the impact of proteolysis on tenderness is mediated by sarcomere length. This similarity in variation between sarcomere length, stress relaxation time, and WBS scores indicate that there is a possibility that a correlation between small- and large-strain measurements in muscle foods exists, even though WBS testing was not done for this present study.

HDP Study: Correlation between Elastic Coefficients and WBS Scores and TPA features

The values of elastic coefficients estimated from ultrasound methods are given in table 6.2. From studies by Chen et al. (1994 and 1996), it can be inferred that the values for $c_{11,}$ c_{22}, and c_{33} were found to be much higher than the estimated values of isotropic moduli in beef muscle. Chen et al. (1994 and 1996) estimated isotropic Young's modulus values from 3.0 kPa to 6.0 kPa in beef muscle, undergoing small strains in the range of 1-5%, which are lower than the reported values in this study by a magnitude of 6. The values of elastic coefficients c_{44} and c_{66} determined experimentally in this study corroborated very well with the values estimated by Gennission et al. (2003). It was inferred that the reported values for the elastic coefficients $c_{11,}$ c_{22}, and c_{33} agreed with the reported values of longitudinal wave speeds in beef muscle (Gennisson et al., 2003) and since there existed no other study on estimation of transverse isotropic elastic coefficients of the stiffness matrix on beef muscle, these estimated values were used in this study.

Correlation values established between the elastic coefficients and WBS scores and TPA features are given in table 6.5. WBS scores showed an overall poor correlation with the elastic coefficients, with a maximum r-value of 0.65 with the elastic coefficient c_{33} and this could be attributed to the inconsistency in reduction in WBS scores after HDP treatment (Table 6.3). TPA cohesiveness showed a very high correlation to c_{11}, c_{22}, c_{44} and c_{66} among all estimated features with r-values of 0.98, 0.92, 0.99, and -0.93. Springiness correlated very well with c_{11}, c_{22}, and c_{44} with r-values of -0.86, -0.86, and -0.85, respectively. Chewiness correlated very well with c_{55} with r-value of 0.95 and resilience correlated very well with c_{66} with r-value of -0.91.

Determination of small-strain behavior of muscle foods is of interest since it offers a better understanding of textural properties than large-strain measurements. It is imperative that small-strain studies be correlated to large-strain behavior since large-strain measurements are the only approved measures of objective indicators of texture and tenderness. In defense of this study, the high correlation established by cohesiveness, chewiness, and springiness with small-strain measurements can be explained thus.

Segars et al. (1977) explained in their arguments that TPA chewiness "probably reflects not only the disintegrative properties of the sample, but also the amount of elasticity of connective tissue prior to disintegration" and so it would correlate with a small-strain parameter like Poisson's ratio, which can be estimated from constitutive relationships using elastic constants and stress relaxation. The relationship between chewiness, springiness, and cohesiveness can be written as:

Chewiness = Hardness*Cohesiveness*Springiness (9)

Cohesiveness is defined as the product's characteristic to withstand a second deformation relative to its behavior under the first deformation and springiness is defined as the ability of the product to spring back after the first deformation (Texture Technologies, 2009). Cohesiveness and springiness can also be defined as measures of combinations of small- and large-strain behavior of a food product based on the TPA curve in figure 6.4. Cohesiveness is the ratio of Area 2/Area 1 and springiness is the ratio of Length 2/Length 1. Based on the calculation of cohesiveness and springiness from the TPA curve, these two features can also be considered as measures of amount of elasticity of the meat tissue in their ability to withstand deformation.

Therefore, these two small-strain parameters can correlate with measurements of stress relaxation time and elastic coefficients.

A study by Spadaro et al. (2002) tried establishing correlation between biomechanical properties of meat. Perpendicular and parallel (with respect to fiber direction) strain estimations of stiffness and dissipation of energy via stress relaxation time were related to palatability estimations of overall tenderness, WBS shear, juiciness, fiber tenderness, content of connective tissue, and sensory panel scores. It was observed that overall tenderness correlated positively with biomechanical properties of parallel and perpendicular stiffness and energy dissipation, and displayed a low and negative correlation with WBS scores. This was also observed with the low correlation established between WBS scores and the elastic coefficients. However, the argument against WBS shear is a simple measure of force that does not account for the complexities involved in the process of compression, bending, and shearing of the sample and due to the structure of the blade used in testing, the actual loading process is also difficult to interpret (Lu and Chen, 1998).

Effects on Palatability

Caine et al. (2003) indicated that that cohesiveness and chewiness both constituted as negative palatability attributes in terms of juiciness, flavor desirability, flavor intensity, overall tenderness, and overall palatability, with the negative correlation of these two TPA features. In the same study, an increase in springiness was found to correlate positively with good palatability attributes. Using this study as a reference, in the aging study, cohesiveness, springiness, and chewiness as large-strain measurements provided moderately good indicators of

small-strain measurements of stress-relaxation time as indicated in table 6.1, and these two features were found to increase from day 1 to day 3 of aging and then reduce from day 3 to day 7 of aging (fig. 6.6), which indicates improvement in palatability as per Caine et al. (2003). This is also further corroborated by the behavior of stress-relaxation time in a similar manner (fig. 6.5) However, springiness was also found to establish a positive correlation with relaxation time since springiness did not indicate any increase between day 1 and day 3 of aging. This also contradicts the study by contradicts the study by Caine et al. (2003), who attributed springiness with positive palatability attributes.

In the HDP-treatment study, the positive correlation between cohesiveness and the elastic coefficients c_{11}, c_{22}, c_{44} and, chewiness and c_{55} indicate that a reduction in the value of these elastic coefficients could possibly improve palatability. This relationship is also consistent with the high negative correlation observed between springiness and c_{11}, c_{22}, and c_{44}, which Caine et al (2003) reported as a positive palatability attribute with its reported high correlation with the palatability attributes mentioned above. From table 6.4, it was observed that the HDP-treatment process reduced TPA cohesiveness in all but one sample and increased TPA springiness, save for in two samples. While this is consistent in improvement in palatability, established correlations between cohesiveness and the coefficients c_{11}, c_{22}, c_{44} and springiness and c_{11}, c_{22}, c_{44} contradict each other when the results are corroborated with table 6.3. In addition, chewiness was found to increase post-treatment which does not corroborate with the positive correlation established in this study. While the reduction in chewiness is compatible with good palatability characteristics indicated by Caine et al. (2003), this variation in reduction in value of chewiness, while simultaneously increasing in the value of TPA cohesiveness after HDP-treatment indicates an

inconsistency in the HDP treatment process which could be due to the variation in other process parameters, like bin size and sample location, which were not accounted for in this study.

CONCLUSIONS

Results from this study indicated that a strong correlation was established between cohesiveness, springiness, and chewiness with small-strain estimations of elastic coefficients. In both studies, chewiness and cohesiveness indicated positive correlation with small-strain measurements, whereas springiness showed a high negative correlation with the elastic coefficients c_{11}, $c_{22,}$ and c_{44}. Results indicate that small-strain measurements of elastic coefficients can help explain mechanical behavior of raw beef muscle undergoing texture modification methods using HDP-treatment and aging. Further studies in this field would require standardizing a methodology for measuring elastic coefficients from beef muscle, and calculating elastic constants from the compliance matrix, which is the inverse of the C_{ij} matrix. This would also require accounting for anisotropy of beef muscle and its hyperelastic behavior which poses a significant challenge, as mentioned in chapter 5. This would however help provide more information on textural characteristics of beef muscle and explain the mechanisms behind aging and HDP-treatment better.

REFERENCES:

AMSA. 1995. Research guidelines for cookery, sensory evaluation, and instrumental tenderness of fresh meat. American Meat Science Association and National Livestock and Meat Board, Chicago, IL.

Antonova, I., P. Mallikarjunan, and S.E. Duncan. 2003. Correlating objective measurements of crispness in breaded fried chicken nuggets with sensory crispness. *J. Food Sci.* 68(4), 1308-1315.

Berry, B.W.. 1983. Measurement of meat texture. *Reciprocal Meat Conference Proceedings* 36, 103-107.

Bertola, N.C., A.E. Bevilacqua, and N.E. Zaritzky. 1994. Heat treatment effect on textural changes and thermal denaturation of proteins in beef muscle. *J. Food Process. & Preserv.* 18, 31-46.

Bertram, H.C., A.K. Whittaker, W.R. Shorthose, H.J. Anderson, and A.H. Karlsson. 2004. Water characteristics in cooked beef as influenced by ageing and high-pressure treatment—an NMR micro imaging study. *Meat Sci.* 66(2), 301-306.

Bowker, B.C., Eastridge, J.S., Paroczay, E.W., Solomon, M.B. 2008. Influence of sarcomere length on aging and hydrodynamic pressure processing of beef muscle [abstract]. *J. Ani. Sci.* 86, E-Suppl. 2, 43.

Caine, W.R., J.L. Aalhus, D.R. Best, M.E.R. Dugan, and L.E. Jeremiah. 2003. Relationship of texture profile analysis and Warner-Bratzler shear force with sensory characteristics of beef rib steaks. *Meat Sci.* 64, 333-339.

Chen, E.J., J. Novakofski, K. Jenkins, and W.D. O'Brien Jr.. 1994. Ultrasound elasticity measurements of beef muscle. *1994 Ultrasonics Symposium,* 1459-1462.

Chen, E.J., J. Novakofski, W.K. Jenkins, and W.D. O'Brien Jr.. 1996. Young's modulus measurements of soft tissues with application to elasticity imaging. *IEEE Trans. Ultrasonics, Ferroelectrics, and Freq. Control* 43 (1), 191-194.

Epley, R.J. 2009. Aging beef. University of Minnesota Extension. Available at http://www.extension.umn.edu/distribution/nutrition/DJ5968.html. Accessed May 23, 2009.

Gennisson, J-L, S. Catheline, S. Chaffai, and M. Fink. 2003. Transient elastography in anisotropic medium: Application to the measurement of slow and fast shear wave speeds in muscles. *J. Acoust. Soc. Am.*114(1), 536-541.

Hedrick, H.B., Stringer, W.C., and C. Clarke. 1993. Recommendations for aging beef. University of Missouri Extension. Available at http://extension.missouri.edu/publications/DisplayPub.aspx?P=G2209. Accessed May 23, 2009.

Hopkinson, S.F., T.P. Ringkob, and C.M. Bailey. 1985. Cutability and the effect of electrical stimulation and aging on tenderness of beef from young intact males and castrates. *J. Ani. Sci.* 60, 675-681.

Jerret, A.R., J. Stevens, and A.J. Holland. 1996. Tensile properties of white muscle in rested and exhausted Chinook Salmon (*Oncorhynchus tshawytscha*). *J. Food Sci.* 61(3), 527-532.

Koohmaraie, M., T. L. Wheeler, and S. D. Shackelford. 1995. Beef tenderness: Regulation and prediction. Available at http://www.ars.usda.gov/SP2UserFiles/Place/54380530/19950004A1.pdf. Accessed April 10, 2009.

Kriz, R. and W.W. Stinchomb. 1979. Elastic moduli of transversely isotropic graphite fibers and their composites. *Expt. Mech.* 19(2), 41-49.

Leptit, J.. 1991. Theoretical strain ranges in raw meat. *Meat Sci.* 29, 271-283.

Lu, R. and Y.R. Chen. 1998. Characterization of nonlinear elastic properties of beef products under large deformation. *Trans. ASAE* 41(1), 163-171.

Martens, H., E. Stabursvik, and M. Martens. 1982. Texture and colour changes in meat during cooking related to thermal denaturation of muscle proteins. *J. Text. Studies* 13, 291-309.

Mies, P.D., K.E. Belk, J.D. Tatum, and G.C. Smith. 2009. Effects of postmortem aging on beef tenderness and aging guidelines to maximize tenderness of different beef subprimal cuts. Available at http://ansci.colostate.edu/files/meat_science/mies.pdf. Accessed August 10, 2009.

Mohsensin, N.M., and J.P. Mittal. 1977. Use of rheological terms and correlation of compatible measurements in food texture research. *J. Texture Studies* 8, 395-408.

Palka, K. and H. Daun. 1999. Changes in texture, cooking losses, and myofibrillar structure of bovine *M. semitendinosus* during heating. *Meat Sci.* 51, 237-243.

Parish, Jr.,F.C. 2009. Facts: Meat Science- Aging of beef. Available at http://www.good cooking.com/steak /aging/aging.htm. Accessed June 1, 2009.

Schilling, M.W., J.R. Claus, N.G. Mariott, M.B. Solomon, W.N. Eigel, and H. Wang. 2002. No effect of hydrodynamic shock wave on protein functionality of beef muscle. *J. Food Sci.* 67(1), 335-340.

Segars, R.A., R.G. Hamel, and J.G. Kapsalis. 1977. Use of Poisson's ratio for objective-subjective texture correlations in beef. An apparatus for obtaining the required data. *J. Texture Studies* 8, 433-447.

Solomon, M.B. J.B. Long, and J.S. Eastridge. 1997a. The hydrodyne: A new process to improve beef tenderness. *J. Ani. Sci.* 75, 1534-1537.

Solomon, M.B., M.N. Liu, J.R. Patel, E. Paroczay, J.S. Eastridge, and S.W. Coleman. 2008. Tenderness improvement in fresh or frozen/thawed beef steaks treated with hydrodynamic pressure processing. *J. Muscle Foods* 19, 98-109.

Spadaro, V., Allen, D.H., Keeton, J.T., Moreira, R., and Boleman, R.M.. 2002. Biomechanical properties of meat and their correlation to tenderness. *J. Texture Studies* 33, 59-87.

Texture Technologies. 2009. Available at http://www.texturetechnologies.com/texture profile analysis.html. Accessed on August 17, 2009.

Wattanachant, S., S. Benjakul, and D.A. Ledward. 2005. Effect of heat treatment on changes in texture, structure, and properties of Thai indigenous chicken muscle. *Food Chem.* 93, 337-348.

Wheeler, T.L., and M. Koohmaraie. 1999. The extent of proteolysis is independent of sarcomere length in lamb *longissimus* and *psoas major*. *J. Ani. Sci.* 77(9), 2444-2451.

LIST OF FIGURES

Figure 6.1: Aging of beef loins in vacuum-packaged bags

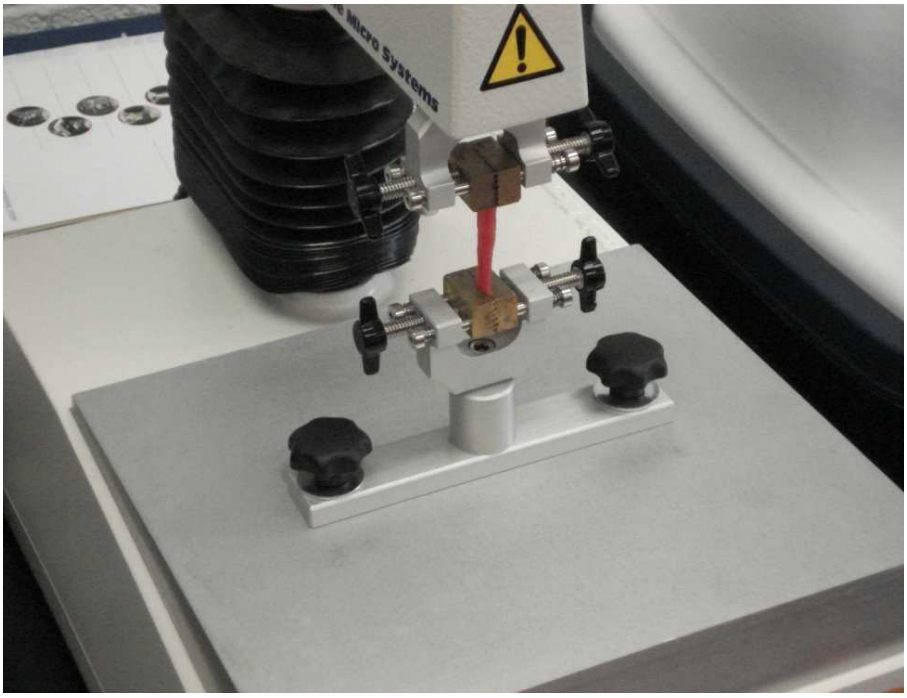

Figure 6.2: Estimation of relaxation time using tensile strain

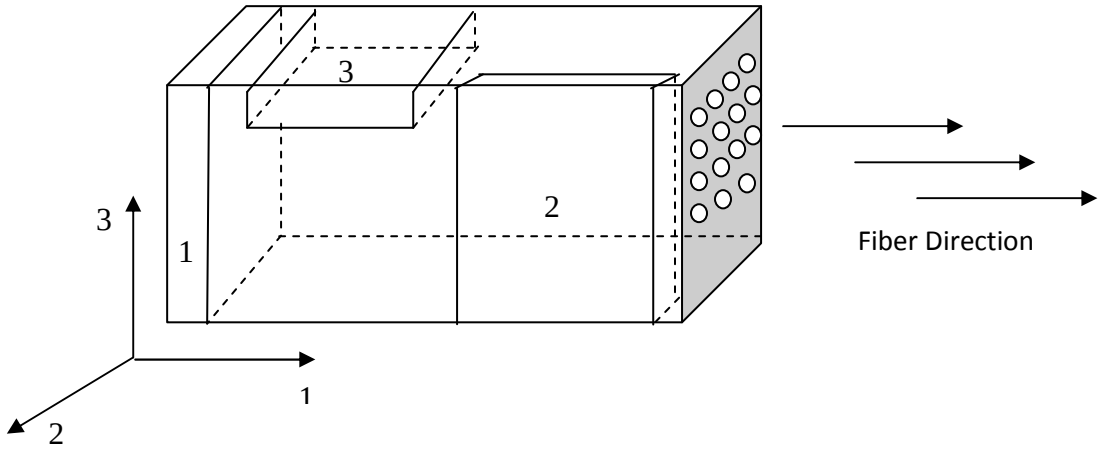

Figure 6.3: Extraction schematic for samples for elastic coefficient estimation using ultrasound

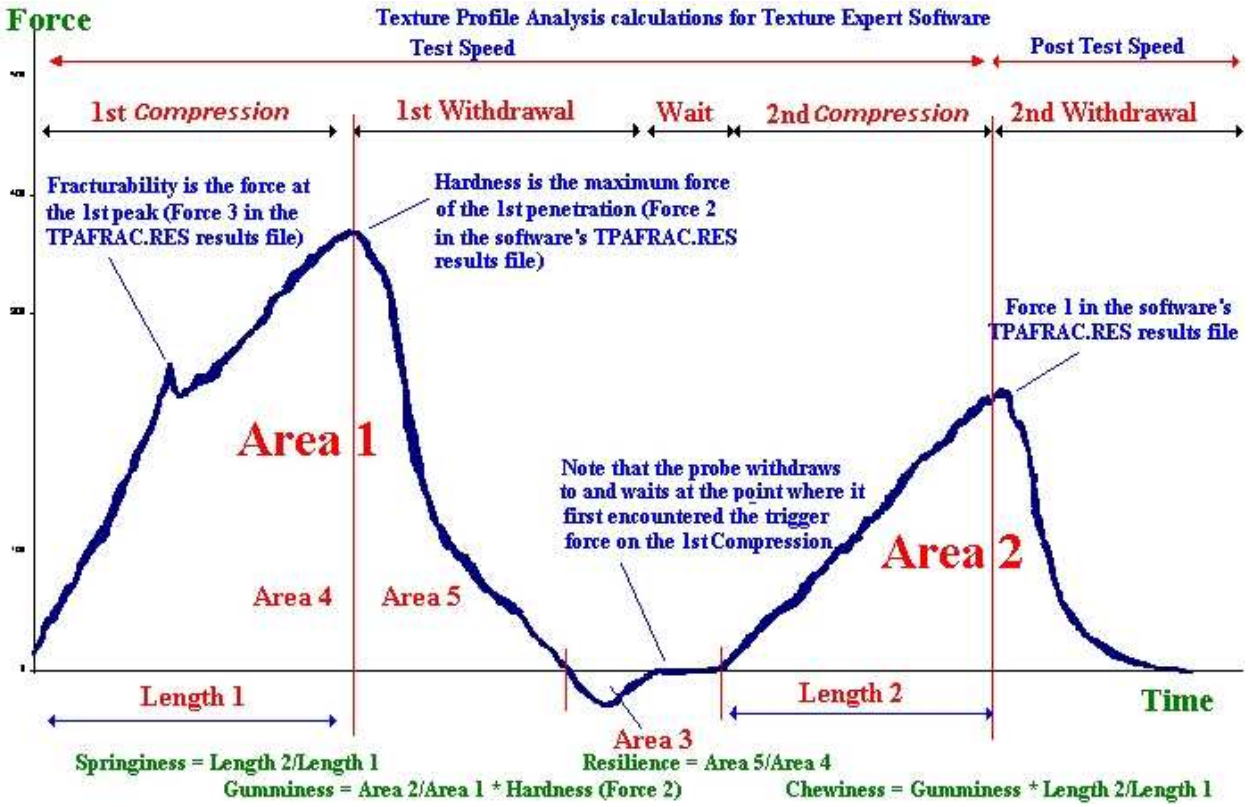

Figure 6.4: Texture Profile Analysis curve (Texture Technologies, 2009)

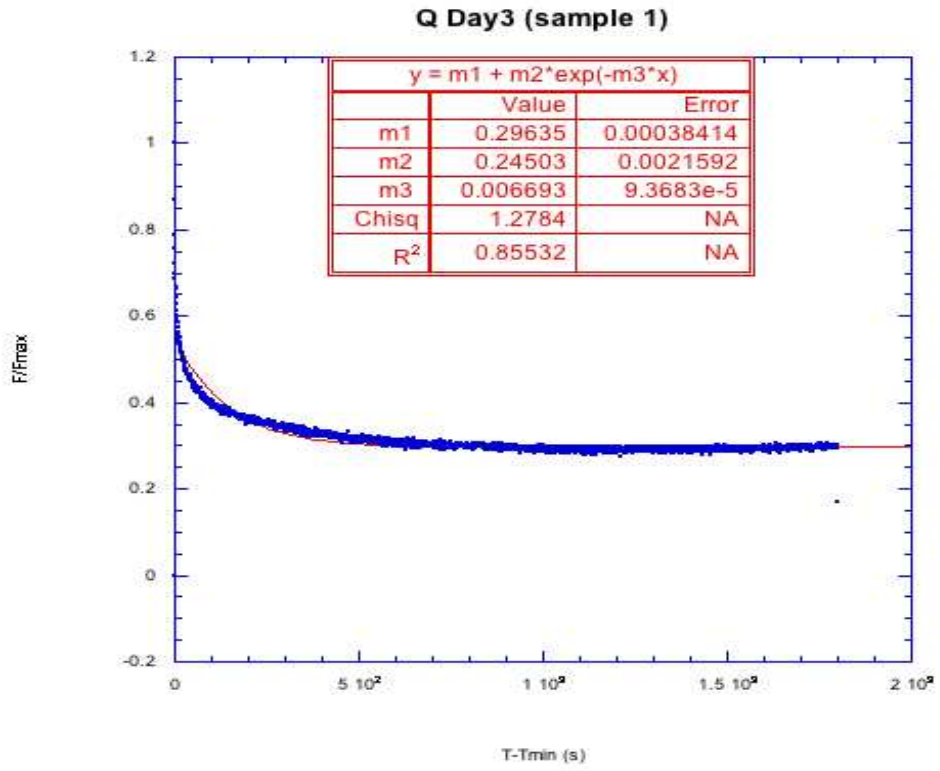

Figure 6.5: Curve-fitted graph for estimation of relaxation time (τ)

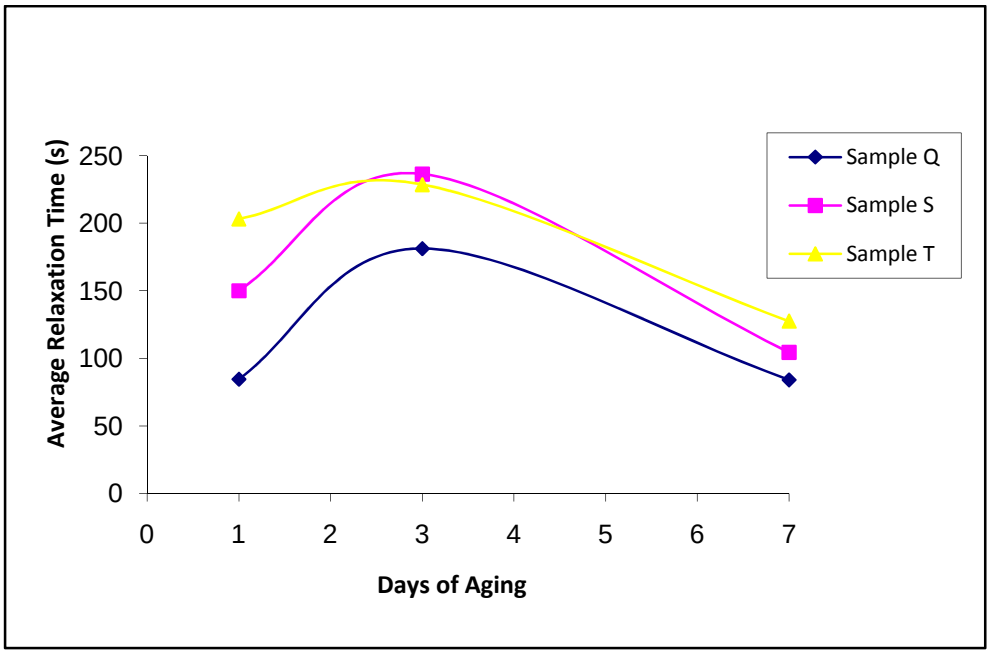

Figure 6.6: Variation of relaxation time with days of aging

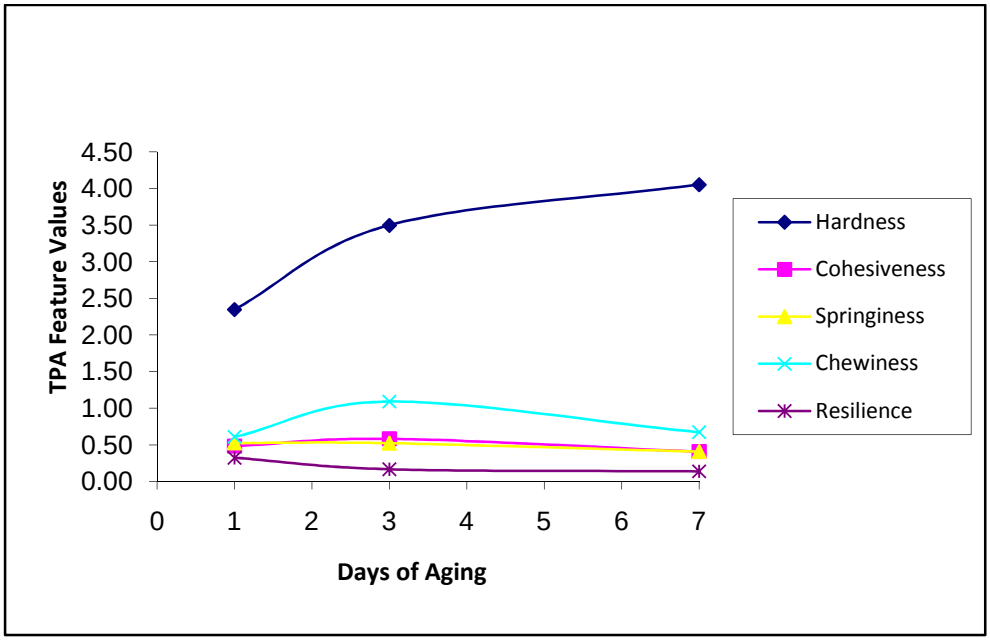

Figure 6.7: Variation of TPA features with aging

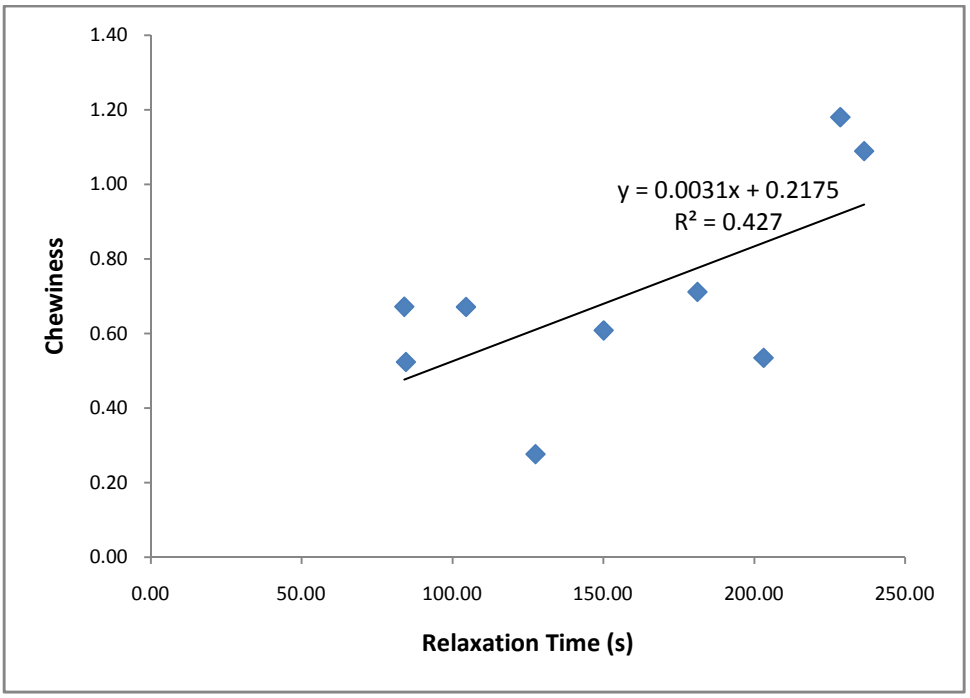

Figure 6.8: Correlation between relaxation time and TPA chewiness

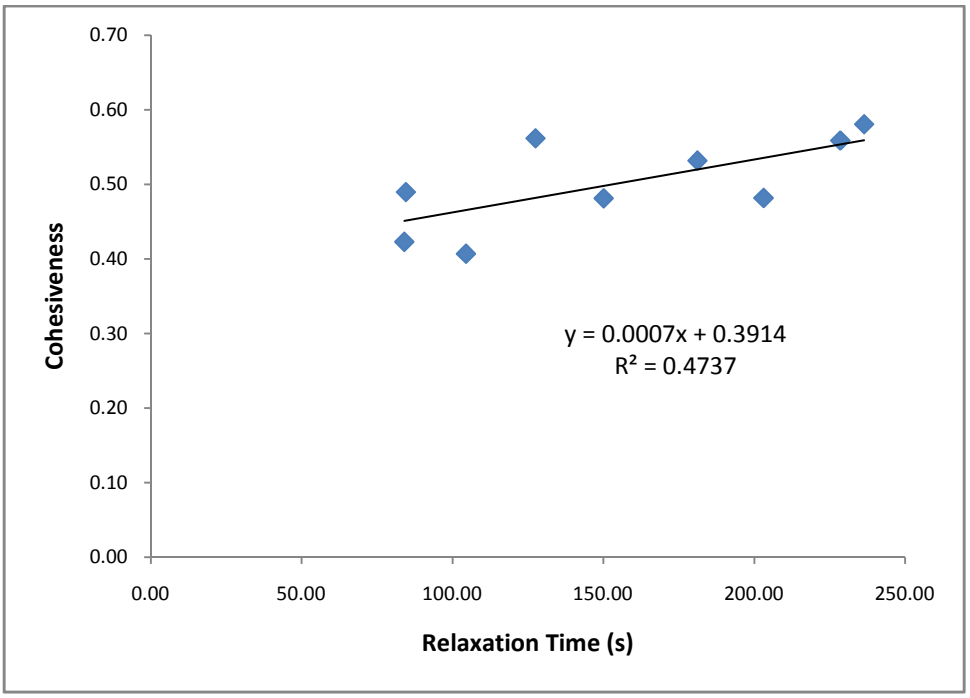

Figure 6.9: Correlation between relaxation time and TPA cohesiveness

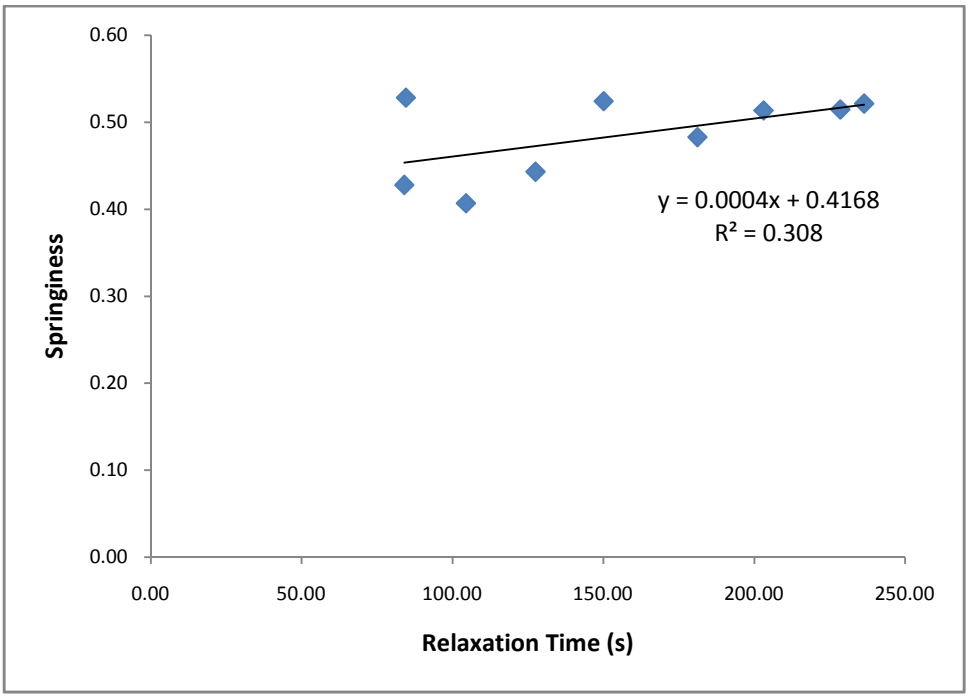

Figure 6.10: Correlation between relaxation time and TPA springiness

LIST OF TABLES

Table 6.1: Pearson's correlation and mean-squared error estimation between TPA features and stress relaxation (τ)

	Average values[1]	*Standard Deviation*[1]	*Pearson's Correlation with τ*[1] *(r)*	*MSE estimation of TPA feature using τ*[1]
Cohesiveness	0.501	0.061	0.690	0.002[a]
Chewiness	0.484	0.047	0.653	0.040
Springiness	0.696	0.280	0.555	0.002[a]

[1] Estimated from n = 9 samples
[a] Indicates best estimation of TPA feature using stress relaxation

Table 6.2: Average values of diagonal coefficients of stiffness matrix C_{ij} estimated using ultrasound techniques

Beef Loin ID	*Charge Amount (g)*	*C_{11} (Pa)*	*C_{22} (Pa)*	*C_{33} (Pa)*	*C_{44} (Pa)*	*C_{55} (Pa)*	*C_{66} (Pa)*
2C	Control	9.8E+08	2.04E+09	1.60E+09	803161.40	279861.95	302418.09
1C	Control	1.1E+09	2.23E+09	1.3E+09	626493.53	352307.15	182641.84
2A1	50	1.3E+09	2.59E+09	1.27E+09	896814.41	276427.50	172506.35
2A2	50	1.6E+09	3.91E+09	1.59E+09	1217942.02	886102.84	245647.82
2B1	75	1.0E+09	2.03E+09	1.21E+09	703567.41	275958.94	275465.13
2B2	75	1.1E+09	2.21E+09	1.47E+09	982729.52	409051.39	135323.41
1B1	75	1.4E+09	2.79E+09	2.91E+09	804695.56	212853.07	285126.43
1B2	75	1.7E+09	3.01E+09	2.6E+09	1311486.91	315171.97	141710.62
1A1	100	1.5E+09	3.19E+09	1.14E+09	1267413.03	201789.73	145832.12
1A2	100	1.5E+09	3.22E+09	2.58E+09	1002194.60	298582.74	156661.03

n= 2-4 samples per average estimated value

Table 6.3: Percentage change in WBS shear-force post HDP-treatment (-ve values indicate increase post-treatment)

Sample ID	*Charge Amount (g)*	*% change in WBS (kg-f)*
4A-1	50	5.29
4A-2	50	14.37
6A-1	50	-13.45
6A-2	50	3.01
6B-1	75	-17.19
6B-2	75	-10.75
4B-1	100	22.86
4B-2	100	1.55

Table 6.4: Percentage change in TPA features post HDP-treatment (-ve values indicate increase in values post-treatment)

Sample ID	*Charge Amount (g)*	*% change in Hardness (kg-f)*	*% change in Cohesiveness*	*% change in Springiness*	*% change in Chewiness*	*% change in Resilience*
3A-1	50	-69.38	2.96	-9.95	-87.76	3.21
3A-2	50	-42.31	5.42	-11.97	-47.24	0.41
5A-1	75	-37.04	3.56	-17.01	-50.91	5.95
5A-2	75	17.46	1.61	2.49	22.64	4.85
3B-1	100	-51.38	4.28	-5.55	-48.29	-0.14
3B-2	100	-40.36	4.81	-37.14	-50.25	-0.95
5B-1	100	50.55	2.42	-25.21	45.85	-16.48
5B-2	100	22.19	-0.79	5.12	24.18	-10.22

Table 6.5: Pearson's correlation coefficients (*r*) and P-values (in parenthesis) for WBS and TPA features with elastic coefficients

	C_{11}	C_{22}	C_{33}	C_{44}	C_{55}	C_{66}
WBS Shear[1]	0.07 (0.93)	-0.22 (0.77)	0.65 (0.35)	0.01 (0.99)	-0.03 (0.97)	0.17 (0.83)
Chewiness[1]	0.49 (0.51)	0.62 (0.37)	-0.42 (0.58)	0.43 (0.57)	0.95 (0.04)	0.04 (0.96)
Hardness[1]	0.48 (0.52)	0.61 (0.38)	-0.45 (0.55)	0.43 (0.59)	0.96 (0.03)	0.05 (0.95)
Springiness[1]	-0.86 (0.13)	-0.86 (0.14)	-0.14 (0.86)	-0.85 (0.15)	-0.59 (0.41)	0.49 (0.51)
Cohesiveness[1]	0.98 (0.02)	0.92 (0.07)	0.36 (0.64)	0.99 (0.01)	0.07 (0.93)	-0.93 (0.07)
Resilience[1]	0.6 (0.39)	0.52 (0.47)	0.35 (0.65)	0.62 (0.38)	-0.5 (0.49)	-0.91 (0.09)

[1] Estimated from n =10 samples

CHAPTER 7

SUMMARY AND CONCLUSIONS

Texture and tenderness are vital to the beef industry considering the financial implications of such attributes on consumer satisfaction and repeat business. Industrial employed methods of aging, injection of papain, electrical stunning have been employed, and yet one out of every four eating experiences with beef are reported unsatisfactory. HDP-treatment technology has reported successful tenderizing effects in various meat cuts, but the variables in the procedure are too many to effectively understand the dynamic behind the process. HDP-treatment methods are also a restricted source of technology due to high capital costs and security and safety issues arising due to the use of explosives in the treatment methods. However, the future of HDP-treatment technology could lie in other methods of generating shock waves, i.e. electrohydraulic method. Companies like Phoenix Science and Technology (Chelmsford, MA) are innovators in pulsed wave generation using electrohydraulic means and their applications, among many, include tenderizing beef. Using electrohydraulic methods may eliminate the variables that make the explosive means of HDP-treatment inconsistent.

The primary goal of this study was to optimize the HDP-treatment process by numerical modeling and understand the process from the perspective of textural changes occurring in beef loins subjected to HDP-treatment. In order to achieve the objective, the study was split into four parts. The first part dealt with non-destructive evaluation of texture and tenderness using ultrasound and image processing techniques. In the same study, the effect of HDP-treatment variables, viz. amount of charge, size of container, and location of sample during treatment were

evaluated. Both ultrasound and image processing techniques could not correlate very well with estimated values of Warner-Bratzler shear (WBS) scores and texture profile analysis (TPA) features. In addition, the effects due to amount of charge indicated no significant difference in the values of WBS scores and TPA features, while location of sample and size of container had significant effects on the values.

The objective of the second study was to utilize a rheological model to simulate deformation behavior of a model protein gel (β-lactoglobulin) as a preliminary study to model textural changes in beef loins undergoing HDP-treatment. Creep recovery and stress relaxation response of the gel was used for prediction of the deformation in each element of the model, from which the overall deformation was estimated. Sensitivity analysis of the model indicated that low frequency oscillations and decreased storage modulus values dominated deformation behavior. The model was entirely non-sensitive to frequency changes above 30,000 rads/s. Values for deformation of the gel were calculated for a spectrum of frequencies between 30,000 rads/s and 300,000 rads/s, under very low pressures (50 kPa). The resulting deformation under very low pressures of 50 kPa indicated that the model was not valid for the high pressures in the order of MPa which HDP-treatments utilize. In addition, the model also indicated the lack of interaction of viscous elements with respect to the deformation behavior and so the next modeling approach was proposed to be based on elastic behavior.

The objective of the third study was to model the elastic behavior of beef loins undergoing HDP-treatment as a transversely isotropic material. Elastic coefficients of the stiffness matrix, C_{ij} of beef loins were estimated from ultrasound longitudinal and shear wave speeds. Average values of the experimentally derived diagonal elastic coefficients c_{11}, c_{22}, c_{33}, c_{44}, c_{55}, and c_{66} were estimated to be 1.03 GPa, 2.14 GPa, 1.45 GPa, 0.715 MPa, 0.316 MPa, and

0.24 MPa, respectively. Results of the simulation using Euler's equation and Tammann Equation of States indicated no deformational response of the model to the shock wave and thus a statistical correlation between numerical estimation of deformation and strain behavior of the model beef loin and WBS and TPA features could not be established. When the model was implemented assuming a unidirectional linear propagation of shock wave, deformation characteristics of the model assuming transversely isotropic indicated realistic deformation behavior, indicating that high values of estimated and assumed elastic coefficients were able to impede deformation as a result of the incident pressure wave. The estimated values of the coefficients were however found to be very high, in the range of gigapascals, but since there existed no other study, the results could not be corroborated.

Results from the modeling indicated very preliminary studies that could not be corroborated due to the lack of literature on the subject of modeling the HDP-process. The objective of the last study was to establish a correlation between small- and large-strain behavior using stress relaxation and elastic coefficients as small-strain estimates and WBS scores and TPA features as large strain estimates. Results from this study indicated that TPA cohesiveness (r = 0.69), chewiness (r = *0*.65), and springiness (r = 0.55) showed a moderately good correlation with stress relaxation time. Statistical correlation in the HDP-treatment study between WBS and TPA features and the elastic coefficients of the C_{ij} matrix indicated TPA cohesiveness and springiness showed a very high correlation to c_{11}, c_{22}, and c_{44} with r-values > 0.85. This indicates that stress relaxation time and elastic coefficients of the stiffness matrix can be promising parameters for predicting textural properties in beef.

FUTURE WORK

It is suggested that future studies in modeling and optimizing the HDP-treatment process must utilize elastic behavior of foods undergoing the treatment, as this research indicated that viscous elements did not play a role in predicting biomechanical behavior. Process conditions such as water temperature, shape and curvature of the vessel, distance of the sample from the source of shock waves, etc. must also be taken into account when modeling the process. There also exists a need to estimate the elastic coefficients and elastic constants of foods like beef, which have been reported to display hyperelastic and non-linear behavior of biological tissues. This requires the calculation of dilatational and deviatoric components of the strain energy tensor and the corresponding elastic constants related to the tensor, considering hyperelastic behavior. Therefore, this poses a significant challenge for researchers when anisotropic behavior of beef muscle is also considered. However a comprehensive study on hyperelastic and anisotropic behavior provides ample information to researchers and this information can help understand more aspects of mechanical behavior of beef muscle, especially with regards to texture and tenderness. Such a detailed approach can help understand small strain changes occurring in muscle during high pressure treatment processes, and help optimize the process of high pressure treatment of muscle foods.